MONITORING LONG-TERM CONTROLLED GRAVE SCENARIOS USING GROUND PENETRATING RADAR

by

WILLIAM T. HAWKINS
B.A. Louisiana State University, 2009

A thesis submitted in partial fulfillment of the requirements
for the degree of Master of Arts
in the Department of Anthropology
in the College of Sciences
at the University of Central Florida
Orlando, Florida

Spring Term
2011

ABSTRACT

Geophysical techniques, such as ground-penetrating radar (GPR), have been successfully used by law enforcement agencies to locate graves and forensic evidence. However, more controlled research is needed to better understand the potential and limitations of this technology in the forensic context. The goal of this study was to determine the potential of GPR using both a 250 MHz and 500 MHz antennae to monitor eight controlled graves with six different burial scenarios using pig carcasses as human proxy cadavers. In addition, a conductivity meter was employed to determine the applicability of using this technology to locate unmarked graves. For the conductivity meter, the data was processed using an EM38 program in conjunction with the SURFER program to display a conductivity contour map of the grid. For the GPR imagery, reflection profile data was processed using the program REFLEXW while horizontal slices were processed using the GPR-SLICE program. Results indicate that the conductivity meter is not a viable option in the detection of clandestine graves when other geophysical tools are available. For the GPR, results indicate that while graves can still be detected after a two-year period, there is a marked decrease in the response, or resolution, of the burial scenarios. Furthermore, burials with grave goods interred along with the carcasses were far more likely to be detected than burials that were interred with no accompanying grave goods. When comparing the performance of the two antennae, the 250 MHz antenna provided increased resolution for large cadavers buried in deep graves.

This work is dedicated to myself, without whom, I would never have completed this thesis.

ACKNOWLEDGMENTS

The research that constitutes this thesis could not have been completed without support from many individuals. My committee provided invaluable commentary and assistance; I would especially like to thank my advisor and head of my committee, Dr. John Schultz, for his numerous critiques of my work. Truly, a strong piece of steel cannot be forged without a particularly intense flame to mold it. Of course, I would also like to thank Dr. Tosha Dupras and Dr. Stacy Barber for their own contributions to finalizing this thesis.

I would also like to thank the numerous people whose help in the field insured the data was collected in as efficient a manner as possible. In no particular order, I would like to thank Joanna Fletcher, Carrie Healy, Mike Martin, Matt Newton, and Brittany Walter, in addition to the several other students and friends who participated whom I may have forgotten.

This project was supported by Award No. 2008-DN-BX-K-132 awarded by the National Institute of Justice, Office of Justice Programs, US Department of Justice. The opinions, findings, and conclusions or recommendations expressed are those of the author and do not necessarily reflect those of the Department of Justice.

TABLE OF CONTENTS

LIST OF FIGURES

LIST OF TABLES

CHAPTER ONE: INTRODUCTION

OVERVIEW

Locating and recovering buried bodies in clandestine graves is a problem that law enforcement agencies are faced with again and again. Forensic anthropologists and archaeologists can contribute in the detection and recovery of clandestine graves and other forensic objects by applying field skills used in the archaeological context to the forensic context (Dupras et al. 2006; Schultz 2007). An example of this contribution is the growing application of geophysical methods in the attempt to detect clandestine graves at the request of law enforcement agencies (Billinger 2009; Calkin et al. 2005; Davenport 2001; Dupras et al. 2006; Ruffell et al. 2009; Schultz 2007). Geophysical tools and techniques may be utilized to detect the location of clandestine graves in an efficient manner. However, the use of such tools and techniques requires extensive training and practice. Law enforcement agencies may not have the resources to procure remote sensing technology nor to train agents in their use; therefore, forensic anthropologists and archaeologists can fill this gap and supply their knowledge and expertise in this area.

Forensic geoscience is a discipline that studies the interaction of human remains and the earth's subsurface layers. It is "…concerned with the application of geological and wider environmental science information and methods to investigations which may come before a court of law" (Pye and Croft 2004:1). Geoscientists use a variety of techniques to study the earth's subsurface that can either be invasive or noninvasive (Dupras et al. 2006; Killam 2004). Invasive techniques include any techniques that disturb the subsurface's soil and have a higher likelihood

of destroying material evidence in the process (Davenport 2001; Killam 2004). Such techniques include probing, shoveling, or using any earthmoving equipment to displace soil. Conversely, noninvasive techniques do not disturb soil and allow researchers to investigate the subsurface with much less risk of destroying material evidence (Davenport 2001; Conyers 2004; Schultz 2007). Geophysical techniques such as ground penetrating radar (GPR) fall into the latter category and are an excellent method of locating a potential crime scene without disturbing the evidence. These techniques enable technicians to study the subsurface for the identification of grave sites. In addition, the use of geophysical techniques allows suspected areas to be cleared without the laborious process of actively digging through the subsurface over a large area.

Controlled Research

To ensure the best application of GPR, controlled research, in which GPR is tested on controlled burials for a long-term period of time, must be funded and pursued. In the published literature showcasing controlled research of GPR, there has been limited work using human cadavers (Freeland et al. 2003) due to the difficulty of procuring and performing research with human remains. Instead, most research utilizes animal carcasses, most often euthanized pig carcasses (*Sus scrofa*), as human cadaver proxies (France et al. 1992; Schultz et al. 2006; Schultz 2008; Strongman 1992).

Controlled experiments offer two advantages. First, their results can be used to form guidelines for working with GPR in a variety of different settings. Local environments and soil types can be tested for their effect on conducting GPR surveys. Secondly, controlled experimentation offers the chance for users to become familiar with working the GPR equipment and processing data. Therefore, controlled research for GPR for this technology should be

pursued to understand the applicability of GPR and provide experience to GPR technicians. This will facilitate better communication to law enforcement agencies concerning the likelihood of success or failure depending upon the area that is to be analyzed.

The group NecroSearch, which comprises the practitioners of numerous disciplines, popularized controlled research for ground-penetrating radar. NecroSearch explored a multidisciplinary approach to clandestine grave detection, including such fields as botany, geophysics, entomology, and geology (France et al. 1992). They determined that GPR was the best geophysical tool to employ for locating clandestine graves in forensic contexts. Other examples of controlled research with GPR have followed. As previously mentioned, most of the studies involved use pig carcasses as proxies for human cadavers, the one exception occurring in a study by Freeland (2003) where a single human cadaver was used. All of the studies have used 'standard' burials; that is, the burials were composed of bodies without any accompanying grave goods. Throughout these studies, clay consistently provided poor resuloution (Freeland 2003) while sandy soil supports better resolutions (Schultz et al. 2006; Schultz 2008). Table 1 provides an overview of the number of studies that involved controlled research for GPR.

Table 1: Examples of Controlled Research in GPR in a Forensic Context

Study	Location	Antenna	Cadaver Type	Depth	Results
France et al. 1992	Colorado	300 and 900 MHz	6 pigs buried	50.8-78.7 cm	-GPR was most effective geophysical tool used -Calibration needed prior to data collection.
Strongman 1992	British Columbia, Canada	500 MHz	1 bear, 2 goats	n/a	-Burials able to be detected after 5 years -Testing adult versus juvenile sizes
Freeland et al. 2003	Tennessee	400 and 900 MHz	1 human cadaver	60 cm	-400 MHz antenna detected grave effectively -900 MHz was unable to penetrate clay past 30 cm. -Clay is not conducive to GPR work
Modroo and Olhoeft 2004	Colorado	450 and 900 MHz	1 pig	76 cm	-GPR effectively located pig regardless of core temperature of the pig. -GPR picked up on air pockets that formed around pig from snow melting.
Schultz et al. 2006	Florida	500 MHz	12 large pigs buried	6 at .50-.60 m, 6 at 1.0-1.1m	-Cadavers in sand were easily detected. -Skeletonization did not significantly affect detection. -Cadavers in clay were increasingly difficult to find with decomposition.
Schultz et al. 2008	Florida	500 MHz	12 small pigs	6 at .50-.60 m 6 at 1.00-1.10 m	-Difficulties in locating small cadavers in sand once skeletonized -Deep graves are detected for a longer period.

The succession of studies has indicated a need for a long-term study where results are consistently monitored, as well as a study involving the use of GPR in detecting burials with grave objects distinct from the buried body. In addition, no controlled research has as yet been undertaken to appraise the use of GPR in a Spodosol environment. Furthermore, there is a need to compare the applicability of different antennae in locating clandestine graves in order to

identify the best frequency for forensic work, especially between those antennae with higher frequency emissions as compared to those with lower frequency emissions.

Research Objectives

The primary objective of this research was to test the application of geophysical techniques in the investigation of different burial scenarios and compare different geophysical techniques. This research continued the next phase in an ongoing project funded by the National Institute of Justice in order to monitor controlled graves with ground-penetrating radar in the long term. Two years was the set time limit for this project. Pig carcasses (*Sus scrofa*) were buried as human proxies in six different burial scenarios. Two control graves without pig carcasses were established to compare the effect of only disturbed soil. The data for the first year, months 1 through 12, was collected by Michael Martin (Martin 2010). Year 2 data, months 13-24, was collected and analyzed by the thesis author.

Two main geophysical techniques were tested: GPR and conductivity. The applicability of use of the conductivity meter was documented by processing the data as a contoured map and observing any changes in the succeeding months. GPR imagery data was processed and compared between the 500 MHz and 250 MHz antennas to ascertain the effect that different burial scenarios may have on the efficacy of detection for each antenna. The effect of interment time on GPR imaging was also investigated. Analyzing these variables allowed the author to establish guidelines for the use of GPR and conductivity in the investigation for clandestine graves.

Thesis Outline

The conent of this thesis will be divided into five chapters. An introduction to the research will be provided in chapter one. Results of the conductivyt meter will be provided in chapter two. The results of 500 MHz atenna will be provided in chapter three. The results of the 250 MHZ antenna will be provided in chapter four. Finally, the summary of the research projects' findings will presented in chapter five.

CHAPTER TWO: THE DETECTION OF VARIOUS BURIAL SCENARIOS USING A CONDUCTIVITY METER

INTRODUCTION

While the ground-penetrating radar (GPR) is the primary tool presented in the forensic literature for grave detection, the utility of the conductivity meter is underrepresented. To date, only a single case study in the forensic literature utilizing a combination of the conductivity meter and GPR to locate a clandestine grave (Nobes 2000). Questions still remain as to its place in the forensic archaeologist's methodological toolkit. The conductivity meter is utilized to infer changes in or composition of the earth's subsurface by inducing electrical currents in the soil to test its conductivity (Clay 2005). By doing so, information about the soil's form and composition can be determined. Even the subtlest changes in soil movements may be detected as soil changes produce contrasts in conductivity that the conductivity meter may detect. Therefore, it is a reasonable assumption that a conductivity meter may be a useful tool by detecting disturbed soils, which composes the grave, i.e. the changes both physical and chemical that distinguishes grave shaft fill from the surrounding soil.

Controlled Research

The conductivity meter is used in the detection of small changes in the soil's composition (Clay 2005). While it can detect metallic objects, these objects have to create a strong enough eddy current for the receiving portion of the antenna to detect (Clay 2005; Dionne 2009). As such, there has been limited use of the conductivity meter in controlled research. However, Dionne (2009) successfully showed, in a controlled research setting utilizing the same

conductivity meter model, that the conductivity meter could be used to locate metallic weapon caches of varying types and depths. However, his findings suggested that the conductivity meter would have difficulties identifying non-ferrous items or objects buried past a meter's depth due to limitations implicit for this model; there is a peak in signal strength at a depth of 40 cm, after which the strength of the signal steadily decreases (Geonics 2006).

To determine the potential of the conductivity meter as a law enforcement tool, controlled research should be pursued. One of the greatest advantages to its use owes to the conductivity meter being extremely versatile; it can be used in wet or dry conditions, in all types of terrain. The conductivity meter also provides a direct read-out, displaying the measure of conductivity in millisiemens per meter (mS/m) (Killam 2004). Unfortunately, this tool is expensive and requires extensive training to be properly utilized. Furthermore, there are serious questions as to the scope of its ability in reading both anomalies a meter into the earth's subsurface and the backfill of a common grave shaft (Dionne et al. 2010).

MATERIALS AND METHODS

Field Site and Controlled Graves

The field site was used for controlled research project is located on the University of Central Florida's main campus property, in UCF's Arboretum. Specifically, the field site lies within property maintained by the Civil Engineering division of the University of Central Florida's College of Engineering and Computer Science, referred to as the Geotechnical Engineering Test Site. It is a secure field site, fenced in with a locked gate. A small portion of this field was mowed and maintained to create a permanent grid of 11 m by 22 m. Permanent

non-metal markers were placed at the corners of the grid so the exact position of the survey transects could be duplicated each time geophysical data was collected.

Figure 1: The Geotechnical Engineering Test Site

A total of eight graves were monitored. Six pig carcasses (*Sus scrofa*) were buried at regular intervals throughout the grid in a variety of burial scenarios (see Table 2) as well as two control holes; it was important to include these control holes to test the response of conductivity to disturbed soil. Testing such a response would determine if forensic investigators could detect the distinctions between a grave with a buried component (the pig proxies and various grave objects) or simple disturbed soil when using the conductivity meter. The euthanized pig carcasses were buried in January of 2009 after sustaining head shots with .22 caliber handgun. As established by Martin (2010) the six pig carcass graves contain the following scenarios (in addition, see Table 2):

1. A blank control grave consisting of only disturbed backfill (50-60 cm) to determine the geophysical response to disturbed soil only.
2. A blank control grave consisting of only disturbed backfill (100-110 cm) to determine the geophysical response to disturbed soil only.
3. A pig carcass buried without additional grave objects at .5 m depth.
4. A pig carcass buried without additional grave objects at 1 m depth.
5. A pig carcass wrapped in a vinyl tarpaulin and buried at 1 m depth.
6. A pig carcass wrapped in a cotton blanket and buried at 1 m depth.
7. A pig carcass buried underneath a layer of lime (calcium hydroxide) at 1 m depth
8. A pig carcass buried underneath a layer of rocks at 1 m depth.

Table 2: Detailed Grave Information for Each of the Burials (From Martin 2010)

Grid Location	**Burial Date**	**Depth of Unit (below surface)**	**Scenario**	**Weight of Pig (lbs)**	**Sex of Pig**
1A	1/30/2009	0.5 m	Shallow pig grave	90	Female
1B	1/30/2009	1.0 m	Deep pig grave	100	Male
1C	1/30/2009	1.0 m	Deep grave with layer of rocks covering pig	90	Male
1D	1/30/2009	1.0 m	Deep grave with pig wrapped in tarpaulin	98	Female
2A	1/26/2009	0.5 m	Shallow control hole	N/A	N/A
2B	1/30/2009	1.0 m	Deep control hole	N/A	N/A
2C	1/30/2009	1.0 m	Deep grave with layer of lime covering pig	95	Male
2D	1/30/2009	1.0 m	Deep grave with pig wrapped in blanket	97	Female
Calibration Unit (outside grid)	1/9/2009	1.0 m	Rebar hole	N/A	N/A

The pig carcasses were laid into the grave pit on their right sides, with their heads towards the north wall and their back against the east wall. Three body locations were measured

from the surface of the grave pit for precise measurements: the head, the abdomen, and the tail (see Table 3). Figure 2 shows the layout of the research grid including each burial scenario.

Table 3: Precise Burial Measurements of Pig Carcasses (From Martin 2010)

Grave Location	Measurement to Head	Measurement to Abdomen	Measurement to Tail
1A	0.33 m	0.24 m	0.26 m
1B	0.86 m	0.76 m	0.77 m
1C*	0.83 m	0.75 m	0.77 m
1D	0.74 m	0.74 m	0.75 m
2C	0.83 m	0.76 m	0.78 m
2D	0.80 m	0.74 m	0.76 m

**Note: layer of rocks added over pig carcass comprising an additional .70 m*

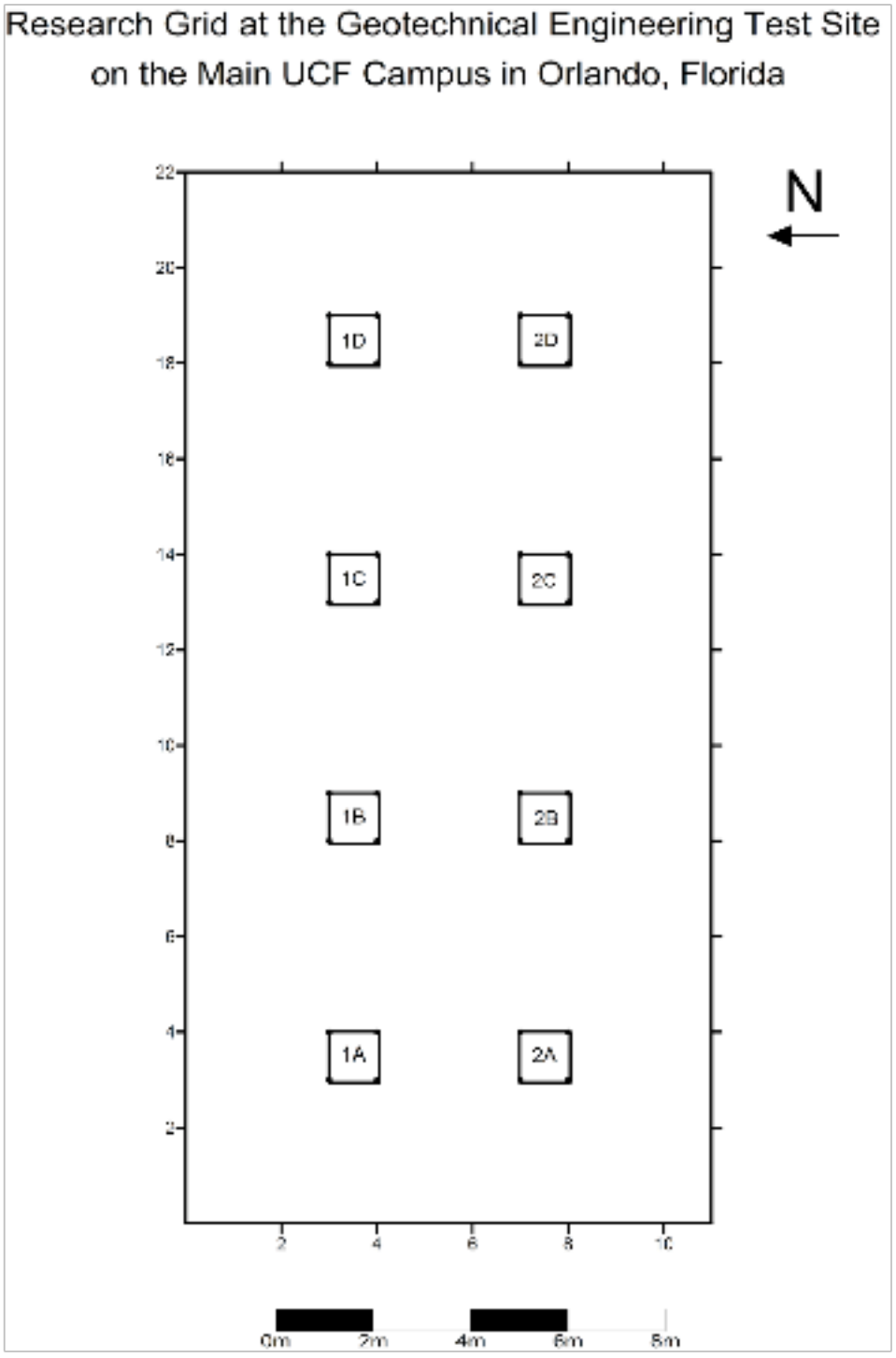

Figure 2: Research Site Grid with Established Burials (From Martin 2010)

Data Collection

Data collection was performed by operating the conductivity meter, a Geonics EM38-RT with an Allegro CX handheld data logger to store the data collected from the field. The conductivity meter was calibrated throughout data collection by choosing a small area known to be without burials of any kind off the research grid.

The conductivity meter is composed of two main portions: the transmitter and the receiver. The transmitter sends out electrical currents into the subsurface. When these currents pass through the soil they will create secondary currents, also known as eddy currents. These eddy currents send out their own electric signals that the receiving portion of the conductivity meter will detect, allowing the conductivity meter to document changes in soil composition. The receiver identifies changes in EM wavelength that is the direct response of changes in conductivity (Beauchaine and Werdemann 2006). Though there are numerous models of conductivity meters, the conventional technology used by both forensic anthropologists and archaeologists is the horizontal loop (or slingram) conductivity meter that can be operated by a single individual and houses both the transmitter and receiver coils (Dupras et al. 2006). The horizontal loop model can be employed either horizontally, where the instrument is laid on its side on the ground, or vertically, where the instrument is held upright. In this research, the vertical mode was used in order to document changes at a greater depth (Clay 2005).

The grid data collection was performed at the end of every month for a total of twelve months. Geophysical data was collected with transect spacings of 25 cm in an east-west direction (see Figure 3).

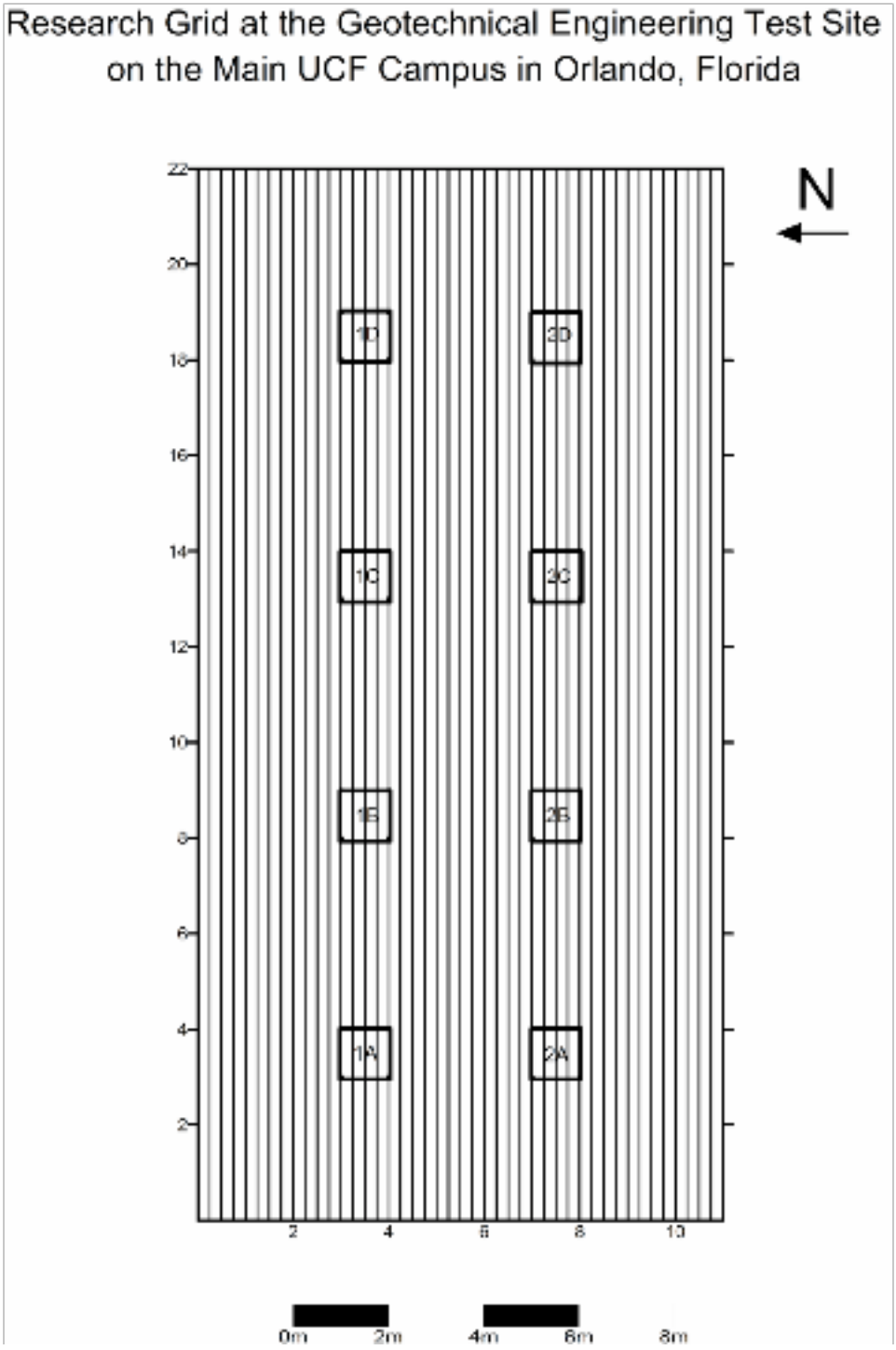

Figure 3: Research Site Grid with Transect Lines (From Martin 2010)

Data Processing

The final phase of this research was the processing of the data gathered in the field. Per protocols established by Martin (2010), conductivity measurements were recorded with a hand-held Allegro CX Field Computer that connects to the conductivity meter; the data collected was then transferred back to a desktop computer from the field computer. Conductivity data was processed using an EM28 computer program and then further processed by Golden Software Surfer 8 (Version 8.4) to display the information in a contour map image. A contour map image uses the X and Y coordinates and the value of the conductivity measurements, represented as Z, to map out the site wherein it is employed. The closer two lines are together on the map, the greater the conductivity of that area.

RESULTS

All images from the processed data are located in Appendix A. At month 13, six conductivity anomalies were noted. These anomalies did not correspond to any pig burial, nor were there any anomalies of any kind noted at the location of the eight graves. In months 14 through 24, the same six anomalous reflections were noted consistently (see Figure 4). Over the monitoring period, little variation existed that could be linked with the location of the eight graves.

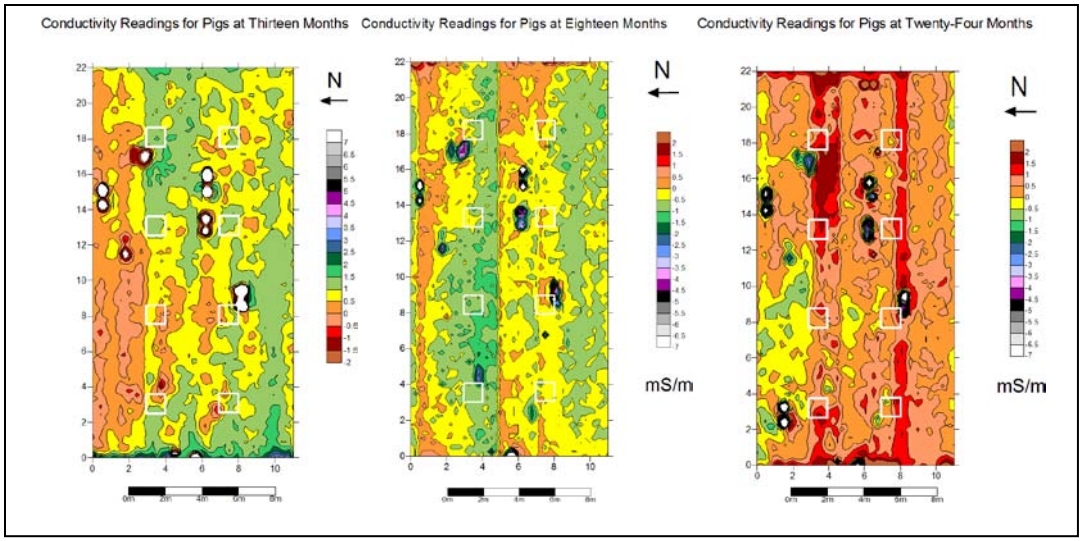

Figure 4: Conductivity Contour Maps at Months 13, 18, and 24 Respectively

DISCUSSION

The use of the conductivity meter in the search for clandestine graves is strongly advised against. Over a two-year period, data collection showed little variability and no significant anomalies for any burial scenarios, a finding consistent with the conclusions from the first year of research (Martin 2010). There are three factors that may account for this: the depth of the graves, the absence of non-ferrous or non-conductive materials, and the physical and chemical composition of the soil.

The strength of the conductivity meter is at its most potent around 40 cm in the subsurface. After this point, the strength of the conductivity meter shares an inverse relationship with successive depths: the deeper the creation of eddy currents, the weaker the returning signal strength will be. This is made clear in the available literature by the manufacturer (Geonics 2006) as well as researchers in the field (Clay 2005).

However, the carcass buried at 24 cm, the shallow pig burial, burial 1A, was not detected. This is most probably due to the conductive nature of the buried materials, in this case the pig carcasses. The function of the conductivity meter is to induce electric currents in the soil. If the buried materials have a low propensity for conducting electricity, it is unlikely that they will return a strong signal. While Dionne (2009) had success with detecting weapon caches of ferrous materials, he had difficulty detecting the presence of non-ferrous materials at shallow depths. It is probable that the organic nature of the buried cadaver proxies did not lend themselves well to being electrically conducted, especially after decomposition and possible skeletonization.

The final possible reason for the inability of the conductivity meter to detect clandestine graves may be due to the physical and chemical nature of the soil that composed the field test site. The soil at the field site was classified a Smyrna pomello soil, a sandy soil characterized by its superior water drainage (Doolittle and Schellentrager 1989; Leighty 1989). In addition, the field soil profile was characterized by a spodic horizon a soil layer with organic, amorphous components (Brady and Weil 1999). The conductivity meter is able to pick up differences in soil contrasts if the contrasting soils have enough physical and chemical contrast (Dionne et al. 2010). Basic physical effects on the soil that affect the utilization of a conductivity meter are the presence of clay in the soil, the temperature of the soil, and the moisture level of the soil (McNeill 1980). Most importantly, however, is the composition of soil, which is founded upon its porosity level. Sand or gravel is found to have the lowest response to conductivity readings (Bevan 1998). There must be a significant amount of contrast between fill and non-fill for the conductivity meter to pick up upon changes in soil distribution (Clay 2005). As the shafts of the burials were filled with sandy soil from the original excavation, it is unlikely that the contrast

between fill and non-fill was significant enough to elicit a response. This is further exacerbated by the passage of two years, which would only result in the soil becoming more homogenous.

The use of the conductivity meter is strongly advised against as a search option for graves. Due to limitations implicit in the equipment, the ability of the investigator to identify buried human remains is improbable. It may be possible for this instrument to detect shallow burials with metal grave goods interred alongside the body; research would need to be conducted with those variables in mind to confirm that hypothesis. The conductivity meter was not developed for the purpose of clandestine grave search; its purpose lies in the identification of soil movement and general subsurface features. Human remains lie outside its scope and therefore the conductivity meter should remain outside of the forensic anthropologists' toolkit when better options such as GPR are available.

CHAPTER THREE: THE DETECTION OF VARIOUS BURIAL SCENARIOS USING A GPR UNIT WITH A 500 MHZ ANTENNA

INTRODUCTION

The use of noninvasive geophysical techniques, such as ground penetrating radar (GPR), is utilized increasingly in the detection of clandestine graves by law enforcement agencies (Davenport 2001; Dupras et al 2006; Ruffell 2005; Schultz 2007). Ground-penetrating radar provides law enforcement with a noninvasive search method and therefore allows for minimal damage to possible evidence in the search for a clandestine grave. It can also display results in real-time, maximizing the efficient use of time in the field. Numerous published case studies using GPR demonstrate the applicability of the equipment to either positively locate clandestine graves or clear suspected areas of a forensic significance, allowing law enforcement to maximize their time searching for the body (Calkin et al. 1996; Davenport 2001; Mellett 1992; Nobes 2000; Ruffel 2009; Schultz 2007)

However, a better understanding of the technology's potential and its limitations is required before its use can be expanded. In order to achieve this better understanding, controlled research projects must be pursued. In controlled research, the use of GPR is employed over a research area where graves, usually containing pig carcasses as human cadaver proxies, are set up to test the applicability of the equipment to detect clandestine graves. Controlled research investigates the various variables affecting the applicability of GPR to detect clandestine graves. Previous studies have documented the changes in GPR grave detection based on differences in body size, specifically envisioning an adult versus juvenile burial (Schultz et al. 2006; Schultz

2008; Strongman 1991). Other studies have tested the ability of GPR detection based on depth, considering the differences between shallow and deep burials (Freeland et al. 2003; Roark et al 1998; Schultz et al. 2006; Schultz 2008). Another variable studied in GPR controlled research is the type of soil of which the grave matrix is composed. Clayey, water-saturated soil have proven to result in increased GPR wave attenuation (Freeland et al. 2003) while sandy soils have proven to be excellent facilitators of wave propagation due to the increased relative dielectric contrast between the buried body and the surrounding soil matrix (Schultz et al 2006; Schultz 2008).

While Strongman (1992) investigated the applicability of the GPR after a 5 year period, he did not employ sequential monitoring in his research project. When Schultz (2006, 2008) employed sequential monitoring, he did so only for a period up to 21.5 months, noting at the end of his research a significant decreases in returning signal strength beginning to become apparent (Schultz et al. 2006; Schultz 2008). Research of this nature has yet to address the differences in the detection of graves modeled after real-life scenarios, with grave objects added to the grave feature. In addition, there has been no significant research testing the usefulness of GPR in a Spodosol environment.

Purpose

Stringent testing of GPR, in its use as a detector for clandestine graves, has been narrowly utilized with only a few simple variables. To more properly assess its application, controlled research must be broadened to include new variables to create a more comprehensive understanding of its applicability. This research does so by having a threefold purpose: first, to determine the ability of the 500-MHz to detect clandestine graves that resemble real-life forensic scenarios; second, to grade each burial scenario throughout the research process to determine

which burial provides the most discernable hyperbola and which provides the poorest; and finally, to determine the applicability of the GPR unit to detect the graves for a monitoring period of two years and thus the long term applicability of GPR in detecting clandestine graves. Additionally, this research monitors the efficacy of the GPR unit in a Spodosol environment. This research comprises the second year of a two-year project. The first year's research, months 1 through 12, was conducted by Martin (2010); the second year's research is the aim of this thesis and comprises months 13 through 24.

MATERIALS AND METHODS

Field Site and Controlled Graves

The field site which hosted this controlled research project was located on the University of Central Florida's (UCF's) main campus property, in UCF's Arboretum. Specifically, the field site lies within property maintained by the Civil Engineering division of UCF's College of Engineering and Computer Science, referred to as the Geotechnical Engineering Test Site (see Figure 5). It is a secure field site, fenced in with a locked gate. A small portion of this field was mowed and maintained in order to create a permanent grid of 11 m by 22 m. Permanent non-metal markers were placed at the corners of the grid so the exact position of the survey transects could be duplicated each time geophysical data was collected.

Figure 5: The Geotechincal Engineering Test Site

A total of eight graves were monitored. Six pig carcasses (*Sus scrofa*) were buried at regular intervals throughout the grid as well as two control holes (see Figures 2 and 3). It was important to include these control holes to test the response of GPR to the disturbed soil, to determine if GPR detected either the pig carcass proxies and any additional grave item or the disturbed soil. The pigs were euthanized and buried in January of 2009, sustaining head shots with .22 caliber handgun. As established by Martin (2010), the six graves contain the following scenarios (in addition, see Table 4).

1. A blank control grave consisting of only disturbed backfill (50-60 cm) to determine the geophysical response to disturbed soil only.
2. A blank control grave consisting of only disturbed backfill (100-110 cm) to determine the geophysical response to disturbed soil only.
3. A pig carcass buried without additional grave objects at .5 m depth.
4. A pig carcass buried without additional grave objects at 1 m depth.

5. A pig carcass buried wrapped in a vinyl tarpaulin and buried at 1 m depth.
6. A pig carcass buried wrapped in a cotton blanket and buried at 1 m depth.
7. A pig carcass buried underneath a layer of lime (calcium hydroxide) at 1 m. depth
8. A pig carcass buried underneath a layer of rocks at 1 m depth.

Table 4: Detailed Grave Information for Each of the Burials (From Martin 2010)

Grid Location	**Burial Date**	**Depth of Unit**	**Scenario**	**Weight of Pig (lbs)**	**Sex of Pig**
1A	1/30/2009	0.5 m	Shallow pig grave	90	Female
1B	1/30/2009	1.0 m	Deep pig grave	100	Male
1C	1/30/2009	1.0 m	Deep grave with layer of rocks covering pig	90	Male
1D	1/30/2009	1.0 m	Deep grave with pig wrapped in tarpaulin	98	Female
2A	1/26/2009	0.5 m	Shallow control hole	N/A	N/A
2B	1/30/2009	1.0 m	Deep control hole	N/A	N/A
2C	1/30/2009	1.0 m	Deep grave with layer of lime covering pig	95	Male
2D	1/30/2009	1.0 m	Deep grave with pig wrapped in blanket	97	Female
Calibration Unit (outside grid)	1/9/2009	1.0 m	Rebar hole	N/A	N/A

The pig carcasses were laid into the grave pit on their right sides, with their heads towards the north wall and their back against the east wall. Three body locations on their body were measured from the surface of the grave pit for precise measurements: the head, the abdomen, and the tail (see Table 5; see also Martin 2010).

Table 5: Precise Burial Measurements of Pig Carcasses (From Martin 2010)

Grave Location	Measurement to Head	Measurement to Abdomen	Measurement to Tail
1A	0.33 m	0.24 m	0.26 m
1B	0.86 m	0.76 m	0.77 m
1C*	0.83 m	0.75 m	0.77 m
1D	0.74 m	0.74 m	0.75 m
2C	0.83 m	0.76 m	0.78 m
2D	0.80 m	0.74 m	0.76 m

**Note: layer of rocks added over pig carcass comprising an additional .70 m*

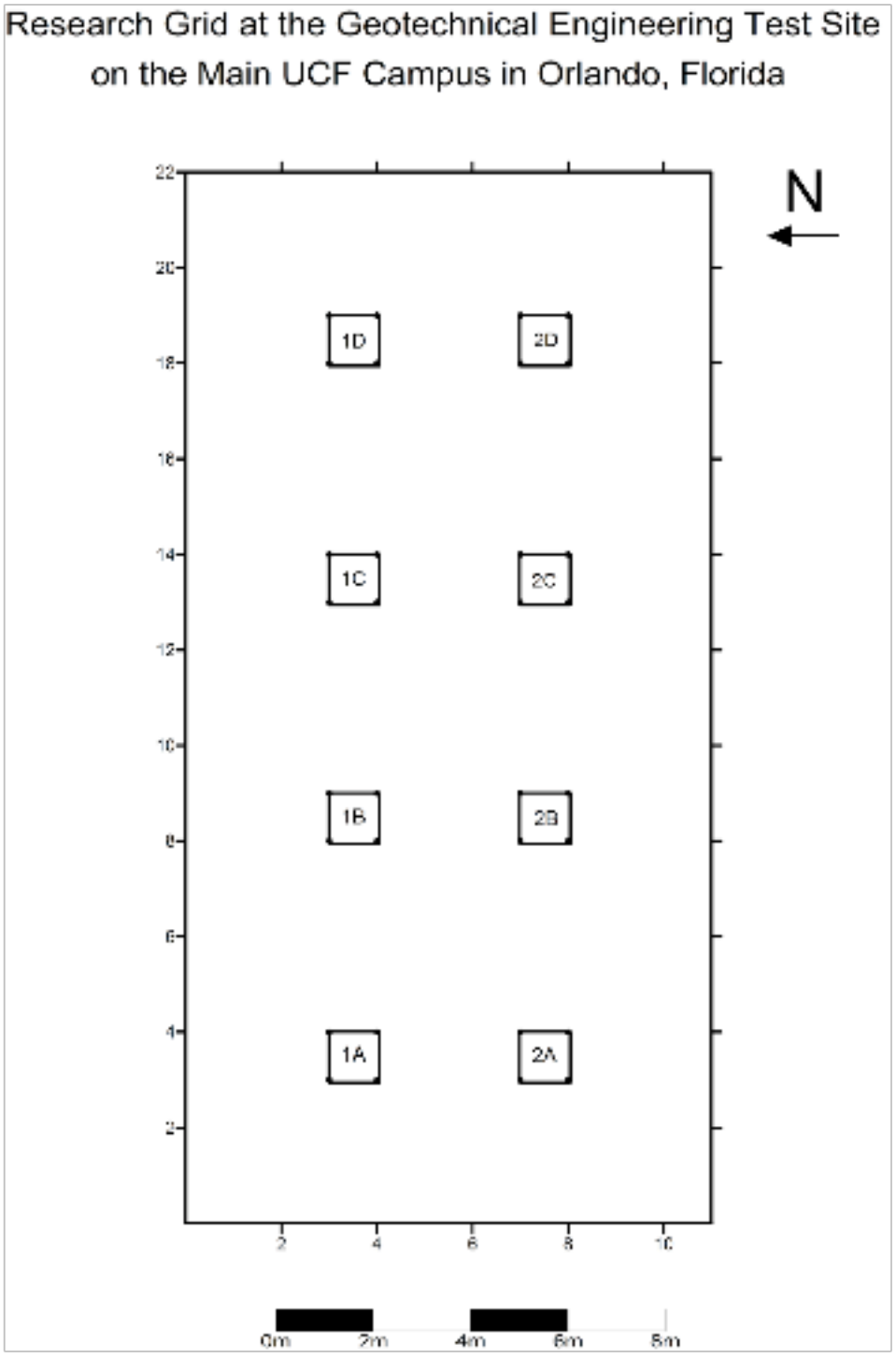

Figure 6: Research Site Grid with Established Burials (From Martin 2010)

GPR Equipment

All GPR equipment is composed of three main parts: the antenna (which both transmits and receives electromagnetic waves), the computer control, and the monitor which displays results in real time (Schultz 2007). The GPR unit generates radar waves, "a form of electromagnetic energy" (Conyers 2004:23), to probe the surface. These waves will travel infinitely unless they are absorbed or conducted away in some way (Conyers 2004). When the electromagnetic strikes an object in the subsurface, a resulting reflected wave will occur that will be received by the receiving portion of the dipole antenna. However, the amplitude of the returning wave- that is, the strength of the returning signal-is directly dependent on the measure of the relative dielectric constant, the contrast between any two materials (Ruffel 2005; Schultz 2007).

The antenna frequency number reflects the frequency at which its radar waves are generated by the antenna (Reynolds 1997). Antenna frequency emissions range from 10 MHz to 1.5 GHz (Watters and Hunter 2004). The choice of antenna frequency has a direct relationship with GPR detection of clandestine graves at various depths. In short, the lower the frequency the deeper the GPR will be able to read. Conversely, the higher the frequency the more precise and detailed the GPR results will be. For example, a 120 MHz antenna may display results up to 50 meters deep, while a 900 MHz antenna can only display results less than a meter deep but with a much better resolution (Schultz 2007). Therefore, a happy medium is often sought after and is often found in a 400-500 MHz antenna (Dupras et al 2006; Schultz 2007).

Data Collection

Grid data collection was performed twice a month for a twelve month monitoring period a using a Mala RAMAC X3M GPR unit, with a 500 MHz antenna, manufactured by Mala Geonics. Data was collected using transect interval spacings of .25 cm in both an east-west direction and a north-south direction (see Figures 3 and 4). Per recommendations by Pomfret (2006), this research collected transects in two directions as this methodology provides maximum detection and resolution of small subsurface features.

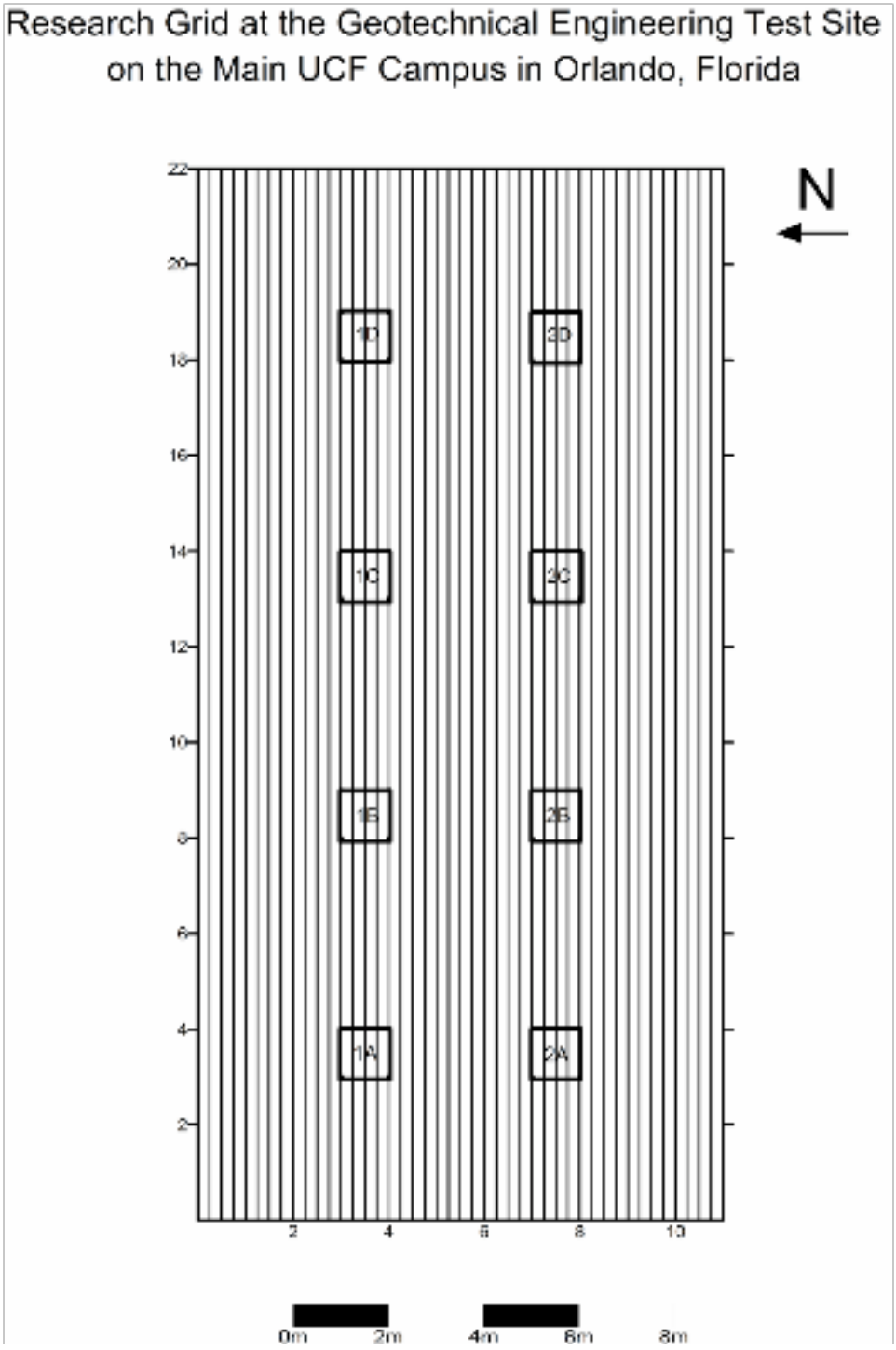

Figure 7: Research Site Grid with West-East Transects (From Martin 2010)

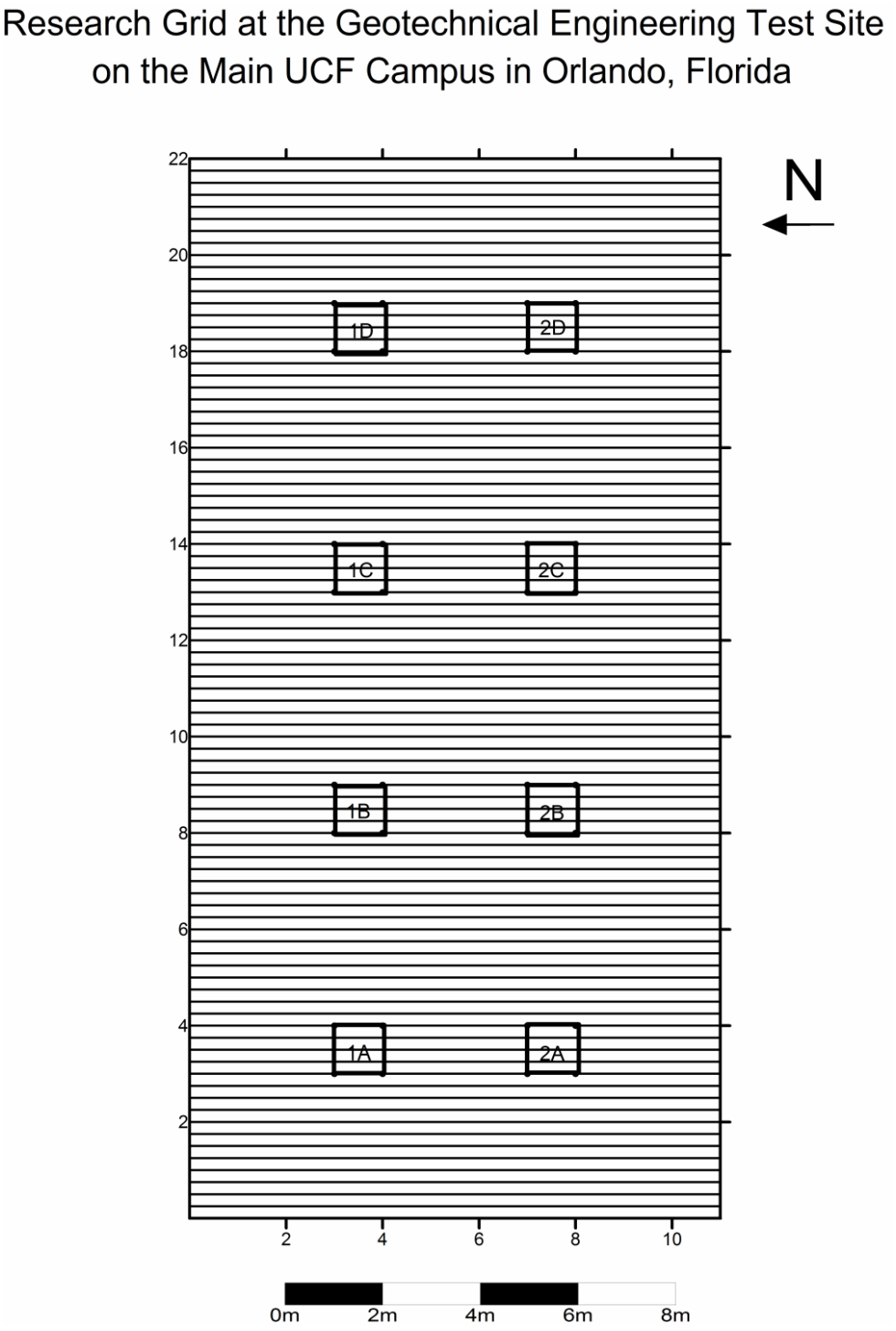

Figure 8: Research Site Grid with North-South Transects (From Martin 2010)

On data collection days, soil moisture values within the graves were noted using a soil moisture meter manufactured by Lincoln Irrigation Incorporation. The probe on the soil moisture meter measures 90 cm in length, and moisture values were recorded on a scale of 1 to 10, with 10 being the wettest. Per protocols developed by Martin (2010), the soil moisture meter was calibrated to 10 using tap water. The soil moisture data was used to determine the relationship between moisture and grave detection. Per Martin (2010), soil moisture was collected at the following locations: each corner of the research grid, one point on both the west and east baselines, three points on both the north and south baselines, the northwest corner of the rebar hole, and each of the northwest corners of the burials within the grid. Two soil moisture measurements were collected for shallow burials (25 and 50 cm) and three measurements for deep burials (24, 50, and 90 cm).

Additionally, the GPR unit was calibrated for accurate depth measurements that may be affected by daily soil moisture. A buried object at a specific depth is used for calibration to determine the sensitivity of the instrument and can allow wave velocity, and thus depth, to be more accurately calculated within the soil (Conyers and Cameron 1998; Conyers 2004; Strongman 1992; Martin 2010). Prior to data collection, the GPR unit was calibrated a metal bar that was pounded into the ground at a1 m depth, a method suggested by Conyers (2004). The calibration test unit was located 2 m away from the east end of the grid.

Data Processing

The final phase of this research was the processing of the data gathered in the field. Processing GPR data using 2-D or 3-D analysis may increase the likelihood of spotting anomalies in the subsurface, a hypothesis that was tested with this research. Two programs were

used: REFLEXW and GPR-SLICE. REFLEXW was used to process raw reflection profiles, a type of data display that presents the data in two dimensions, depth and distance (covered by the GPR's survey wheel). GPR-SLICE, on the other hand, is a three dimensional display and shows the entire scanned grid, as opposed to a single profile. The program has the ability to put all transects gathered in the X and Y planes and fuse them together, creating what is called a horizontal slice or Z-slice. This is done in part by welding together each of the reflection profiles collected, making it imperative that small spacing of transects is utilized in order to minimize the amount of empty space that is used to create the horizontal slice.

RESULTS

Reflection Profiles

Analysis using the REFLEXW program was confined to two rows in the east-west transects (Row 1 and Row 2), each comprised of five 0.25 m transects or profiles. As illustration, Profile 1 (Figure 9) represents the north side of the burial pit and Profile 5 (Figure 13) represents the south side of the burial pit, the middlemost profile, Profile 3 (Figure 11), represented the transect that ran over the approximate center of the grave. It became apparent that the middlemost profile represented the greatest quality in returning signals, presenting the most reliable data of the details of the subsurface. In Profile 2 (Figure 10), the three burials interred at 1.0 m depth were evident; however, there was no hyperbola for burial 1A, whereas in Profile 3 (Figure 11) there was a discernable hyperbola for the shallow burial. Guidelines for analyses were created in conformity with those established by Martin (2010). While the two sets of five

transects were examples of reflection profiles over the graves, only the third reflection profile, the middlemost, was used. The reflection profiles for the data collection period following month 13 (months 14-24) are located in Appendix B.

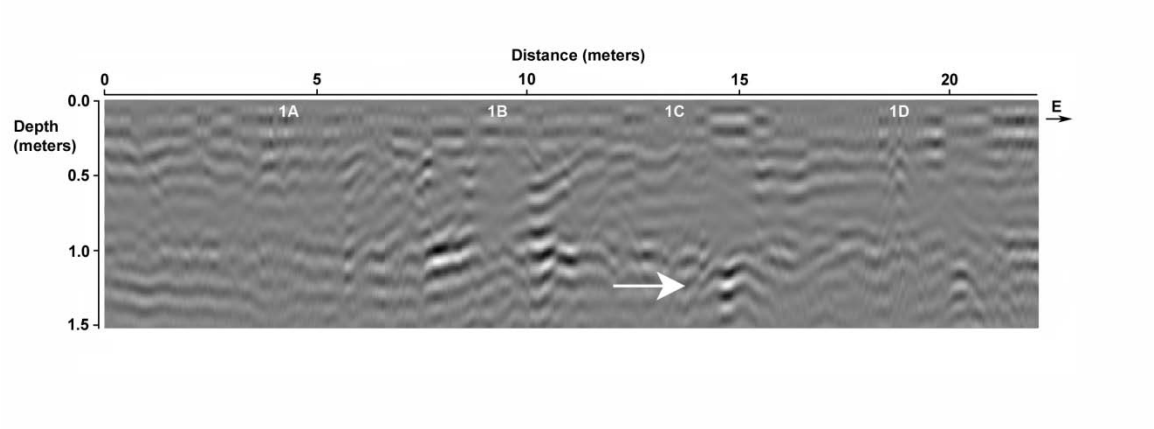

Figure 9: Profile 1 of Row 1 at 13 Months

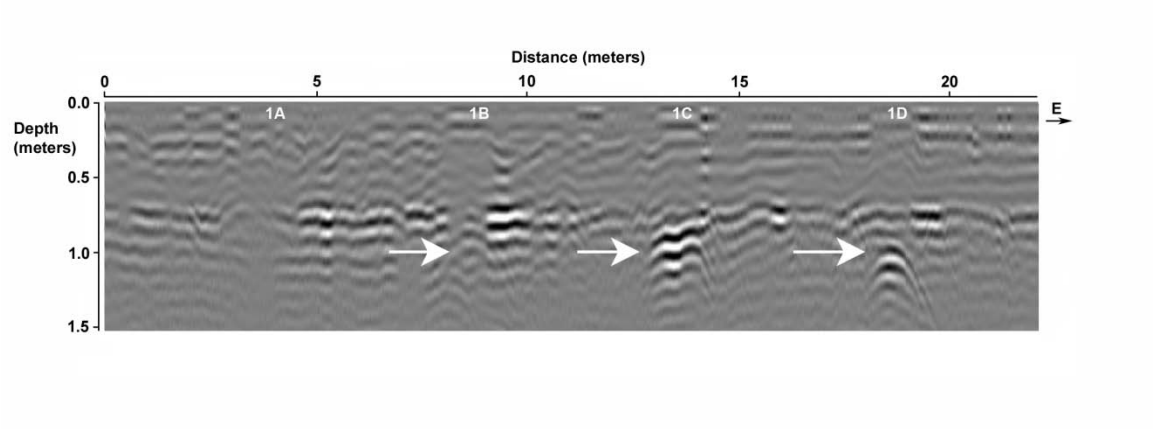

Figure 10: Profile 2 of Row 1 at 13 Months

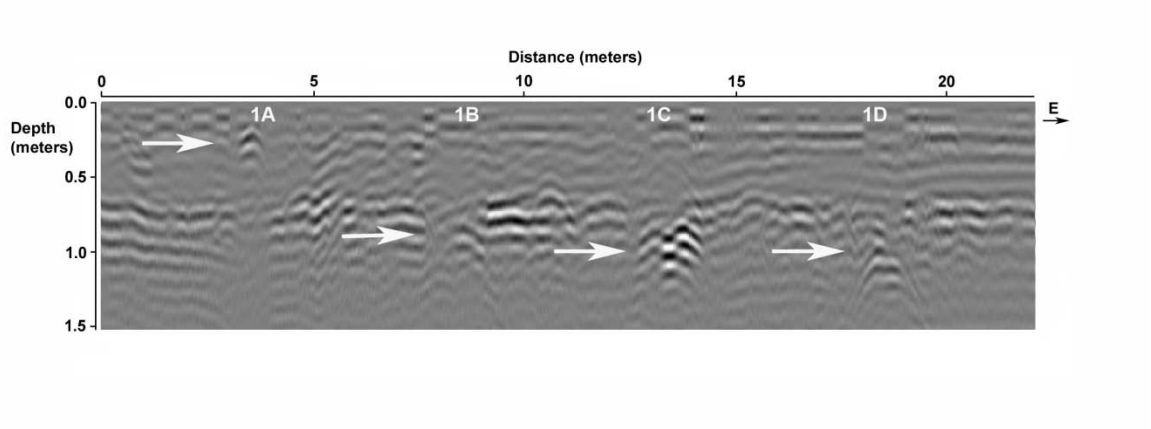

Figure 11: Profile 3 of Row 1 at 13 Months

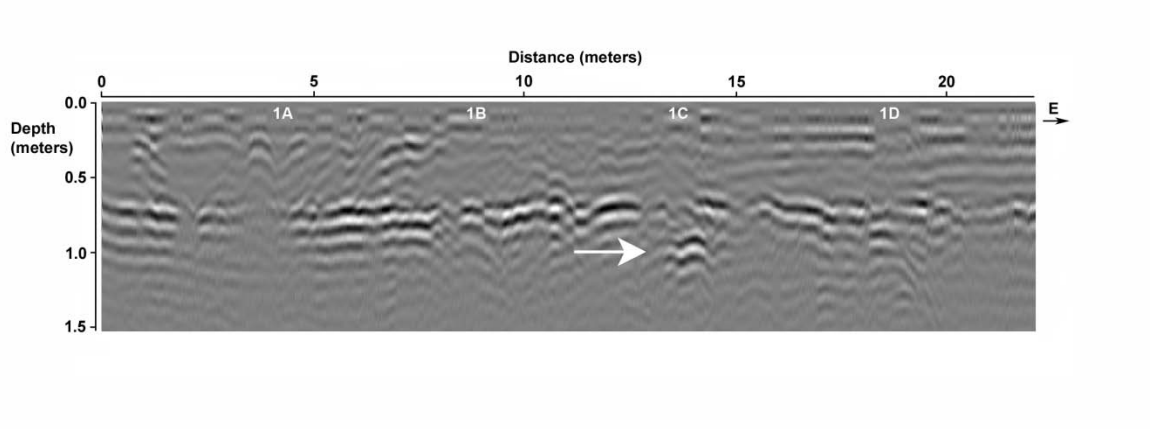

Figure 12: Profile 4 of Row 1 at 13 Months

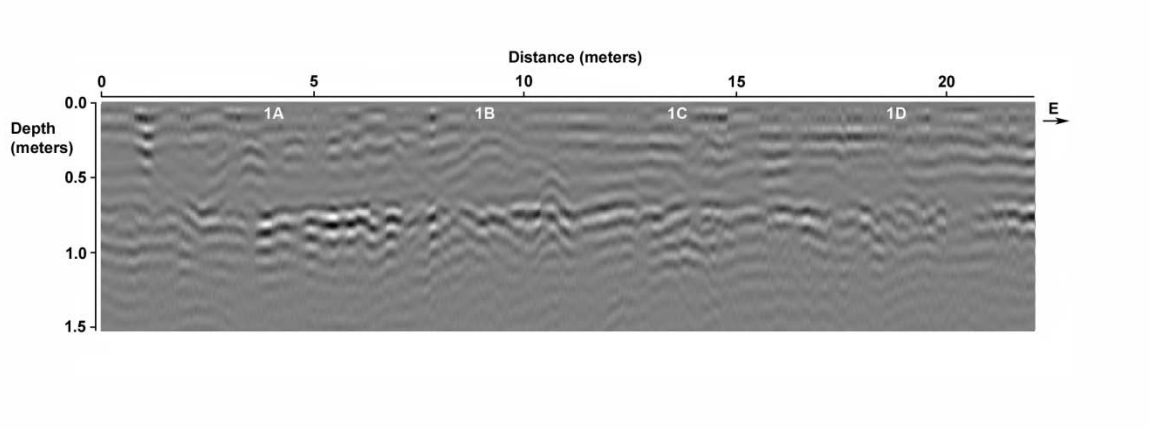

Figure 13: Profile 5 of Row 1 at 13 Months

Month 13 summary data indicates that all four burial scenarios in Row 1- the shallow pig burial (1A), the deep big burial (1B), the pig buried under a layer of gravel (1C), and the pig buried wrapped in a tarpaulin (1D)- produced discernable hyperbolae. Of the row, burial 1C shows far and above the strongest response, followed by 1D, 1A, and 1B, respectively (Figure 37).

Row 2 displays weaker signals. Neither one of burials 2A and 2C, the shallow control grave and the pig buried under lime, respectively, produces a discernable hyperbola. Burial 2B, the deep control hole, produces a response significantly underneath the meter mark, perhaps indicating that it is the burial floor that produces a response, not the disturbed soil of the grave shaft. Burial 2D, the pig wrapped in a blanket, produces a discernable hyperbola (Figure 38).

At month 14, burial 1A no longer produces a visible hyperbola. The hyperbola for burial 1B is still present but very weak, and the hyperbolae for burials 1C and 1D are still discernable (Figure 39). In Row 2, the hyperbola for burial 2D is no longer produced. The reflection from the grave floor of 2B is still present, as is a faint indication of a response from burial 2C (Figure 40). This pattern repeats itself in Month 15, although, in Row 2, the hyperbola from burial 2D is present again. The hyperbola for burial 1B is weaker than the previous month (Figures 41 & 42).

At month 16, burial 1C, the pig buried under gravel, is the burial that produces a response in Row 1 (Figure 43). In Row 2, the response from the grave floor of control hole 2B is still discernable, as are two very faint responses from burials 2C and 2D (Figure 44). At Month 17, the response from burial 1C is joined by a sudden increase in the response from grave 1D (Figure

45). In Row 2, burial 2B's grave floor is the only feature producing a response to the GPR equipment (Figure 46).

At month 18, there is a marked decrease in the overall visibility of the responses. Burial 1D, the pig wrapped in a tarpaulin, manages a weak response that can be identified after processing, as well as the grave floor of burial 2B (Figures 47 & 48). This overall weakness of signal strength is repeated in Month 19, with the salient exception of burial 1C, the pig buried under gravel, which creates a surprisingly strong response. In contrast, in Row 2, even the grave floor of burial 2B is no longer discernable as it had been months previous (Figures 49 & 50).

Months 20, 21, and 22 repeat this pattern. There is no discernable response from the shallow pig burial or shallow control hole or deep big burial (burials 1A, 1B, and 2A, respectively). There is no discernable response from the pig buried under lime (burial 2C). The pig buried under gravel, the pig wrapped in a tarpaulin and the deep control grave floor show intermittent responses throughout the months at seemingly random patterns. The pig wrapped in a blanket creates a weak response in Month 20 but thereafter is lost to the background noise of the typical survey (see Figures 51-56). At month 23, burial 2C is barely discernable; no other grave produces a response (Figures 57 & 58).

The final month, month 24, sees a return in burial response strength in both rows. In Row 1, burials 1C and 1D are discernable after processing. Additionally, in Row 2, burials 2B, 2C, and 2D are discernable again after processing (Figures 59 & 60). For a summary of the quality of imagery throughout the research project, see Table 6.

Table 6: Monthly imagery results for each burial scenario based on reflection profiles from the 500 MHz antenna; months 1-12 adapted from Martin (2010)

Burial Scenario								
	1A	1B	1C	1D	2A	2B	2C	2D
Month								
1	Good	Poor	Excellent	Poor	None	None	Good	None
2	Good	Good	Good	Poor	None	Poor	Poor	Poor
3	Poor	Good	Excellent	Poor	None	Poor	Poor	Poor
4	Excellent	Excellent	Excellent	Good	None	Poor	Good	Good
5	Excellent	Excellent	Excellent	Excellent	None	Poor	Excellent	Good
6	Excellent	Good	Excellent	Good	None	None	None	None
7	Excellent	Good	Excellent	Poor	None	None	None	None
8	Excellent	Poor	Excellent	Poor	None	None	None	None
9	Good	Poor	Excellent	Poor	None	Poor	None	None
10	Good	None	Good	Good	None	None	None	None
11	Excellent	None	Excellent	None	None	Poor	None	None
12	Good	None	Good	None	None	None	None	None
13	Poor	Poor	Good	Poor	None	Good	None	Poor
14	None	Poor	Good	Good	None	Poor	Poor	None
15	None	Poor	Good	Good	None	Poor	None	Poor
16	None	None	Poor	None	None	Poor	Poor	Poor
17	None	None	Good	Poor	None	Poor	None	None
18	None	None	None	None	None	Poor	None	None
19	None	Poor	Good	Poor	None	None	None	None
20	Poor	None	Good	None	None	Poor	None	Poor
21	Poor	None	None	None	None	Poor	None	None
22	None	None	Poor	None	None	None	None	None
23	None	None	None	None	None	None	Poor	None
24	None	None	Good	Good	None	Poor	Poor	Poor

Horizontal Slices

Horizontal slices are composed using the software program GPR-SLICE (Version 7). Horizontal slices, also referred to in the literature as Z-slices or time slices, are planview representations of the grid composed in a 3-D cube, each slice of the cube taken at a different

depth and representing that depth's planview. Therefore, each horizontal slice is an amalgamation of both the X and Y orientation's data and compiled into Appendix C. Each image is taken at a single depth, usually a depth of 1.0 m though some variability is inherent in this approximation.

At month 13, three responses are noted that correspond to burial 1C (the pig buried under gravel), burial 1D (the pig wrapped in a tarpaulin), and burial 2B (the deep control grave, most likely the grave floor). No other responses from the graves are detected (Figure 61).

Two images are taken from the 3-D cube for month 14, a shallow view (at approximately 1.0 m depth) and deep view (at approximately 1.5 m depth). In the shallow image, burials 1C and 1D produce a strong response as well as a weak returning signal from burial 1B, the deep pig grave (Figure 62). In the deep image, burials 2B and 2C (the pig buried under lime) exhibit strong responses (Figure 63). This pattern is repeated in month 15. There is a singular addition, a strong returning signal on the deep image at burial 1C, but otherwise the aforementioned pattern held (Figures 64 & 65).

In month 16, a single horizontal slice is used at approximately 1.0 meters in depth. This slice featured four responses: burials 1C, 1D, 2C, and 2D (the pig wrapped in a blanket). The responses from Row 2 are noticeably weaker than the responses from Row 1 (see Figure 66).

In month 17, two horizontal slices were used. The shallow view, closer to one 1.0 m in depth, features a singular, strong response for burial 1C (Figure 67). The deep view, approximately a 1.5 m in depth, produces a strong response from the grave floor of burial 2B and a weak response from burial 1D (Figure 68).

In month 18, returning responses could only be found at a very shallow depth (at approximately .90 m). Burials 1C, 1D, and 2C gave weak responses (Figure 69). Burials 1A and 2A give responses, but this can be considered a response to moisture in the shallow burial and control graves creating a 'false' positive. In month 19, the only responses are from burial 1C and 2B (Figure C70).

In month 20, the shallow and deep pattern of imagery from months 14 and 17 is repeated. Burials 1C and 1D, at approximately .90-1.0 m of depth, produce typical responses. Burial 2B, or more likely its grave floor, exhibits a strong response at over a meter's depth (Figures 71 & 72).

However, beginning at month 21, the graves cease to produce responses discernable in the planview representation. Save for the single exception of what could be a weak response at burial 1C (the pig buried under gravel) at month 22, data from months 21, 22, and 23 exhibits no response from any burial in either row. Even the burials with grave objects produced no discernable response. Horizontal slices were taken at approximately one meter of depth; however, there were no responses above or below this parameter (Figures 73-75).

At month 24, the final month of this research project, there is a response produced by burials 1C and 2B, the pig buried under gravel and the deep control grave, respectively (Figure 76). These responses are weak and no other burials produce a response. For a summary of the quality of horizontal slice imagery throughout the research project, see Table 7.

Table 7: Monthly imagery results for each burial scenario based on horizontal slices from the 500 MHz antenna; months 1-12 adapted from Martin (2010)

Burial Scenario								
	1A	1B	1C	1D	2A	2B	2C	2D
Month								
1	None	Excellent	Excellent	Good	None	Poor	Good	None
2	None	Good	Excellent	Poor	None	None	Good	None
3	None	None	Excellent	Good	None	None	Poor	None
4	None	Good	Excellent	Excellent	None	Good	Excellent	Excellent
5	None	Good	Excellent	Excellent	None	None	Excellent	Good
6	None	None	Excellent	Good	None	None	None	Good
7	None	None	Excellent	Good	None	None	Good	Poor
8	None	None	Excellent	Excellent	None	None	None	Poor
9	None	None	Excellent	Excellent	None	None	None	None
10	None	None	Excellent	Excellent	None	None	Good	None
11	None	None	Excellent	Excellent	None	None	None	None
12	None	None	Excellent	Poor	None	None	None	None
13	None	None	Good	Good	None	Poor	None	None
14*	None	Poor	Excellent	Excellent	None	Excellent	Good	None
15*	None	None	Excellent	Good	None	Excellent	Excellent	None
16	None	None	Excellent	Excellent	None	None	Poor	Poor
17*	None	None	Excellent	Poor	None	Excellent	None	None
18	Poor	None	Poor	Poor	None	None	Poor	None
19	None	None	Poor	None	None	Good	None	None
20*	None	None	Excellent	Poor	None	Excellent	None	None
21	None	None	None	None	None	None	None	None
22	None	None	Poor	None	None	None	None	None
23	None	None	None	None	None	None	None	None
24	None	None	Poor	None	None	Poor	None	None

DISCUSSION

The 500 MHz Antenna and Grave Detection

The 500 MHz antenna proved capable of detecting a variety of burial scenarios past a year. Until 17 months had passed, most of the grave scenarios were still returning a strong enough signal for the GPR unit to display as a hyperbola. However, around the 18 month period,

the hyperbolae for all burials began to uniformly lose their visibility, and the ability of the 500 MHz antenna to detect all graves was severely reduced. These results resemble those found by Schultz (2006, 2008). In his studies, as his research approached the 21.5-month mark, he noted that he was able to perceive dynamic changes in the visibility of burial responses. However, in the present study, the overall strength of the returning signals began to become diminished by month 18 (Figures B9 and B10); this diminished quality occurs earlier than previous studies in sandy matrices (Schultz et al 2006; Schultz 2008) and may point to differences in the detection of clandestine grave in a Spodosol environment.

The Effect of Burial Scenario on Grave Detection

A major component of this research was observing the difference in the detection of varying burial scenarios. There was a clear difference between the ability of some graves to be detected, especially by the second year of burial.

Two control holes, burials 2A and 2B, were constructed in order to test the ability of the GPR unit to detect disturbed soil of a grave without a carcass. The shallow control hole, throughout months 13 to 24, never produced a distinct response. The shaft of the deep control hole also did not produce a response; however, the floor of the deep control hole did produce a strong response throughout the research period, repeating the pattern seen in the first year of data collection (Martin 2010). These results indicate that while disturbed soil do not provide enough contrast from the surrounding soil matrix to produce a response to the GPR unit, grave features such as grave floors can provide enough contrast in the surrounding matrix to be detected. This finding is consistent with archaeological research utilizing the GPR in which archaeological

features such as the floors of pit houses were identified using GPR technology (Conyers 2006, 2010).

The two pig carcasses buried without grave objects, burials 1A and 1B, produced weak responses at the beginning of the project before resulting in a condition where no response was produced. One carcass was buried at a shallow depth of approximately .5 m, whereas the second carcass was buried at a deeper depth of approximately 1.0 m. Both graves had a very weak response in month 13, exhibiting hyperbolae that could be barely distinguished against the background noise of the research grid. The burial at 1.0 m continued to produce a weak response for the next two months. The shallow burial, burial 1A, did not produce a response to the GPR unit between months 14 and 24, either through REFLEXW or GPR-SLICE processing.

The results of the two burials without accompanying grave goods are not surprising, especially for the shallow burial. Bodies buried at .5 m are still subject to the fluctuations of temperature from the surface atmosphere (Rodriguez 1996). Therefore the shallow pig carcass burial would be expected to decompose at quicker rate than the deep pig carcass burial, especially considering the heat that is produced during Floridian summers. Most likely, the pig carcasses at both shallow and deep burials were already fairly decomposed by month 13. Previous research has indicated that burials without grave objects would be difficult to detect in sandy soils after a 21-month period (Schultz et al. 2006; Schultz 2008). It would appear that the Spodosol environment may result in reduced GPR detection within a faster time frame.

The remainder of the graves consisted of specialized burials: a carcass buried under gravel (burial 1C), a carcass buried under a layer of lime (burial 2C), one carcass wrapped in a tarpaulin before being buried (burial 1D), and the last carcass wrapped in a cotton blanket before

being buried (burial 2D). Of these specialized burials, the pig buried under gravel, burial 1C, provided the strongest and most consistent hyperbolic response. This burial provided the highest resolution of all burials involved in the research project, both in the first and second year (Martin 2010). The second highest resolution was provided by the pig carcass buried wrapped in a tarpaulin, followed by the pig carcass buried under lime, and the pig carcass wrapped in the blanket. This ranking was consistent with the findings from the first year of the research project (Martin 2010).

The pig carcass buried under gravel, burial 1C, most likely produced the best response from the GPR unit because of the dense of the nature of the gravel and its relation to the relative dielectric constant. The gravel would produce a sharp contrast in the soil that would allow it to create a response able to distinguish it from the surrounding soil (Reynolds 1996). Additionally, the gravel would neither decompose nor be shifted, which would explain why the returning signal from this grave was so consistent throughout the research year.

A similar explanation suffices for the second strongest and most consistent grave response, the response from burial 1D, the pig carcass wrapped in a tarpaulin. Due to the impermeable nature of the tarpaulin, it would neither decompose nor be moved throughout the soil, trapping the decomposing fluids. Therefore, a high relative dielectric constant would continue to exist for the carcass, making it easily discernable from the surrounding soil, past the time frame when remains would normally be integrated in the surrounding soil matrix.

The remaining two specialized graves featured grave objects had a lower resolution throughout months 13-24. In the case of burial 1C, the carcass was buried under a layer of lime, a soil form of pulverized limestone in which the primary composition consists of calcium

carbonate. In the case of burial 1D, the carcass was wrapped in a cotton blanket. It is conceivable that these two grave objects would be more likely to decompose in the soil, since the addition of water would help break either substance down. This would create a lower relative dielectric constant, or reduced contrast, between both graves and the surrounding soil, thus creating a weaker returning signal for the GPR to pick upon (Reynolds 1996).

The Effect of Interment Time on Grave Detection

Overall, there is a direct relationship between the passage of time and the rate at which the retuning signal strength of the burial scenarios is reduced. From month 13 to month 24, the returning signal strength of all burials is greatly weakened. At month 13, all four burials in Row 1 can be discerned; in Row 2, only two burials, burial 2B (the deep pig carcass grave) and burial 2D (the pig carcass wrapped in a cotton blanket), can be discerned. When considering the data taken from months 1-12, this represents a marked reduction of signal strength. For example, when comparing the reflection profiles of month 6 to month 18, the resolution of the graves in month 18 have a marked lower resolution as compared to month 6 when all four graves from Row 1 created strong hyperbolae (Martin 2010; see also Figure 14). The condition of the signals is only exacerbated by the end of the research period, when all burials produce intermittent weak responses, at best.

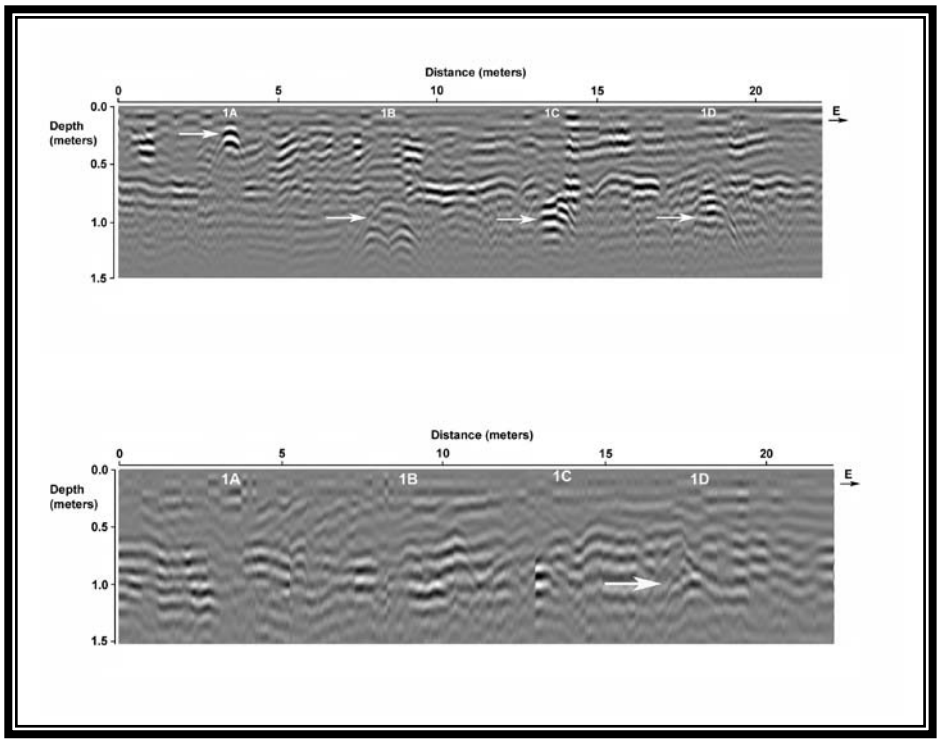

Figure 14: Comparison between Month 6 (superior) and Month 18 (inferior) (Month 6 adapted from Martin 2010)

Data obtained from horizontal slices confirm this relationship between time of interment and signal quality; the horizontal slice at month 13 contains very clear returning signals from burials 1C (the pig carcass buried under gravel) and 1D (the pig carcass wrapped in a tarpaulin) as well as a faint signal from burial 2B (the deep pig carcass burial). By month 24, the responses from burial 1C and 2B are extremely faint after little to no response in the previous months (see Appendix C).

The data clearly shows that as time progresses, the ability of clandestine graves to be detected by a GPR unit is reduced. This finding was not unforeseen, however. As previously stated, the strength of a returning EM signal to the GPR unit is based upon the relative dielectric constant; the relative dielectric constant, in turn, is based upon material composition and the level of moisture implicit in the buried material (Reynolds 1997). Bodies buried at a depth

greater than a meter experience complete skeletonization at 2 to 3 years, with minimal tissue loss in the first year (Rodriguez 1996). This process can be increased with fluctuating temperatures and higher moisture levels in the ground. The soil at the research site had clayey components consistent with a water-saturated soil (Martin 2010).

Additionally, it has been documented that tissue preservation in soils in subtropic regions, such as Florida, is extremely poor and the process of skeletonization is amplified (Manhein 1996). Therefore, it is unsurprising to find that detection of clandestine graves by a GPR unit were difficult to detect at the two year benchmark in a Spodosol setting in Florida, as the pig carcasses were likely decomposed. With the tissues decomposed, the relative dielectric constant of the graves will be greatly decreased overall, resulting in poorer returning signals (Doolittle and Bellatoni 2010). As the process of skeletonization continues and the grave shaft becomes more compact (and, in turn, more similar to the surrounding soil), the likelihood of detection of a grave by GPR will decrease to an infinitesimal point.

The Effect of Moisture on Grave Detection

Soil moisture readings were collected throughout the research period, culminating in the series of data presented in Appendix F. It had become apparent that grave resolution strength did not decrease in a consistent, linear degradation. For example, the returning signal for burial 1C, the pig carcass buried under gravel and the most consistent of grave responses, elicited a very low, practically indistinguishable, response in month 18. However, the next month, month 19, saw the returning signal strength back to a level of quality seen in months 13 through 15.

When data from the available soil moisture readings is utilized, there is evidence that this change in signal strength may be due to moisture in the soil. For month 18, the readings for

moisture using the soil moisture meter were ‘0’ at all depths (Table 23). Conversely, month 19 saw an increase in soil moisture; with readings of ‘3’ and ‘4’ on a ten point scale (Table 25). Though this signifies low to middle moisture levels, it is nonetheless a significant increase from the previous month’s complete lack of moisture.

This pattern seems relevant throughout the research period. For example, month 20 shows a much stronger response from burial 1C, whereas in month 21 no response from this burial could be discerned. When looking at the soil moisture level record, month 20 shows a moisture level of 2 at the all three depths for burial 1C (Table 27). In month 21, the moisture level at all three depths is 1 (Table 28). Though it is slight, it is a decrease in moisture that may signify the importance of moisture level to grave detection. Additionally, the soil moisture level was much higher through all the burials in month 20 than in month 21, indicating wetter soil for the former.

An increase in soil moisture appears to ‘sharpen’ the grave signals. This runs counter-intuitive to a GPR technician’s theoretical understanding. Water has one of the highest signal attenuation rates as well as dielectric constants (Conyers 2004). It is known to absorb or reflect the EM radiation to such an extent as to render it unreadable to the GPR unit; however, it is also known that the greatest variable responsible for the response of a buried object to the GPR’s EM radiation is the materials relative dielectric constant (Reynolds 1997). It is probable then that there is an increased strength in returning signal is due to an increase in relative dielectric constant due to the increased soil moisture level; however, this increase in moisture is not significant enough to cause an increase in wave attenuation. If the soil became oversaturated with water, there is little doubt that the EM signal would not reach the grave due to signal

attenuation. The moisture level is just enough to increase the contrast of the graves to the surrounding soil without increasing wave attenuation. Dry bones have been found to be to electrically similar to dry soil (Davis et al. 2000). If skeletonization has occurred in the carcasses, water may temporarily cause the remains to become electrically dissimilar from the surrounding soil

Soil

Although this research was conducted in the same Florida climate as Schultz's research (2006, 2008), the soil matrix in this research was composed of a Smyrna pomello soil with a spodic horizon (Doolittle and Schellentrager 1989; Leighty 1989). The spodic horizon is significant due to the high density of acidic resins that help compose the layer. These acidic resins can travel down the soil horizons with the help of moisture. Six of the eight burials were buried at a meter's depth, below this spodic horizon. In the reflection profiles, this layer can be seen as a series of thick bands (see Appendix B).

During the first year of data collection, the burials interred at a meter's depth could be clearly discerned, despite any masking effect from the spodic horizon (Martin 2010). It is likely then that a clandestine grave in the spodic horizon will have an increased signal reduction rate than in comparison to sandy soils. However, clandestine graves buried in this layer may be detected during the first year of interment and even through the second year of interment.

CONCLUSION

The applicability of the 500-MHz antenna in clandestine grave detection was tested using the controlled research guidelines outline previously in the chapter. The findings of this research point to limitations in the use of the GPR unit. Specifically, there appears to be a natural time constraint to the ability of clandestine graves to be detected. First, the shallow control hole gave no response whatsoever throughout the research project. The deep control grave, however, gave a response at the presumed grave floor that was consistent throughout the research process. The pig carcasses buried without grave objects gave no consistent response whatsoever. Skeletonization of bodies buried at around one meter is thought to be completed between the second or third years of interment, even less if shallower. It is likely therefore that the pig carcasses interred in the research grid are skeletonized or nearly so. Of the carcasses buried with grave object, burial 1C (the pig carcass buried under gravel) gave the most consistent response, followed by burial 1D (the pig carcass wrapped in a tarpaulin), burial 2C (the pig buried under lime), and burial 2D (the pig carcass wrapped in a cotton blanket).

Ultimately, however, all responses become indistinguishable from the background noise by at least month 22, indicating that no matter the burial scenario, there are certain time constraints as to when the grave and the surrounding soil become indistinguishable from one another. Though there were strong indications that moisture level increased the ability of returning signals to be discerned, this phenomenon, too, was limited by the time of interment. Nevertheless, the more distinct a grave is from the surrounding soil (i.e. the pig carcass buried under gravel versus the deep pig carcass burial without grave objects) the greater its relative

dielectric constant and the more likely it will be able to produce a strong signal for the GPR equipment to read.

REFLEXW proved to be the better processing tool as all graves detected by SLICE were detected by in reflection profiles; more importantly, several other graves that were not detectable in horizontal slices were discerned in reflection profiles. It was also easier to discern the different depths of the burial through a reflection profile, while it may be possible to miss a burial if the GPR technician does not go deep enough into the SLICE program's 3D cube. However, a combination of both imagery techniques produced the greatest understanding and conceptualization of the data.

Though these limitations present a significant challenge to the applicability of the 500 MHz antenna to detect clandestine graves through a GPR unit, it must still be noted that complete signal loss was not reached until the very end of the two year interment period for all graves. The GPR equipment utilizing a 500 MHz antenna still remains a worthwhile tool to employ in the search for clandestine graves.

CHAPTER FOUR: THE DETECTION OF VARIOUS BURIAL SCENARIOS USING A GPR UNIT WITH A 250 MHZ ANTENNA

INTRODUCTION

Ground-penetrating radar (GPR), a non-invasive remote sensing tool, has been used successfully by law enforcement agencies to detect clandestine grave (Davenport 2001; Dupras et al 2006; Ruffell 2005; Schultz 2007). This technology allows law enforcement to search prospective scenes without destroying potential evidence; it also allows agencies to operate at peak efficiency in their searches by displaying results in real-time, thus enabling areas to be cleared or marked for further invasive search. Numerous examples exist within the available literature exhibiting the use of GPR technology in the search for clandestine graves (Calkin et al. 1996; Davenport 2001; Mellett 1992; Nobes 2000; Ruffel 2009; Schultz 2007).

Most of the available literature consists of case reports that exhibit the effectiveness of the utilization of GPR in the field; however, a better understanding of the technology's potential and its limitations can be achieved through controlled research. Specifically, controlled research utilizing a 250 MHz antenna with additional GPR equipment is needed as there has been only one instance of the use of a lower frequency emission antenna in a controlled research setting in a study by Powell (2004), where a 200 MHz antenna was assessed in the ability to locate shallow graves containing various remains of kangaroo, pig, and human origin. However, this study was conducted in Australia, in environmental conditions unlikely to be repeated in most of the continental United States. Only in a single forensic case by Nobes (2000) is there an example of a lower frequency emission antenna such as the 250 MHz antenna being utilized in a forensic context. By operating the GPR equipment over a research area containing gravesites of pig

carcasses, used as human cadaver proxies, the applicability of the technology, with the 250 MHz antenna, can be tested.

Previous studies have already documented the general changes in GPR grave detection based on differences in body size, specifically envisioning an adult versus juvenile burial (Schultz et al. 2006; Schultz 2008; Strongman 1991). Other studies have observed the ability of GPR detection at shallow burial depths, comprising less than a meter (Freeland et al 2003; Roark et al. 1998; Schultz et al. 2006; Schultz 2008); others investigate its use at depths a meter or greater (Schultz et al. 2006; Schultz 2008). The effect of soil type has also been investigated where clayey, water-saturated soil have proven to result in GPR wave attenuation (Freeland et al .2003) while sandy soils have proven to be excellent facilitators of wave propagation due to the high relative dielectric soil between the buried material and surrounding soil matrix (Schultz et al. 2006; Schultz 2008).

The next phase in GPR research is to conduct a controlled study testing the long-term applicability of GPR by monitoring each consecutive month for a period of two years or more. While Strongman (1992) investigated the applicability of the GPR after a 5 year period, he did not employ sequential monitoring in his research project. When Schultz (2006, 2008) employed sequential monitoring, he did so for a period up to 21.5 months only, noting significant decreases in hyperbola resolution strength at the end of his research (Schultz et al. 2006; Schultz 2008). Therefore, further research in the effect of time interment on grave detection is needed, as well as research that addresses the differences in the detection of grave scenarios based on real-life forensic situations.

Purpose

Controlled research must be broadened to include new variables to create a more comprehensive understanding of the applicability of GPR, especially the use of lower frequency emission antennae such as the 250 MHz antenna. This research does so by having a threefold purpose: first, to determine the ability of the 250-MHz to detect clandestine graves that resemble real-life forensic scenarios; second, to grade each burial scenario throughout the research process based on response strength; and finally, to observe the ability of the GPR unit to detect the graves at the end of the two-year research period and thus the long-term applicability of GPR in detecting clandestine graves. This research comprises the second year of a two-year project. The first year's research, months 1 through 12, was conducted by Mike Martin (2010); the second year's research is the aim of this thesis and comprises months 13 through 24.

MATERIALS AND METHODS

Field Site and Controlled Graves

The field site which will host this controlled research project is located on the University of Central Florida's (UCF's) main campus property, in UCF's Arboretum. Specifically, the field site lies within property maintained by the Civil Engineering division of UCF's College of Engineering and Computer Science, referred to as the Geotechnical Engineering Test Site (Figure 15). It is a secure field site, fenced in with a locked gate. A small portion of this field was be mowed and maintained in order to create a permanent grid of 11 m by 22 m. Permanent non-

metal markers were placed at the corners of the grid so the exact position of the survey transects could be duplicated each time geophysical data was collected.

Figure 15: The Geotechincal Engineering Test Site

A total of eight graves were monitored. Six pig carcasses were buried at regular intervals throughout the grid as well as two control holes (Figure 17). It was important to include these control holes in order to test the response of GPR to the disturbed soil, to see if GPR picked up on the buried component (the human remains or pig proxies) or the disturbed soil. The pig carcasses were euthanized and buried previously in January of 2009 after sustaining headshots with a .22 caliber handgun. As established by Martin (2010), the six pig graves contain the following scenarios (in addition, see Table 8):

1. A blank control grave consisting of only disturbed backfill (50-60 cm) to determine the geophysical response to disturbed soil only.
2. A blank control grave consisting of only disturbed backfill (100-110 cm) to determine the geophysical response to disturbed soil only.
3. A pig carcass buried without additional grave objects at .5 m depth.
4. A pig carcass buried without additional grave objects at 1 m depth.
5. A pig carcass wrapped in a vinyl tarpaulin and buried at 1 m depth.
6. A pig carcass wrapped in a cotton blanket and buried at 1 m depth.
7. A pig carcass buried underneath a layer of lime (calcium hydroxide) at 1 m. depth
8. A pig carcass buried underneath a layer of rocks at 1 m depth.

Table 8: Detailed Grave Information for Each of the Burials (From Martin 2010)

Grid Location	**Burial Date**	**Depth of Unit**	**Scenario**	**Weight of Pig (lbs)**	**Sex of Pig**
1A	1/30/2009	0.5 m	Shallow pig grave	90	Female
1B	1/30/2009	1.0 m	Deep pig grave	100	Male
1C	1/30/2009	1.0 m	Deep grave with layer of rocks covering pig	90	Male
1D	1/30/2009	1.0 m	Deep grave with pig wrapped in tarpaulin	98	Female
2A	1/26/2009	0.5 m	Shallow control hole	N/A	N/A
2B	1/30/2009	1.0 m	Deep control hole	N/A	N/A
2C	1/30/2009	1.0 m	Deep grave with layer of lime covering pig	95	Male
2D	1/30/2009	1.0 m	Deep grave with pig wrapped in blanket	97	Female
Calibration Unit (outside grid)	1/9/2009	1.0 m	Rebar hole	N/A	N/A

The pig carcasses were laid into the grave pit on their right sides, with their heads towards the north wall and their back against the east wall. Three body locations were measured

from the surface of the grave pit for precise measurements: the head, the abdomen, and the tail (See Table 9; see also Martin 2010).

Table 9: Precise Burial Measurements of Pig Carcasses (From Martin 2010)

Grave Location	Measurement to Head	Measurement to Abdomen	Measurement to Tail
1A	0.33 m	0.24 m	0.26 m
1B	0.86 m	0.76 m	0.77 m
1C*	0.83 m	0.75 m	0.77 m
1D	0.74 m	0.74 m	0.75 m
2C	0.83 m	0.76 m	0.78 m
2D	0.80 m	0.74 m	0.76 m

**Note: layer of rocks added over pig carcass comprising an additional .70 m*

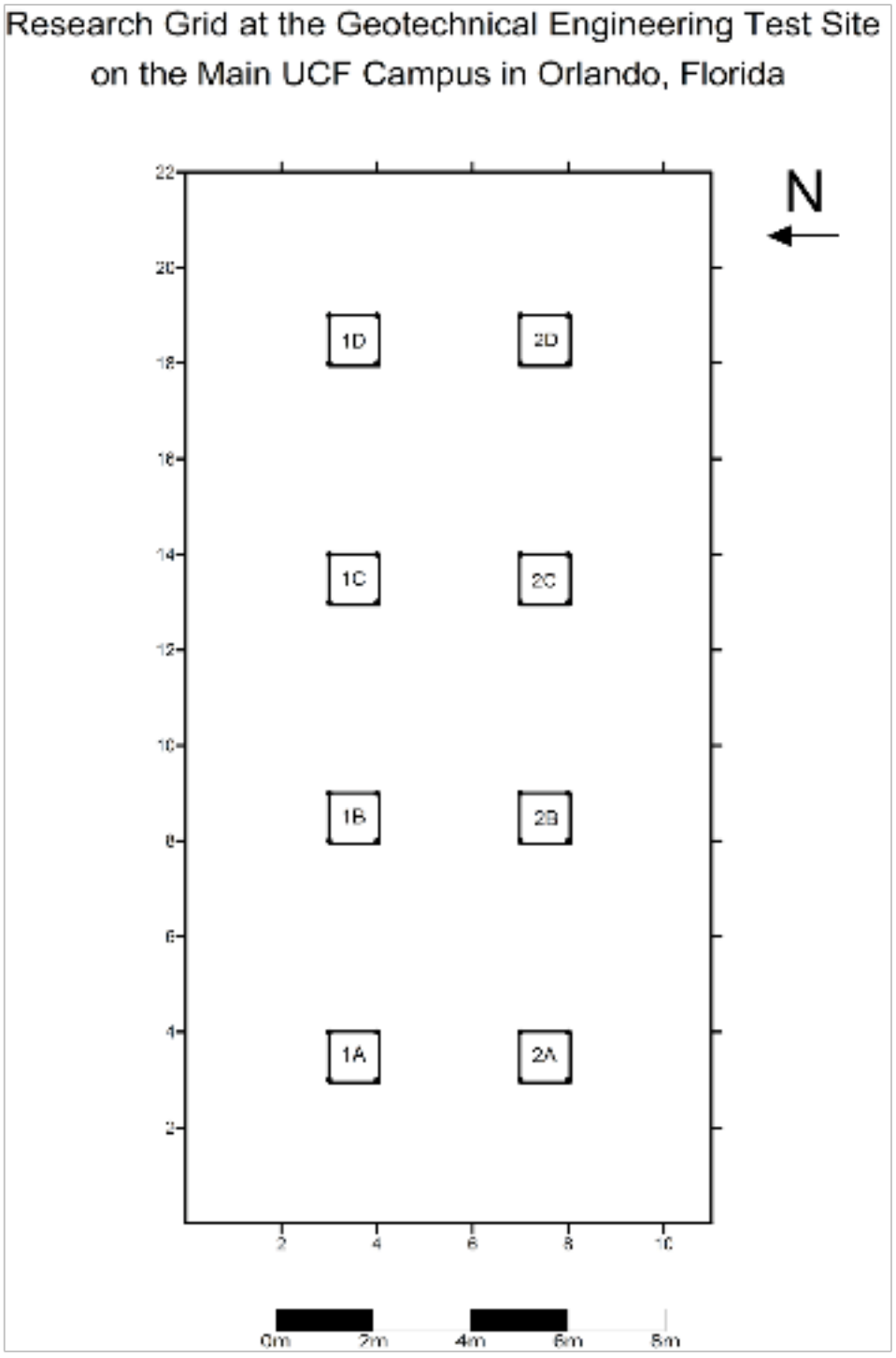

Figure 16: Research Site Grid with Established Burials (From Martin 2010)

GPR Equipment

All GPR equipment is composed of three main parts: the antenna (which both transmits and receives electromagnetic waves), the computer control, and the monitor which displays results in real time (Schultz 2007). The GPR unit generates radar waves, "a form of electromagnetic energy" (Conyers 2004:23), to probe the surface. These waves will travel infinitely unless they are absorbed or conducted away in some way (Conyers 2004). When the electromagnetic strikes an object in the subsurface, a resulting reflected wave will occur that will be received by the receiving portion of the dipole antenna. However, the amplitude of the returning wave- that is, the strength of the returning signal-is directly dependent on the measure of the dielectric constant, the contrast between any two materials (Ruffel 2005; Schultz 2007).

The antenna frequency number reflects the frequency at which its radar waves are generated by the antenna (Reynolds 1997). Antenna frequency emissions range from 10 MHz to 1.5 GHz (Watters and Hunter 2004). The choice of antenna frequency has a direct relationship with GPR detection of clandestine graves at various depths. In short, the lower the frequency the deeper the GPR will be able to read. Conversely, the higher the frequency the more precise and detailed the GPR results will be. For example, a 120 MHz antenna may display results up to 50 meters deep, while a 900 MHz antenna can only display results less than a meter deep but with a much better resolution (Schultz 2007). Therefore, a happy medium is often sought after and is often found in a 400-500 MHz antenna (Dupras et al. 2006; Schultz 2007). However, a 250 MHz antenna was utilized in the present thesis in order to test its applicability in the detection of clandestine graves.

Data Collection

Grid data collection was performed twice a month for a twelve month monitoring period a using a Mala RAMAC X3M GPR unit, with a 500 MHz antenna, manufactured by Mala Geonics. Data was collected using transect interval spacings of .25 cm in both an east-west direction and a north-south direction (see Figures 3 and 4). Per recommendations by Pomfret (2006), this research collected transects in two directions as this methodology provides maximum detection and resolution of small subsurface features.

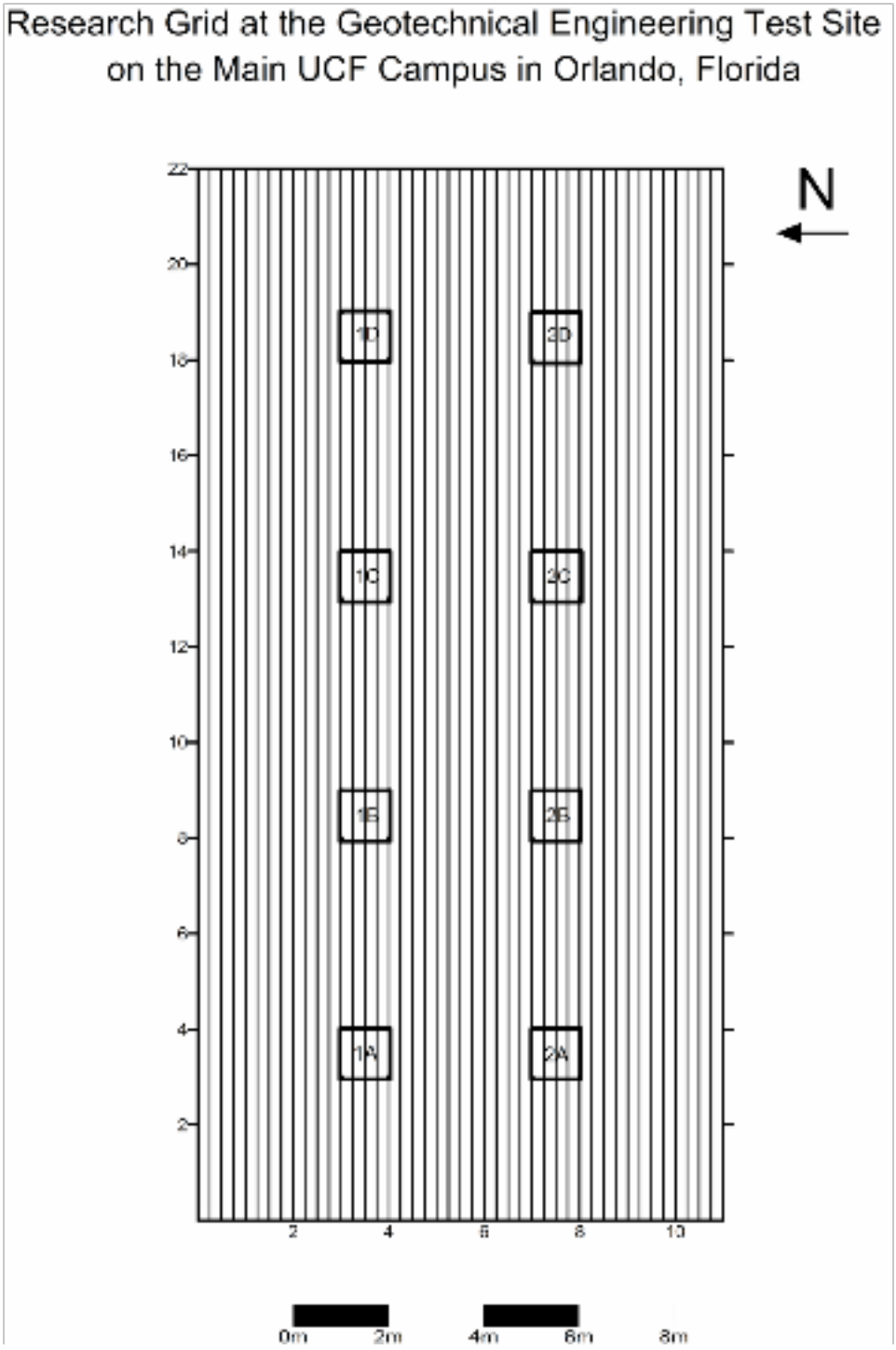

Figure 17: Research Site Grid West-East Transects (From Martin 2010)

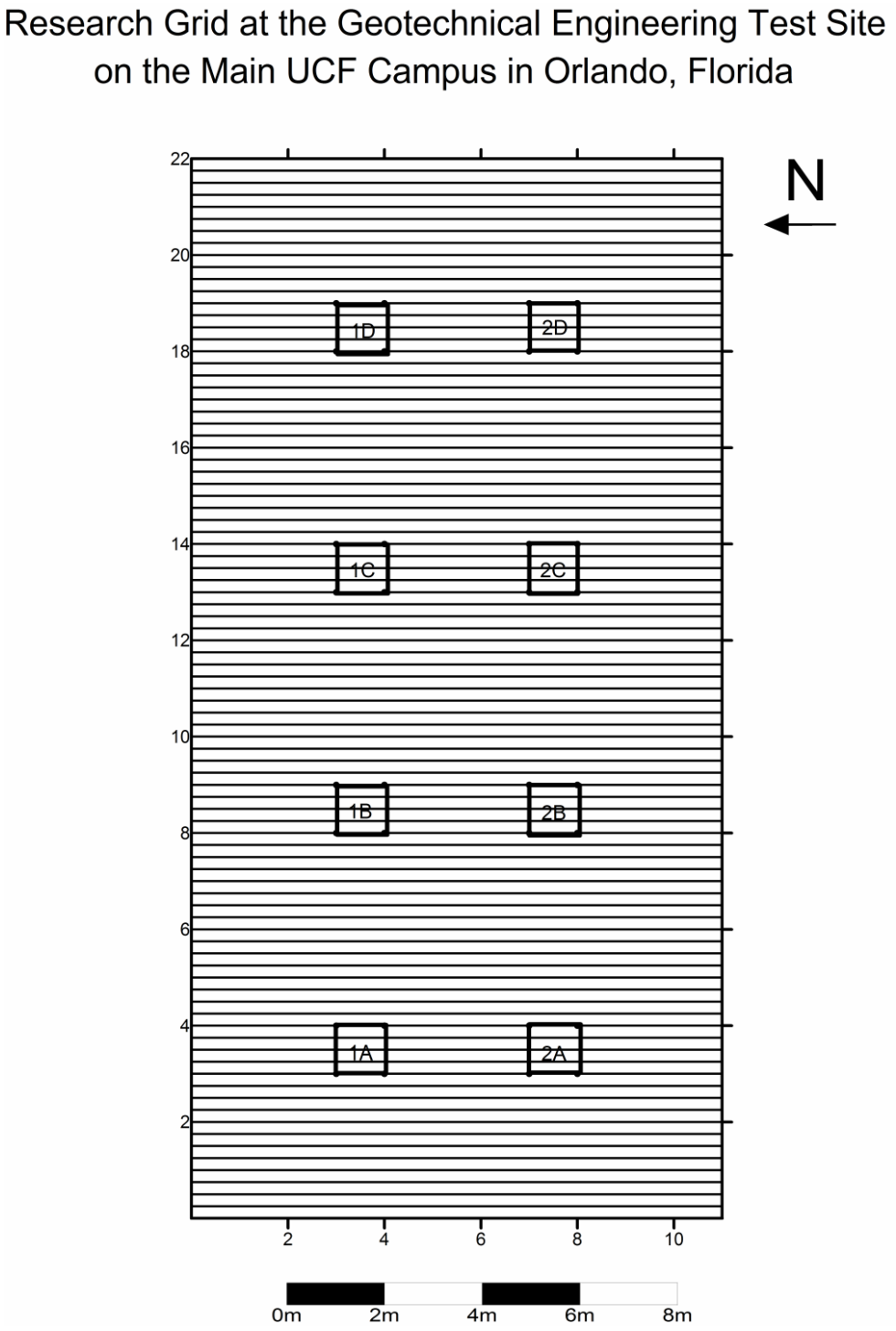

Figure 18: Research Site Grid with North-South Transects (From Martin 2010)

On data collection days, soil moisture values within the graves were noted using a soil moisture meter manufactured by Lincoln Irrigation Incorporation. The probe on the soil moisture meter measures 90 cm in length, and moisture values were recorded on a scale of 1 to 10, with 10 being the wettest. Per protocols developed by Martin (2010), the soil moisture meter was calibrated to 10 using tap water. The soil moisture data was used to determine the relationship between moisture and grave detection. Per Martin (2010), soil moisture was collected at the following locations: each corner of the research grid, one point on both the west and east baselines, three points on both the north and south baselines, the northwest corner of the rebar hole, and each of the northwest corners of the burials within the grid. Two soil moisture measurements were collected for shallow burials (25 and 50 cm) and three measurements for deep burials (24, 50, and 90 cm).

Additionally, the GPR unit was calibrated for accurate depth measurements that may be affected by daily soil moisture. A buried object at a specific depth is used for calibration to determine the sensitivity of the instrument and can allow wave velocity, and thus depth, to be more accurately calculated within the soil (Conyers and Cameron 1998; Conyers 2004; Strongman 1992; Martin 2010). Prior to data collection, the GPR unit was calibrated a metal bar that was pounded into the ground at a1 m depth, a method suggested by Conyers (2004). The calibration test unit was located 2 m away from the east end of the grid.

Data Processing

The final phase of this research was the processing of the data gathered in the field. Processing GPR data using 2-D or 3-D analysis may increase the likelihood of spotting anomalies in the subsurface, a hypothesis that was tested with this research. Two programs were

used: REFLEXW and GPR-SLICE. REFLEXW was used to process raw reflection profiles, a type of data display that presents the data in two dimensions, depth and distance (covered by the GPR's survey wheel). GPR-SLICE, on the other hand, has the ability to put all transects gathered in the X and Y planes and weld them together, creating what is called a horizontal slice or Z-slice. This type of display is three dimensional in nature and shows the entire scanned grid, as opposed to a single profile.

RESULTS

Reflection Profiles

The two rows in the east-west transect that intersected the graves (Row 1 and Row 2), were each comprised of five profiles of 0.25 m transect spacing and were used as points of reference in the analysis of the data. For example, Profile 1 (Figure 19) represents the north side of the burial pit and Profile 5 (Figure 23) represents the south side of the burial pit. The middlemost profile, Profile 3 (Figure 21), represents the transect that ran over the approximate center of the grave.

The middlemost profile represented the greatest quality in returning signals. In Profile 2 (Figure 20), the three burials interred at 1.0 m depth are evident; however, there is no hyperbola for burial 1A, whereas in Profile 3 (Figure 21) there is a discernable hyperbola for the shallow burial. In Profile 4, all graves are similarly present; however, the hyperbola for burial 1A is warped. Therefore, the third reflection profile, the middlemost, provides the highest quality and was utilized throughout the research project. This form of analysis follows guidelines established

by Martin (2010) in the first year of research. The reflection profiles for the data collection period following month 13 (months 14-24) are located in Appendix D.

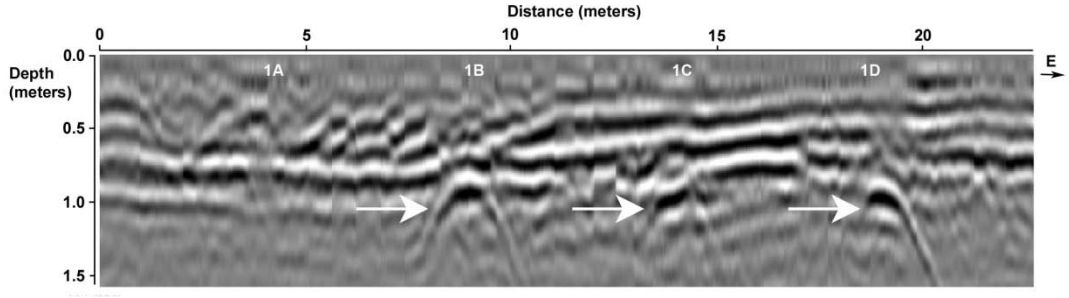

Figure 19: Profile 1 of Row 1 at 13 Months

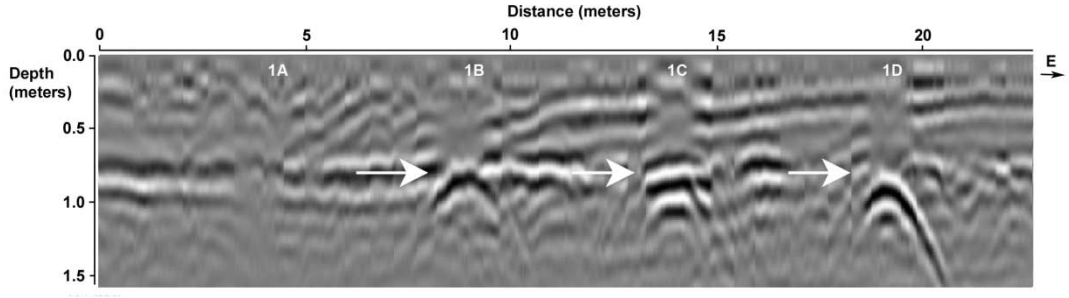

Figure 20: Profile 2 of Row 1 at 13 Months

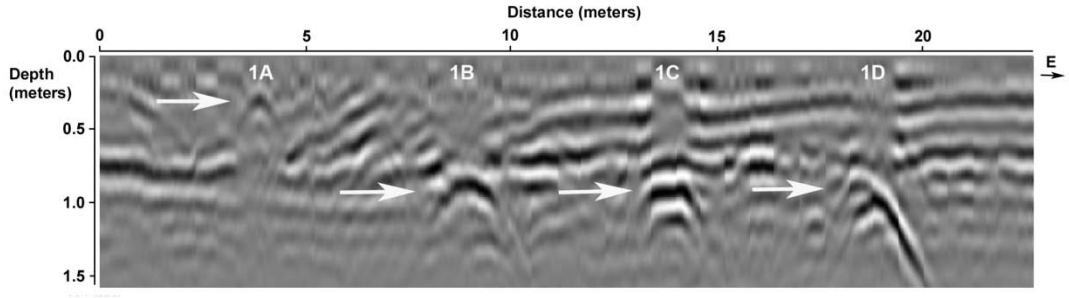

Figure 21: Profile 3 of Row 1 at 13 Months

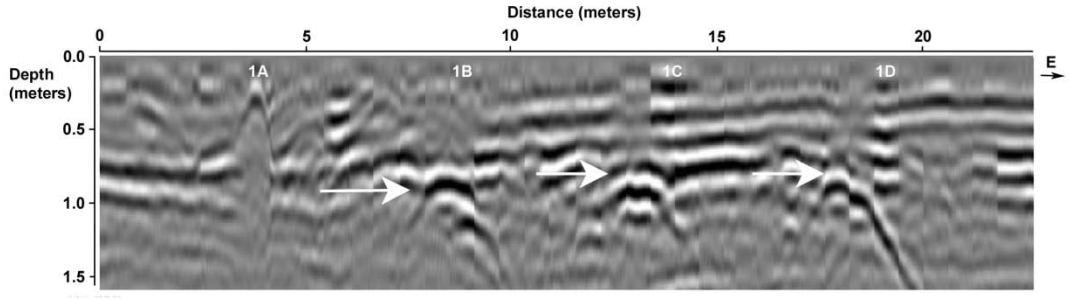

Figure 22: Profile 4 of Row 1 at 13 Months

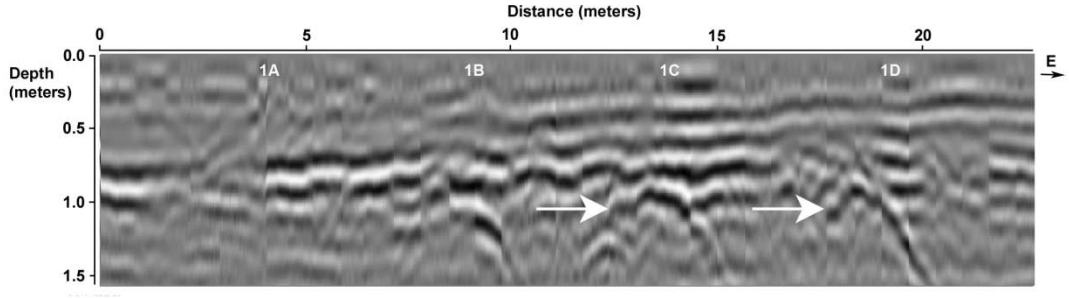

Figure 23: Profile 5 of Row 1 at 13 Months

Month 14 features three easily discernable hyperbolae in burials 1B through 1D in Row 1; the grave shaft of burial 1A produces an extremely weak response (Figure 79). In Row 2, responses can be easily discerned for burials 2B through 2D. There is a column of weak interference that might indicate the shaft of burial 2A (Figure 80). In month 15 this pattern is repeated precisely (Figures 81-82).

In month 16, all discernable hyperbolae suffer a reduction in resolution. Only the hyperbolae of burials 1C and 1D (the pig carcass buried under gravel and the pig carcass wrapped in a tarpaulin, respectively) can be discerned in Row 1 (Figure 83). In Row 2, the pattern from the previous month holds, with burials 2B, 2C, and 2D offering discernable hyperbola, but the resolution is reduced (Figure 84). This reduction in resolution quality is increased in month 17. Burials 1A and 1B (the shallow and deep standard burials, respectively) cannot be discerned; burials 1C and 1D are barely discernable (Figure 85). In the second row, burials 2B, 2C, and 2D (the deep control hole, the pig carcass buried under a layer of lime, and the pig carcass wrapped in a cotton blanket, respectively) produce a very weak response (Figure 86).

The data from month 18 shows very weak responses from both rows. Burials 1A and 2A do not produce a response; the hyperbolae from burials 1C and 1D have a poor resolution (Figure 87). Burials 2A and 2B do not produce a discernable response: the hyperbolae from burials 2C and 2D produce are barely discernable (Figure 88).

At month 19, however, the resolution of the responses for all burials increases substantially. A discernable hyperbola is produced by all four burial scenarios in Row 1, with the hyperbola for burial 1A occurring at a much shallower level than for the other burials of Row 1

(Figure 89). In Row 2, discernable hyperbolae are created for burials 2C and 2D, with a weaker response from burial 2B, though burial 2A (the shallow control grave) still does not produce a response (Figure 90).

At month 20, the hyperbolae for both burial 1B and 2B have diminished in resolution. There is no discernable response from burials 1A and 2A. The remaining burials, the burials with grave goods, feature distinct, discernable hyperbolae (Figures 91 & 92).

In month 21, all burial responses again show a decline in resolution. There is only one discernable hyperbola, from burial 2C, the pig carcass buried under a layer of lime (Figures 93 & 94). Yet, in month 22, the pattern from month 20 repeats itself as though uninterrupted. There are distinct hyperbolae for burials 1C, 1D, 2C, and 2D, with a weak response from 1B and no responses from burials 1A, 2A, and 2B (Figures 95 & 96). In month 23, responses from burials 1C and 1D are barely discernable, as are the response from burials 2B and 2C in Row 2 (Figures 97 & 98). No other grave is detected.

In the final month, month 24, burial 1A (the shallow pig carcass burial without grave objects) produces a weak response while there is no response from burial 1B. Burial 1C also produces a weak response, while burial 1D (the pig carcass wrapped in a tarpaulin) produces a stronger response, though still poor in resolution (Figure 99). In Row 2, burial 2A produces no response. Burials 2B, 2C, and 2D all produce similar weakened responses to the GPR unit (Figure 100). A summary of all recorded responses throughout the 12-month process is found below in Table 10.

Table 10: Monthly imagery results for each burial scenario based on reflection profiles from the 250 MHz antenna; months 1-12 adapted from Martin (2010)

Burial Scenario								
	1A	1B	1C	1D	2A	2B	2C	2D
Month								
1	Good	Poor	Good	Good	None	Good	Good	Poor
2	Good	Good	Good	None	None	Good	Good	None
3	Poor	Poor	Poor	Poor	None	None	Good	None
4	Excellent	Excellent	Excellent	Excellent	None	Good	Excellent	Excellent
5	Excellent	Excellent	Excellent	Excellent	None	Good	Excellent	Excellent
6	Excellent	Excellent	Excellent	Excellent	None	Good	Excellent	Excellent
7	Excellent	Excellent	Excellent	Excellent	None	Good	Excellent	Excellent
8	Excellent	Excellent	Excellent	Excellent	None	Good	Excellent	Excellent
9	Good	Good	Excellent	Excellent	None	Good	Good	Excellent
10	None	Poor	Excellent	Excellent	None	Excellent	Excellent	Excellent
11	Poor	None	Excellent	Excellent	None	Excellent	Good	Excellent
12	Poor	None	Excellent	Good	None	Good	None	Poor
13	Good	Excellent	Excellent	Excellent	None	Good	Good	Excellent
14	Poor	Excellent	Excellent	Excellent	None	Poor	Poor	Good
15	None	Good	Excellent	Excellent	None	Poor	Poor	Good
16	None	None	Good	Poor	None	Good	Good	Good
17	None	None	Poor	Poor	None	Poor	None	Poor
18	None	None	Poor	Good	None	Poor	Poor	Good
19	Good	Poor	Good	Good	None	Poor	Poor	Good
20	None	Poor	Poor	Good	None	Poor	Good	Good
21	None	None	None	None	None	None	Good	Poor
22	None	Poor	Good	Good	None	None	Excellent	Poor
23	None	None	Poor	None	None	Poor	Good	None
24	Poor	None	Poor	Good	None	Good	Poor	Good

Horizontal Slices

All imagery for horizontal slice data can be found in Appendix E. At the start of the research, at month 13, there are five responses indicative of the burials. These responses occur at burials 1C, 1D, 2B, 2C, and 2D, at approximately 1.0 m in depth (Figure 101). All horizontal

slices were taken at approximately 1 m in depth unless otherwise indicated. At month 14, at the same depth, these signal responses are joined by a response from burial 1B (Figure 102).

At month 15, there is no response from burial 2C and the response from burial 1B is extremely faint. Burials 1C, 1D, and 2D are still easily discernable (Figure 103). At month 16, only these three burials produce a response: burials 1C, 1D, and 2D (Figure 104).

Month 17 exhibits a strong response from burial 2B. Burials 1C and 1D still produce a response; however, the response from burial 1D is extremely faint (Figure 105). Month 18 sees a return to the pattern at month 16, with burials 1C, 1D, and 2D producing discernable responses, and no other burials producing a response (Figure 106).

Month 19 sees a return in response strength in both rows. All burials save burials 1A and 2A produce a strong response that can be easily discerned, occurring slightly below 1.0 m (Figure 107). However, by month 20, this anomalous pattern has disappeared. Again, burials 1C, 1D, and 2D are the only burials producing any responses (Figure 1088).

By month 21, no active responses can be discerned (Figures 109). This continues in months 22 and 23 (Figures 110 & 111). At month 24, however, there are discernable response from any burial scenario, including burials 1C, 1D, 2C, and 2D (Figure 112). For a summary of the quality of the horizontal slice imagery throughout the research project, see Table 11.

Table 11: Monthly Imagery results for each burial scenario based on horizontal slices for the 250 MHz antenna; months 1-12 adapted from Martin (2010)

Burial Scenario								
	1A	1B	1C	1D	2A	2B	2C	2D
Month								
1	None	Poor	Good	Good	None	None	Good	Poor
2	Good	Good	Excellent	Poor	None	Poor	Poor	Poor
3	Good	Good	Good	Good	Poor	Poor	Poor	Good
4	None	Excellent	Excellent	Excellent	None	None	Excellent	Excellent
5	None	Good	Good	Good	None	None	Good	Good
6	None	Excellent	Excellent	Excellent	None	None	Excellent	Excellent
7	None	Excellent	Excellent	Excellent	None	None	Excellent	Excellent
8	None	Good	Excellent	Excellent	None	None	Excellent	Excellent
9	None	None	Excellent	Excellent	None	None	None	Poor
10	None	None	Excellent	Excellent	None	None	None	Poor
11	None	None	Good	Poor	None	Good	None	Poor
12	None	None	Good	Poor	None	None	None	Poor
13	None	None	Excellent	Excellent	None	Good	Poor	Excellent
14	None	Excellent	Excellent	Good	None	Good	Good	Good
15	None	Poor	Excellent	Excellent	None	Excellent	None	Good
16	None	None	Good	Poor	None	None	None	Poor
17	None	None	Poor	Poor	None	Excellent	None	Poor
18	None	None	Poor	Poor	None	None	None	Poor
19	None	Poor	Excellent	Poor	None	Good	None	Poor
20	None	None	Poor	Poor	None	None	None	Poor
21	None	None	None	None	None	None	None	None
22	None	None	None	None	None	None	None	None
23	None	None	None	None	None	None	None	None
24	None	None	Poor	Poor	None	None	None	Poor

DISCUSSION

The 250 MHz Antenna and Grave Detection

The 250 MHz antenna proved adept at detecting clandestine graves. However, patterns were identified concerning the resolution of the hyperbolae that the burials produced. Generally, there was a reduction of resolution strength as the time of interment increased. The burials with grave objects still produced a discernable response at the end of the two-year period while the

burials without grave objects and control graves did not. Additionally, a pattern was perceived based on the amount of moisture in the soil. If the soil moisture was increased, the ability of the burials to be discerned was strengthened. The ability of the 250 MHz antenna to detect clandestine graves has been underreported in the literature and therefore a careful analysis of the variables that may affect its ability to detect clandestine graves is overdue.

The Effect of Burial Scenario on Grave Detection

Different burial scenarios produced different responses, causing some burials to be easily detected and others to produce no responses whatsoever. Each burial scenario was analyzed as to its ability to be detected by the GPR unit.

Burials 2A and 2B, the two control holes constructed at .5 m and 1.0 m respectively, were designed to test the ability of disturbed soil, without any carcass or body, to respond to the GPR unit. From month 13 to month 24, the shallow control grave never produced a discernable response. The grave floor of burial 2B could be detected; however, the grave shaft produced no response. Burial 2B could be discerned from months 13-20 and months 23-24, proving to produce as consistent a response as it did during the first year of research (Martin 2010). The results indicate that grave features such as grave floors provide enough contrast from the surrounding soil matrix to produce a discernable response, though simple undisturbed soil will not. This finding is consistent with GPR work in archaeological contexts wherein the GPR equipment can detect the floors of pit houses and other archaeological features (Conyers 2006, 2010).

Burials 1A and 1B represented burials without grave objects. The pig carcass of burial 1A was buried at 0.5 m of depth to simulate a shallow grave; the carcass of burial 1B was buried

at 1.0 m to simulate a deep grave. From month 13 to month 15 these two graves produced discernable hyperbolae; however, from month 16 to 18, they produced no discernable response whatsoever. There was a brief return in hyperbola resolution strength at month 19, followed by a period of no discernable response from months 21-23, and discernable response produced again at month 24. Even when hyperbolae were produced, they were often weak in strength especially as the second year of research continued.

The poor resolution strength of the burials without grave objects is likely due to increased decomposition. The pig carcasses of the standard burials were probably near completion of skeletonization by the middle of the second year based on common decomposition rates (Rodriguez 1996). Furthermore, being interred in a subtropic climate may have accentuated the decomposition process as has been previously documented (Manhein 1996). If the pig carcasses were skeletonized, the resulting burial would probably not produce a significant relative dielectric contrast with the surrounding soil as dry bone provides very little contrast to surrounding soils (Davis et al. 2000). This conclusion is supported by findings by Schultz (2006, 2008) who found that, by the twenty-first month of monitoring, pig carcasses interred in sandy soil in a Floridian climate were likely to begin to lose their resolution strength. As the hyperbolae of all burial scenarios lost substantial resolution strength before the twenty-first month mark, it is possible that being interred in a Spodosol matrix may result in faster decomposition rates than sandy soils.

The four burials with grave objects- the carcass buried under gravel (1C), the carcass buried wrapped in a tarpaulin (1D), the carcass buried under lime (2C), and the carcass buried wrapped in a cotton blanket (2D)- produced consistent responses throughout the research period.

In fact, collectively, the four burials produced discernable hyperbolae for all 12 months, excluding month 18 for burial 2C, month 20 for burial 1C, month 21 for burial 1C, 1D, and 2, and month 23 for burial 2D.

The ability of the GPR unit to detect burials with grave objects was greater than its ability to detect burials without grave objects or control holes. Not only did the GPR detect the graves more consistently throughout the research project, but the burials with grave objects produced stronger responses, producing hyperbolae with more discernable tails and bodies (see Appendix D & E). When considering all 12 months, the burials were ranked as follows, in decreasing order of signal response: burial 1C, burial 2C, burial 1D, and burial 2D. This ranking presents a departure from Martin (2010), who found that the pig carcass wrapped in a tarpaulin (1D) provided a better response that the pig carcass buried under lime (2C). However, while the early months of collection (months 13-15) do showcase a stronger response from burial 1D, subsequent months show burial 1D rapidly losing resolution strength while the response from burial 2C remains fairly constant. It is possible that while the tarpaulin kept in the decomposing fluids of the pig carcass, at some point in the second year of research project it was able to integrate more fully with the surrounding soil, released from the tarpaulin, whereas the lime covering burial 2C would likely be unmoved by natural causes.

Burial 1C, the pig carcass under gravel, provided the strongest response throughout the second year of the research pattern just as it did during the first year (Martin 2010).Gravel would not be moved by natural processes, nor would it decompose or likewise be integrated in the surrounding soil. Burial 2D provided as weak a response in the second year as it did in the first

year, comparatively (Martin 2010). Due to its organic nature, the cotton blanket would be more easily integrated into the surrounding soil matrix as it decomposed.

The Effect of Interment Time on Grave Detection

The 250 MHz antenna is capable of detecting clandestine graves even after two years of interment. However, especially when compared to the first year of research, there is a general decrease in signal resolution as time progresses. Additionally, burials without grave objects could not be detected around 16 months though there was an anomalous return of signal strength at month 19. This is likely due to a decrease in the relative dielectric contrast between the burial and the surrounding soil matrix. If there is a low relative dielectric contrast then the GPR unit will not be able to detect a body in the earth's subsurface (Reynolds 1997). Studies regarding decomposition rates have noted that bodies buried at a depth greater than a meter will experience complete skeletonization between 2-3 years, a process that can be accelerated by the presence of high temperatures above soil and high moisture levels in the ground (Reynolds 1996).

It is likely then that the pig carcasses currently interred are near or at the point of skeletonization as the Florida climate is notorious for its high, fluctuating temperature and the soil at the research site had significant moisture due to clayey components in the soil (Martin 2010). With skeletonization, the relative dielectric constant of the burial would decrease significantly, resulting in poorer resolution strength of the burials to the GPR unit (Davis et al. 2000; Doolittle and Bellantoni 2010).

The Effect of Moisture on Grave Detection

Increases and decreases in resolution strength were noted for all burial scenarios throughout the research project that seemed too random for a simple correlation to time of interment versus resolution strength. Moisture levels in the soil appeared to have a direct effect on resolution strength seen in the grave reflections of the profiles. When analyzing burials 1A and 1B from month 18 to month 24, this pattern becomes apparent. Burials 1A and 1B both produced no discernable response at month 18 (Figure 87), a month that corresponded with soil moisture readings of '0' at all depths (Table 22). However, several rainfalls led to higher moisture levels during month 19 with resulting moisture readings of '1' and '2'throughout all depths (Table 24). Burials 1A and 1B produced an easily discernable response at month 19 after the increase in soil moisture levels (Figure 89).

A similar pattern occurred between months 20 and 21. Though burial 1A did not produce a response at month 20, burial 1B produced a weak response (Figure 91). At month 21, neither burial produced a response (Figure 93). Corresponding moisture readings were between '3' and '4' throughout all depths at month 20 (Table 26) before dipping to an average level of '1' throughout all depths at month 21 (Table 29). Again, a decrease in moisture levels created a decrease in response resolution quality. Visibility continued to vary until month 24, but the relationship between visibility and moisture level was never as strong as it was in comparisons of month 18 to month 19 and month 20 to month 21. In order to demonstrate this pattern succinctly, the correlation between visibility and moisture level of burial 1B was plotted for the entire year (Figure 24).

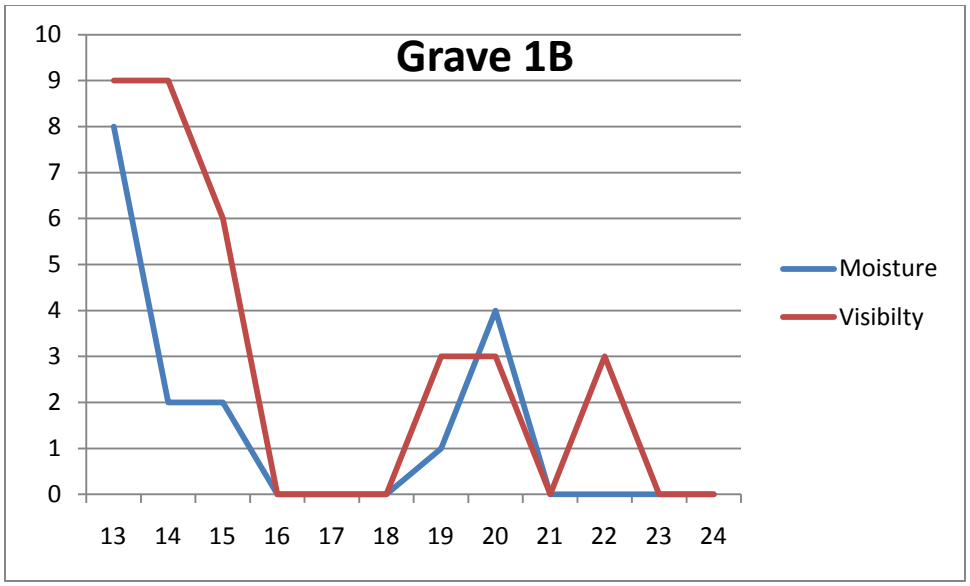

Figure 24: Moisture and Visibility Correlation for Burial 1B, Months 13-24

A slight increase in soil moisture appears to possibly correlate to an increase in resolution strength of the burial hyperbolae. Water is known to scatter the EM waves of a GPR, which would seem to indicate that an increase in soil moisture would result in poorer resolutions. However, the greatest variable responsible for the resolution of a buried object is its relative dielectric constant (Reynolds 1997). Perhaps, then, so long as the increase in soil moisture is not enough to produce greater wave attenuation, it will produce an increased strength in resolution strength due to an increase in relative dielectric constant of the burial. If the soil became oversaturated with water, there is little doubt that the EM signals would not detect the graves due to attenuation of the signal. The moisture level is just enough to increase the contrast of the graves to the surrounding soil without increasing wave attenuation. It is likely that it increases the electrical properties of the buried carcasses, thus creating a strong dielectric constant which would result in better hyperbola resolution (Doolittle and Bellantoni 2010)

Soil

This research was also conducted in a Florida climate in a soil matrix composed of a Smyrna pomello soil with a spodic horizon (Doolittle and Schellentrager 1989; Leighty 1989). The spodic horizon is significant due to the high density of acidic resins that help compose the layer. These acidic resins can travel down the soil horizons with the help of moisture. Six of the eight burials were buried at a 1 m depth, below this spodic horizon, a layer that can be seen as a series of thick bands in the reflection profiles (see Appendix D). The spodic horizon did not represent a significant obstacle for the penetration of the EM waves, just as it did not in the first year of research (Martin 2010).

CONCLUSION

The 250 MHz antenna proved to be an excellent tool to be employed in the detection of clandestine graves. Though there was an overall decrease in signal strength as time progressed, most of the burials could still be detected at month 24. Burials with grave objects produced stronger and more consistent responses and were easier to detect. A lack of soil moisture in the ground resulted in weaker grave resolution, while a moderate increase in soil moisture levels increased the resolution strength of the graves. These findings help to fill in a significant gap in the literature concerned with forensic geophysical searches; previously, there has not been significant investigation in the use of a 250 MHz antenna in the detection of clandestine graves.

Based on the ranking of specialized burials, it is evident that the greater the relative dielectric constant a material provides with the surrounding soil the greater the likelihood that it will be detected by the GPR unit. Standard burials, carcasses or cadavers buried in a Spodosol

environment without grave goods, will likely be unable to be detected by the 250 MHz after a two year period has passed.

REFLEXW proved a superior processing tool as opposed to SLICE, as all responses detected in SLICE were detected in REFLEXW; however, REFLEXW allowed for additional responses to be detected that SLICE did not. Though REFLEXW was found to be superior, it is worth noting that the imagery produced by SLICE may be seen to provide a better visual display. Therefore, using both programs in conjunction with one another should be employed by the GPR operator.

In conclusion, the GPR utilizing the 250 MHz antenna was an excellent tool to detect clandestine graves. Though there are natural constraints upon its ability to detect graves, its noninvasive and time-efficient qualities remain a boon to the investigators who choose to employ it.

CHAPTER FIVE: CONCLUDING REMARKS AND ESTABLISHING GUIDELINES

CONCLUSIONS

Overall, this research demonstrated that use of remote sensing geophysical techniques should be encouraged by law enforcement seeking to locate clandestine graves, so long as certain limitations regarding their utilization be kept in mind. This controlled research sought to confirm the overall ability of the GPR unit to detect clandestine graves as well as the conductivity meter, overall trends in grave detection, and comparisons between the two modes of processing and their resulting imagery as well as the applicability of the 500 MHz antenna versus the 250 MHz antenna in grave detection.

The use of the conductivity meter in grave detection proved to be a futile effort. Six major responses were noted after the data was processed and mapped; however, these responses in no way correlated to any of the burials within the grid. This finding was consistent with the previous year of research (Martin 2010). It is unclear if a metal additive to the grave goods would have improved the conductivity meter's ability to detect the burials as pervious research has shown it has difficulty detecting large metallic objects any deeper than .75 m (Dionne 2009). Therefore, the applicability of this tool in the detection of clandestine graves, especially those buried at or greater than 1 m is advised against.

The ability of the GPR unit, utilizing both antennae, proved to be an excellent tool for subsurface detection of clandestine graves. However, limitations concerning the applicability of the GPR unit were uncovered for both antennae. First, there was a positive correlation between time of interment and reduction in resolution strength that was confirmed through the course of

the research. Second, burials without accompanying grave goods were the first to lose distinctive hyperbolae. Those burials with grave goods produced stronger and more consistent responses throughout the research project. Also, burials lost their resolution at a faster rate in the Spodosol environment than in a sandy soil matrix, with a significant loss of response resolution occurring in the Spodosol environment around 18 months whereas this sudden resolution reduction did not occur in sandy soils until 21.5 months (Schultz 2006, 2008). Finally, data suggested that the level of soil moisture in the ground had a direct correlation with response resolution: the more moisture inherent in the soil the sharper the resolution of the hyperbolae due to the moisture increasing the electrical conductivity of the buried material as opposed to the surrounding soil, creating a higher relative dielectric constant. More research is encouraged to investigate this finding and to determine at what level soil moisture increases response resolution without increasing wave attenuation.

Previous research has indicated that a GPR antenna should be selected that both allows for a deep enough depth penetration while providing a detailed view of the subsurface; this medium has normally been found in the 400-500 MHz antenna (Dupras et al. 2006; Schultz 2007). This research, in addition to utilizing the 500 MHz antenna, also utilized the 250 MHz antenna. The use of the 250 MHz antenna has been limited in case studies and controlled research. Though some researchers have documented the use of lower frequency antennae in both case studies and controlled research (Powell 2004; Nobes 2000), direct comparisons between the operation of the two different frequency antennae for a long term period in the same survey has been limited (Schultz and Martin 2011); this research sought to correct that oversight. It is generally understood that the lower the frequency emission, the greater the depth of

penetration of the GPR component. Conversely, the higher the frequency emission, the shallower, but more detailed the data will be (Conyers 2004; Reynolds 1997). It was expected, then, that the research would confirm the guidelines set by previous researchers to utilize the 500 MHz antenna for its increased subsurface detail. (Dupras et al. 2006; Schultz 2007).

However, this research found the 250 MHz antenna to be a more viable option for the detection of graves containing large cadavers in this soil matrix and at this depth. Graves that produced no discernable signal when using the 500 MHz antenna were able to be identified when processing data gathered from the 250 MHz antenna (see Figures 49 & 50 versus Figures 89 & 90). This conclusion echoed the findings of the previous year's research (Martin 2010). While the 500 MHz antenna offers a more detailed view of the subsurface, it may be that it was too detailed for this particular subsurface, responding to too many features so as to make it difficult for the graves to distinguish themselves from the background noise (Schultz and Martin 2011). The data from the 250 MHz antenna, in contrast, allowed the graves to be more clearly delineated from the background by providing less detailed scanning of the subsurface. The spodic horizon may have come into play as well with its organic layer producing many different responses that the higher frequency of the 500 MHz antenna discerned while the 250 MHz antenna 'ignored'. The findings of this research indicate that in a Spodosol environment the 250 MHz antenna may be a better option for the detection of clandestine graves, a conclusion that was also found in the previous year's research (Martin 2010; see also Figures 48-59 versus Figures 88-99).

GUIDELINES

In conclusion, this research suggested a series of guidelines to be implemented when utilizing GPR in a search for clandestine graves. The search site must be reviewed prior to utilization of the GPR unit in order to be aware of the topography, soil content, foliage, and any landmarks or features that may interrupt the structure of a potential grid. The GPR must be operated over a fairly level surface, and all foliage must be clipped or mowed down to ensure that the GPR technician is able to move freely and securely. Ground-penetrating radar is best utilized in a field setting with clipped grass and an absence of trees and brush in order to minimize the masking effect of a root system when using the GPR. The presence of too many subsurface anomalies will mask the presence of clandestine graves, and objects such as tree roots or urban infrastructure (such as piping) may even result in false positives. Dry, sandy sediment soil is best for the application of GPR while clayey soils will result in major wave attenuation (Conyers 2006). Prior knowledge of a search site will allow the GPR technician to formulate plausible predictions to law enforcement about the likelihood of success in their endeavor.

Second, once the site is properly assessed and prepared, a grid must be constructed with transects spaced close enough to ensure grave detection but far enough to afford more efficiency in the operations as well as minimize the amount of time a search can be performed. In this research, the GPR unit was operated along transect spacing of 0.25 m apart. This spacing provided an excellent medium between the two previous constraints, allowing human cadaver-sized graves (here, the pig carcass proxies) to be detected across a set of five transects while minimizing the amount of time needed in the field. If time permits, the research indicates that a GPR survey should be conducted in both X (north-south) and Y (east-west) directions, as this

will allow the GPR technician to process data efficiently as a horizontal slice, in addition to covering the area a second time for a more thorough search. Also, if the area being surveyed is small enough and the time constraints few, utilization of both antennae, the 500 and 250 MHz antennae, is advised for a broader dataset with which to investigate

Third, calibration is key to gathering as precise a set of data as possible. In this research, the GPR unit was calibrated to a piece of rebar pounded into an empty grave shaft at a precise depth of 1.0 m. Thereafter, before each GPR survey, the wave velocity was calibrated and the data was standardized to accurately show depth when processing both reflection profiles using REFLEXW and SLICE. In the field, it may be necessary to either calibrate the GPR unit before joining law enforcement onsite or to find an anomaly whose relative depth is known (such as a pipe line, underground cable, etc.).

Finally, after data has been collected, processing using a combination of both reflection profiles (REFLEXW) and horizontal slices (SLICE) is suggested. Doing so will allow the GPR technician to possibly be able to discern anomalies that were not discernable before the data was cleaned and edited. Furthermore, a processed data set is a persuasive data set, and will allow the GPR technician to show law enforcement or other third parties, such as court systems, exactly where an anomaly is produced with minimal confusion without the possibility of miscommunication. Showing an anomaly in both a reflection profile and horizontal slice will allow law enforcement to better grasp the size of an object buried in the subsurface.

In sum, the employment of GPR may provide law enforcement or other third parties with much needed information in the search for clandestine graves. Those who seek to employ GPR technology to search for clandestine graves should bear in mind the unlikelihood of finding a

clandestine grave after a significant period of time has passed. While studies have shown that coffins and other prepared burials can be detected with GPR after significant interment time, this is due to the air pocket created by the coffin or the presence of metallic or other grave goods (Dionne et al. 2010). Burials without these attributes, including many examples of clandestine graves found in the literature, will be unlikely to produce a discernable response after the passage of a decade. However, utilization of the GPR is always recommended so long as the above guidelines are followed and its limitations understood. Only then can its potential be properly achieved.

APPENDIX A: CONDUCTIVITY CONTOUR MAPS

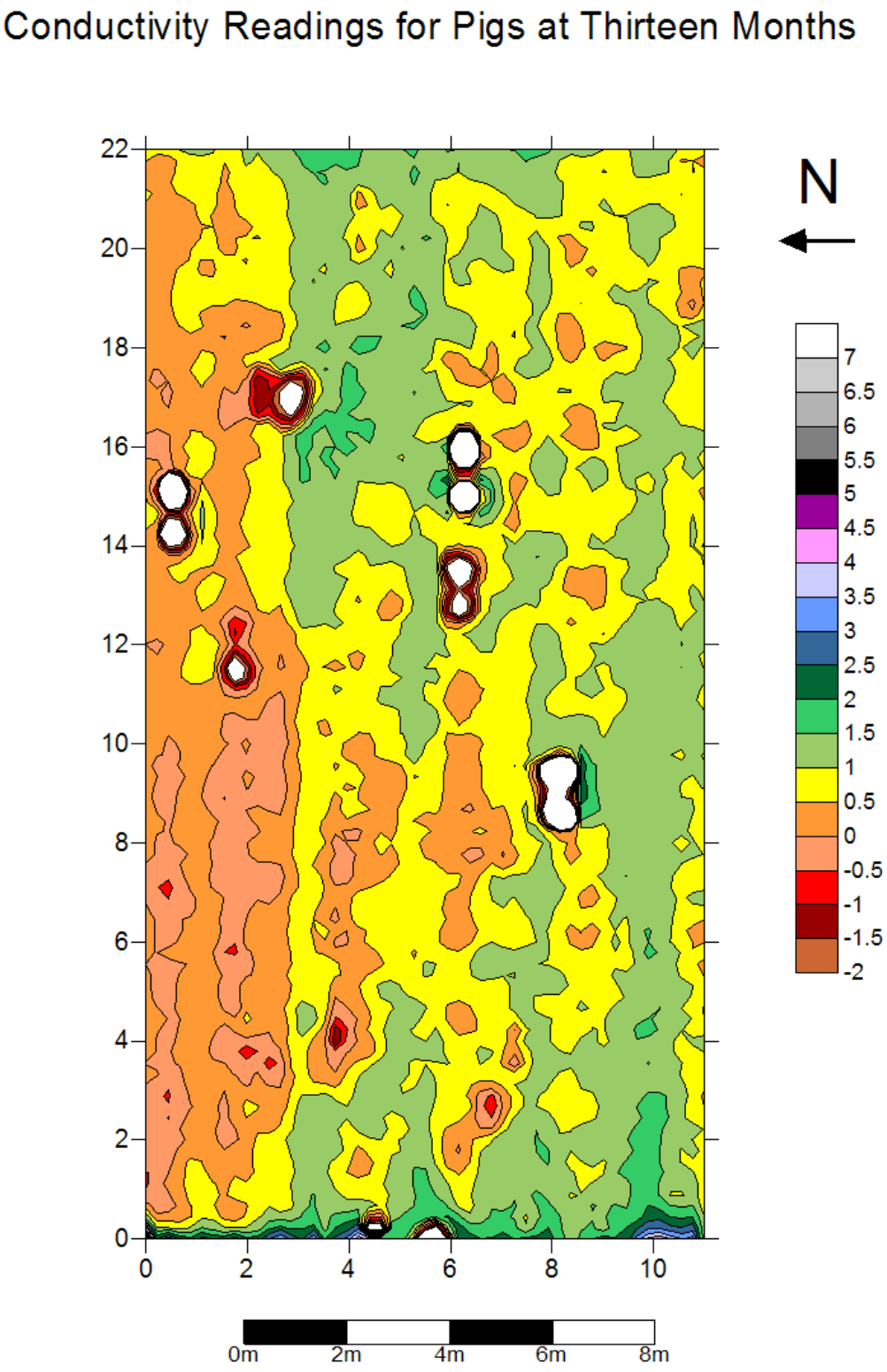

Figure 25: Conductivity Readings at 13 Months of Interment

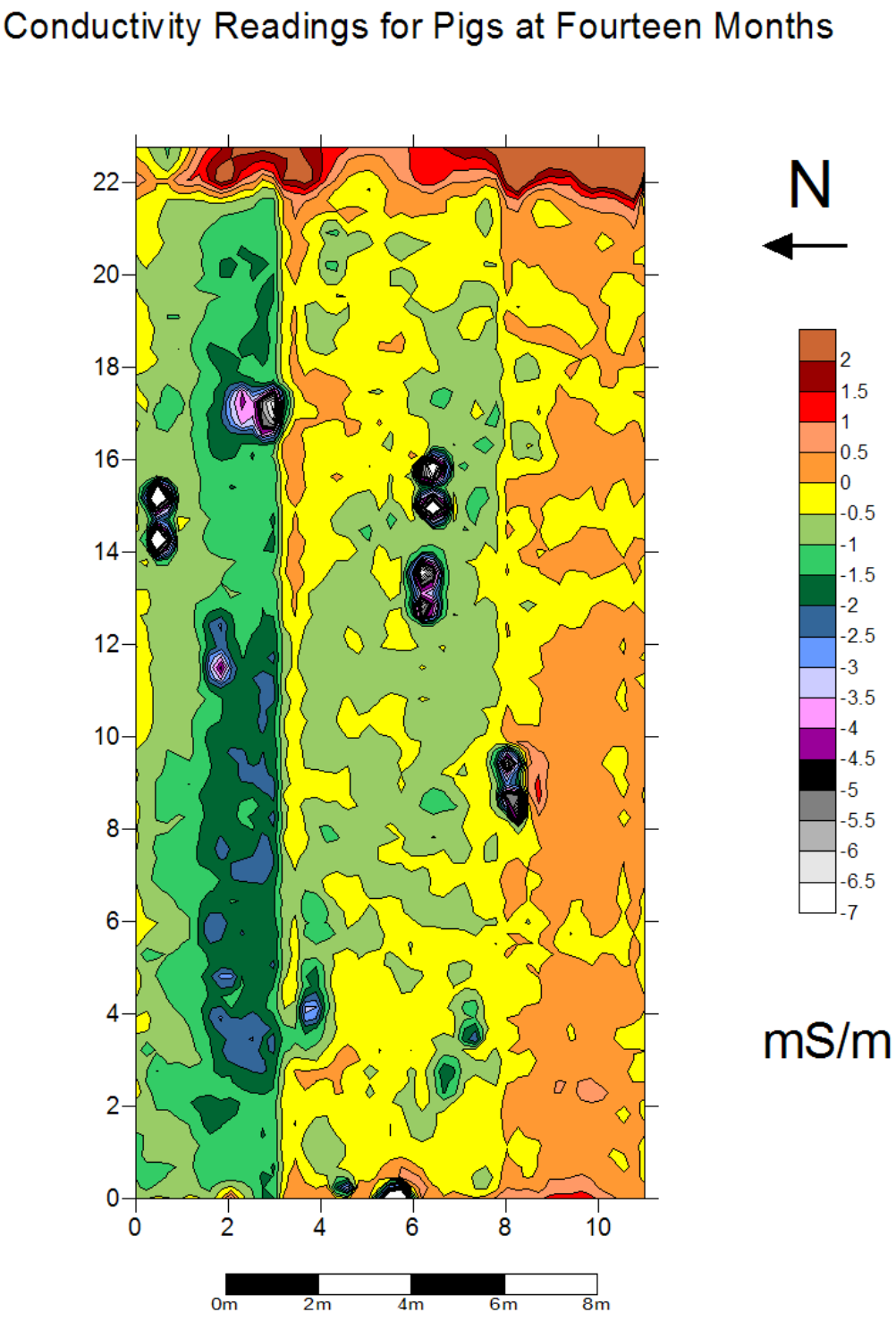

Figure 26: Conductivity Readings at 14 Months of Interment

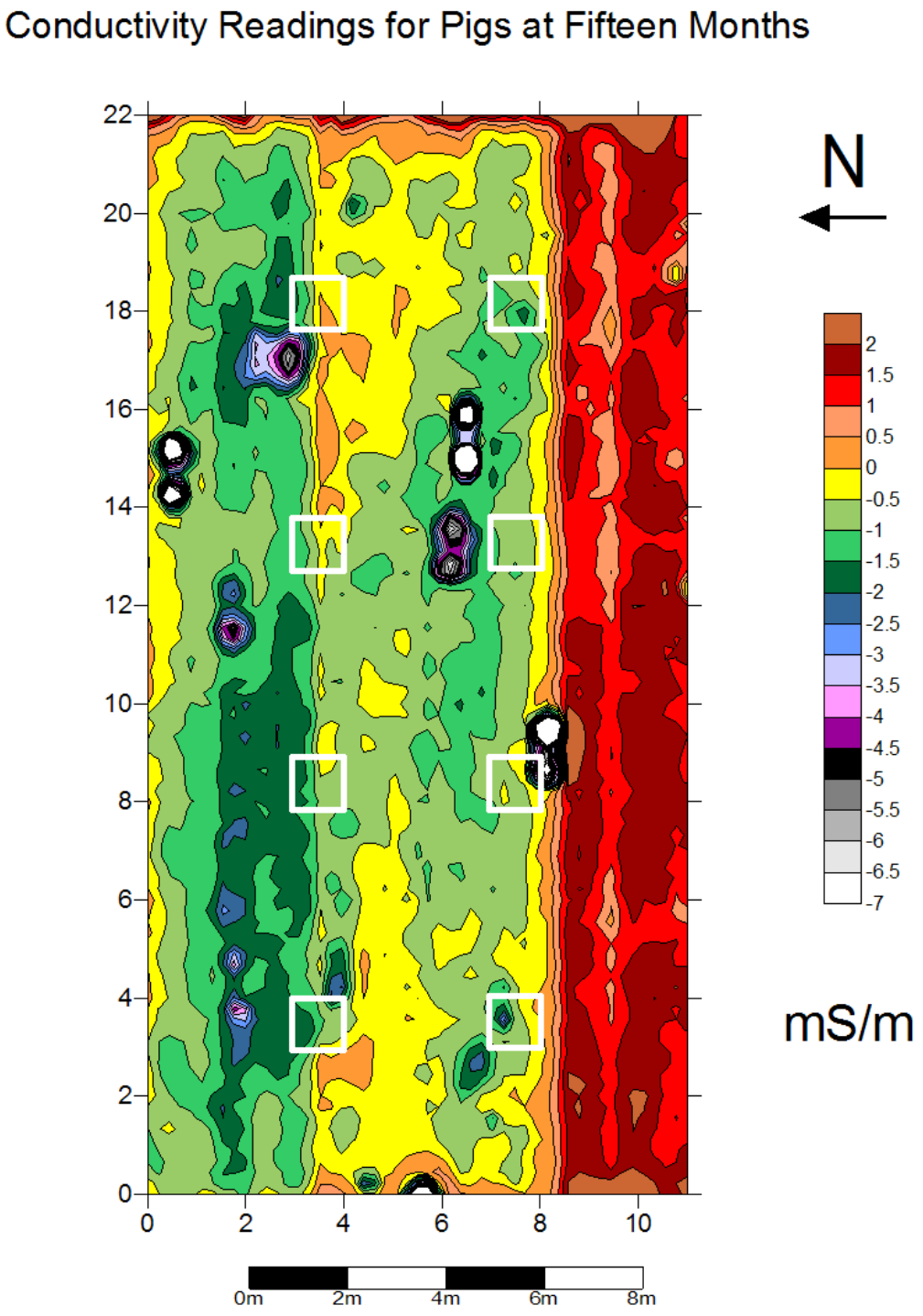

Figure 27: Conductivity Readings at 15 Months of Interment

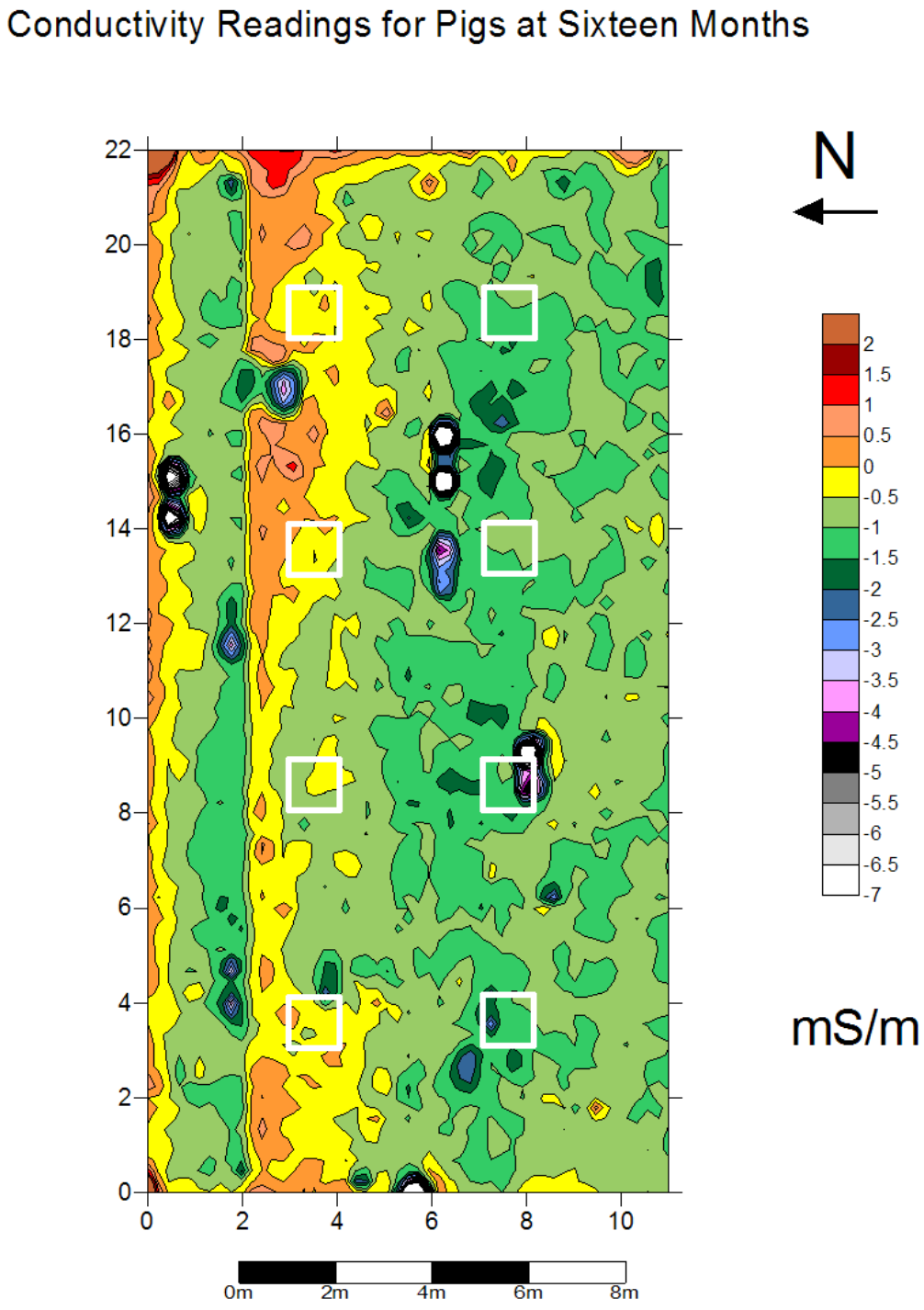

Figure 28: Conductivity Readings at 16 Months of Interment

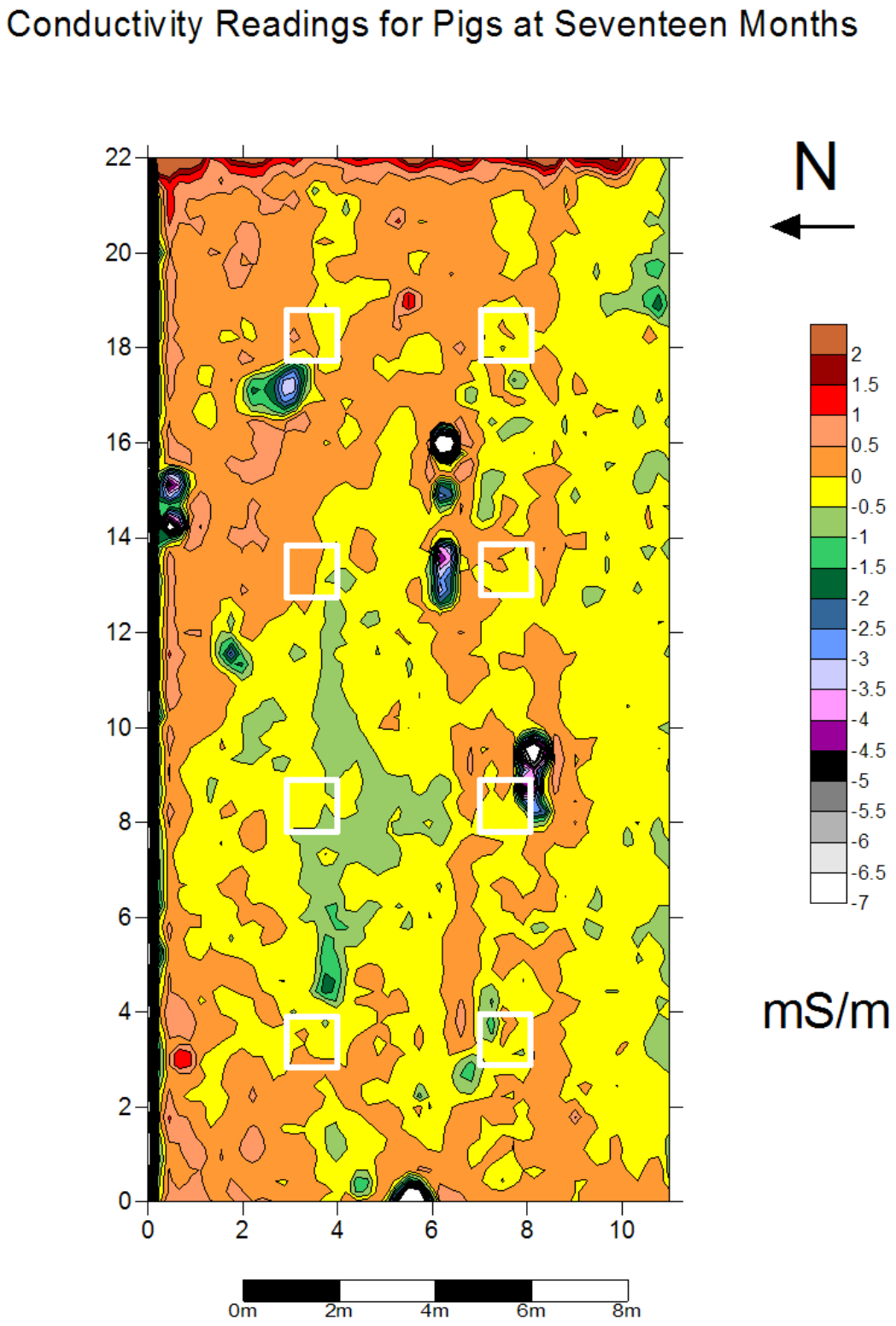

Figure 29: Conductivity Readings at 17 Months of Interment

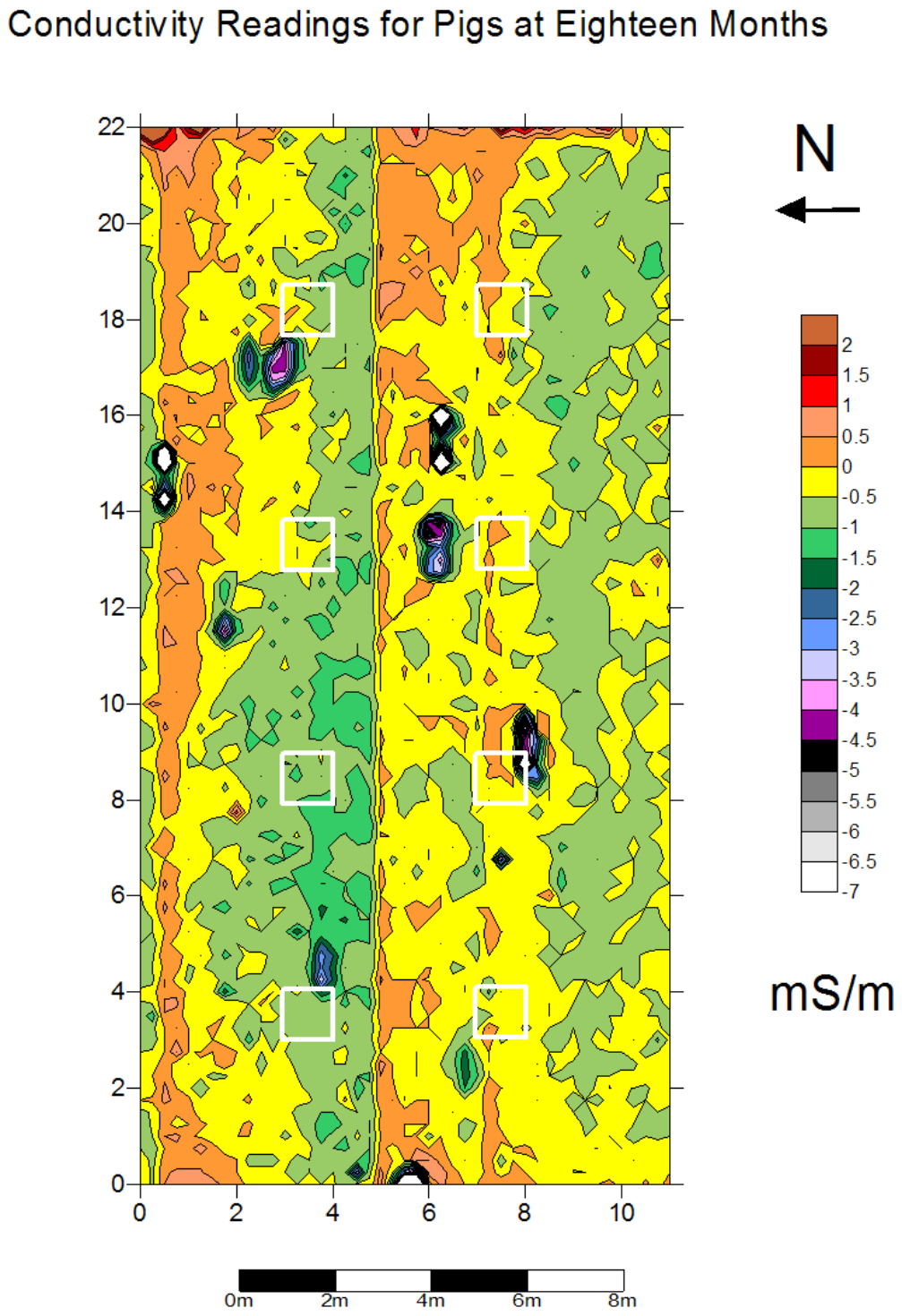

Figure 30: Conductivity Readings at 18 Months of Interment

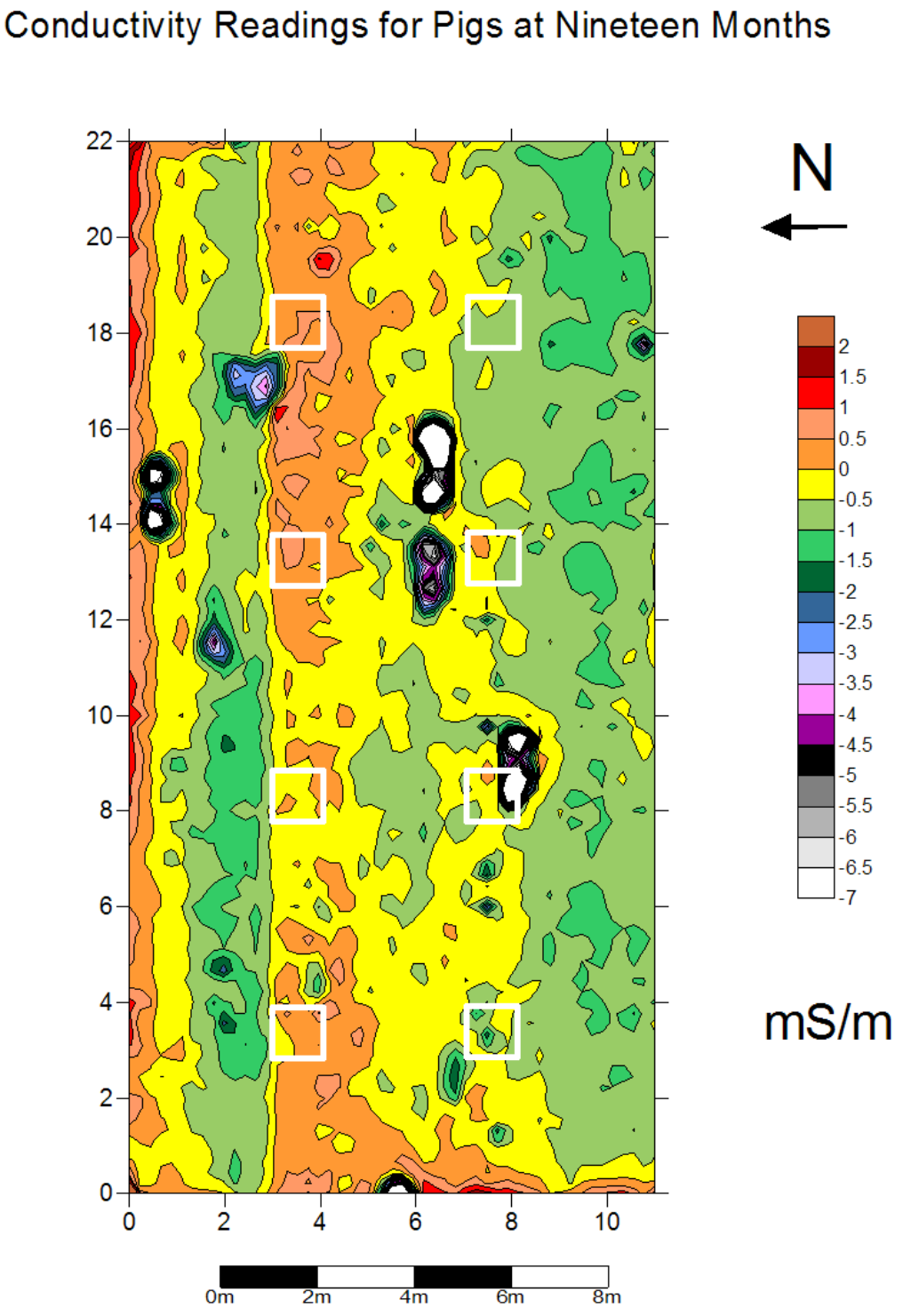

Figure 31: Conductivity Readings at 19 Months of Interment

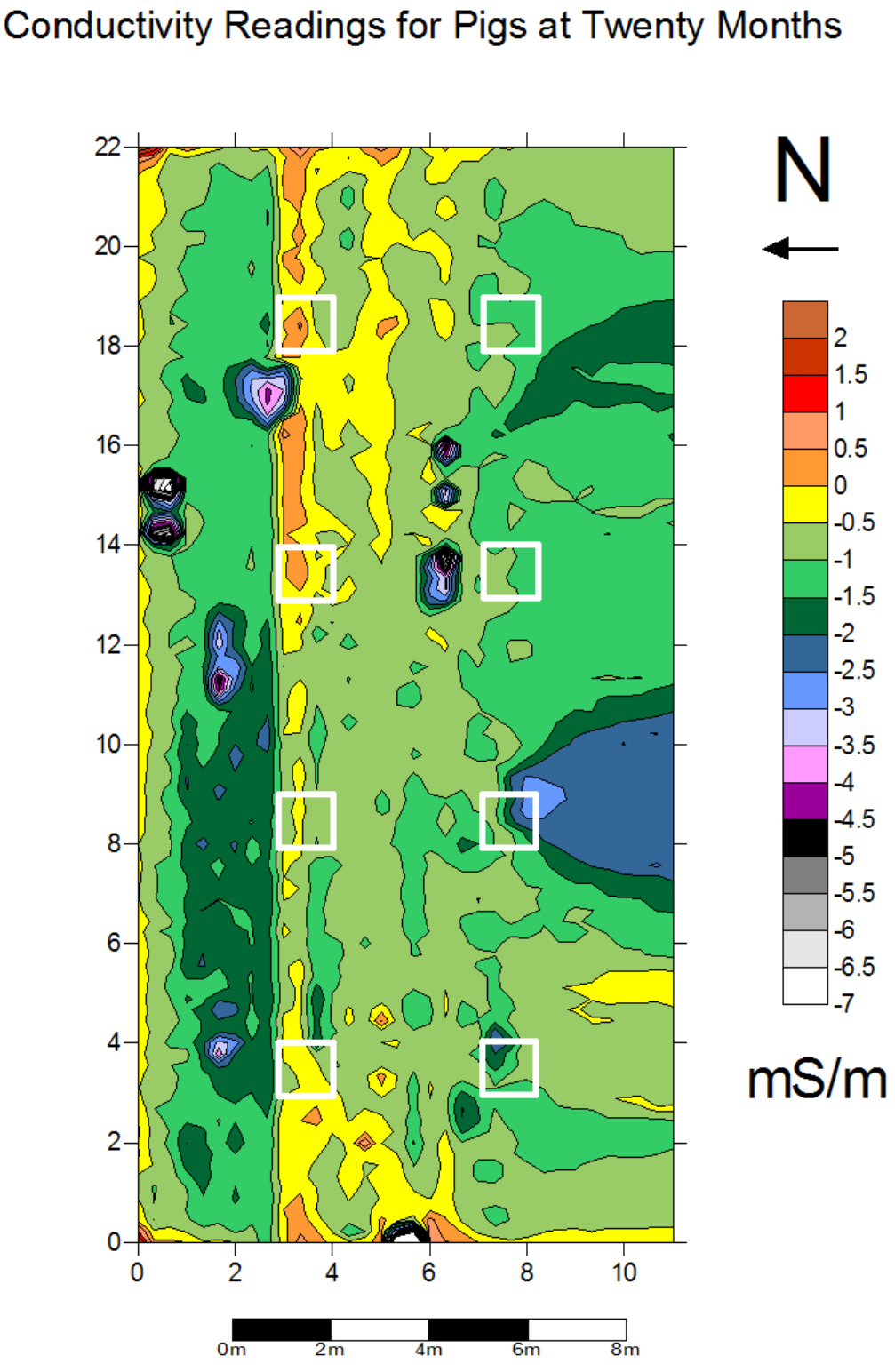

Figure 32: Conductivity Readings at 20 Months of Interment

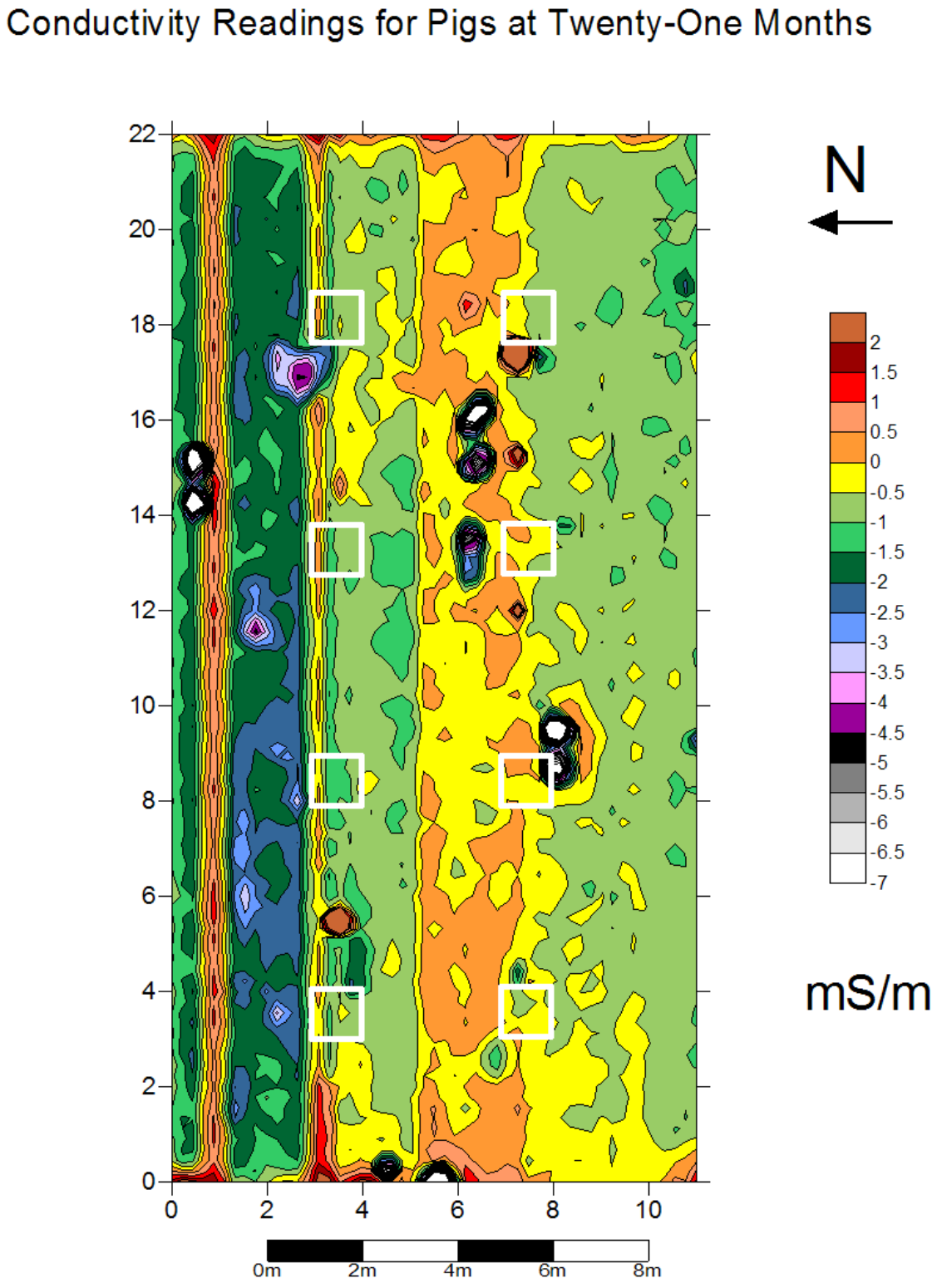

Figure 33: Conductivty Readings at 21 Months of Interment

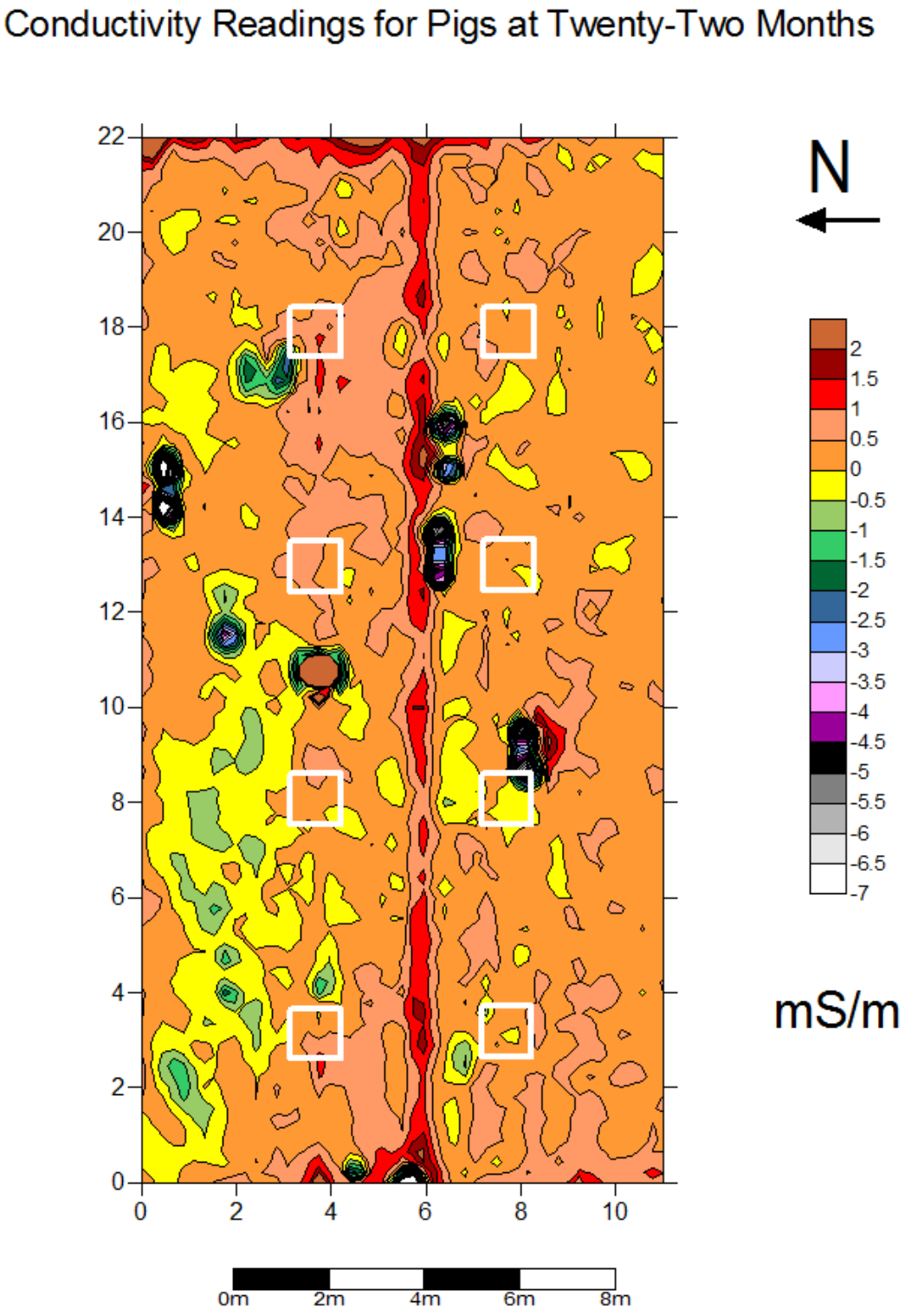

Figure 34: Conductivity Readings at 22 Months of Interment

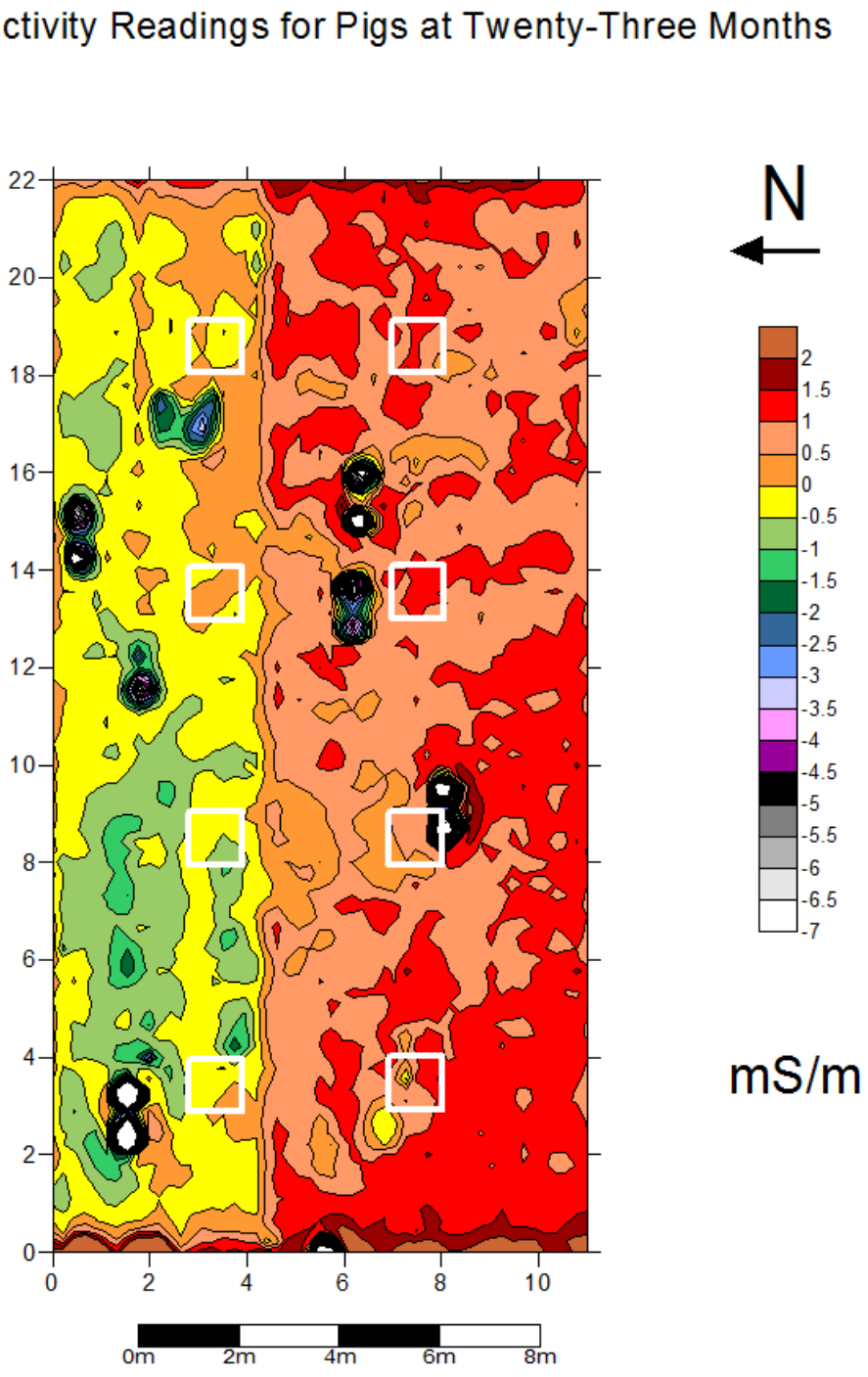

Figure 35: Conductivity Readings at 23 Months of Interment

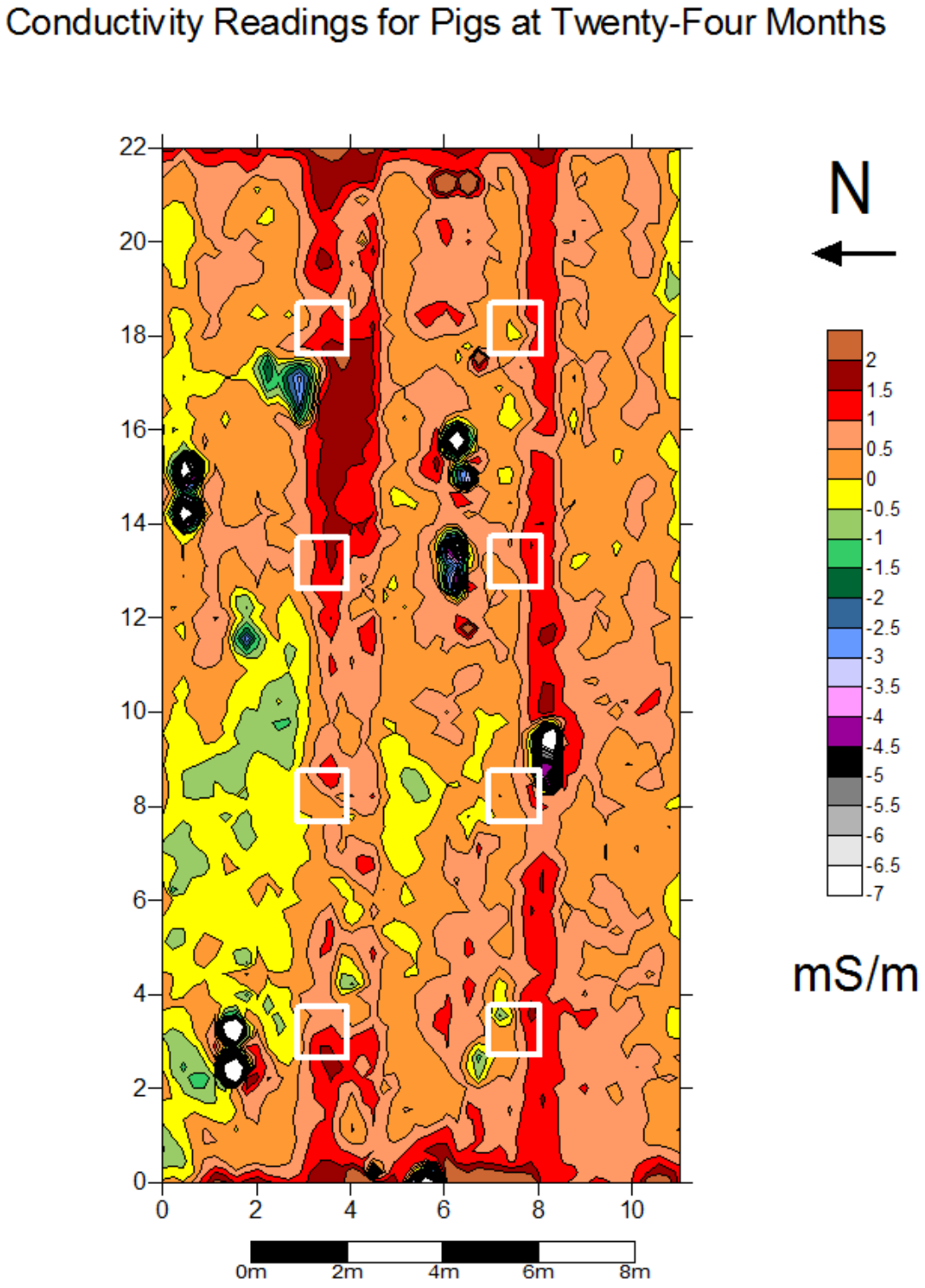

Figure 36: Conductivity Readings at 24 Months of Interment

APPENDIX B: GROUND-PENETRATING RADAR 500-MHZ REFLECTION PROFILES

MONTH 13

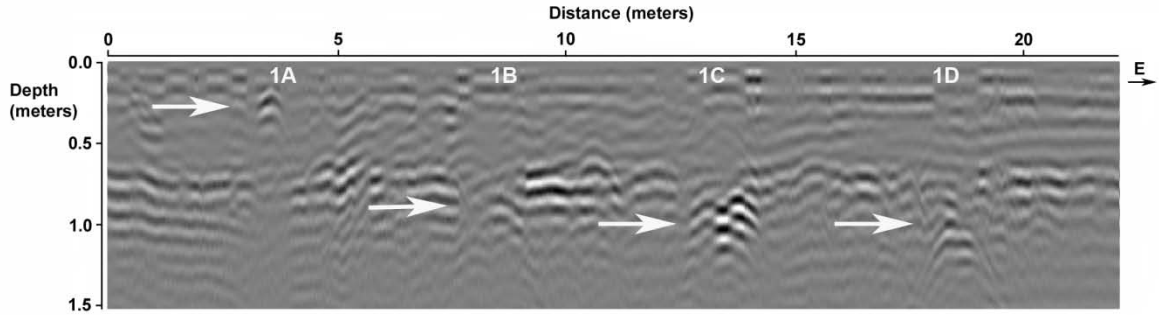

Figure 37: GPR reflection profile using the 500 MHz antenna of Row 1 at 13 months

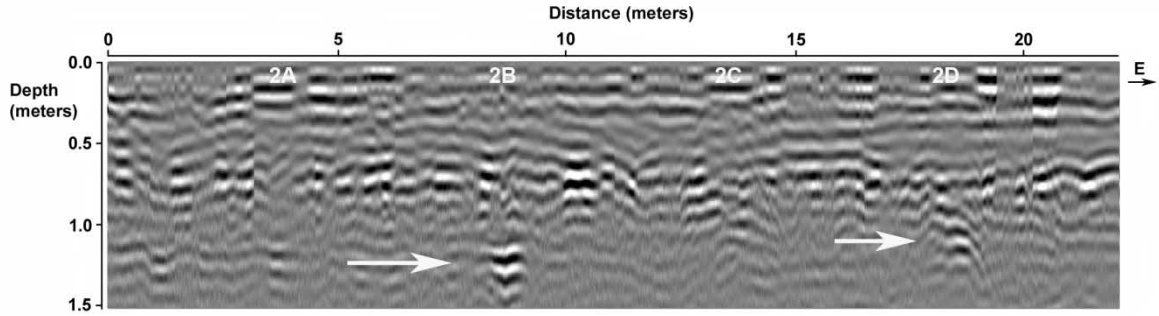

Figure 38: GPR reflection profile using the 500-MHz antenna of Row 2 at 13 months

MONTH 14

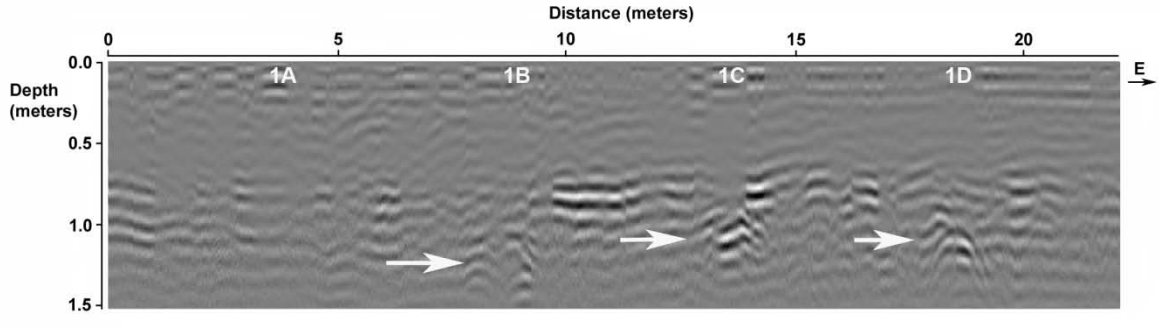

Figure 39: GPR reflection profile using the 500-MHz antenna of Row 1 at 14 months

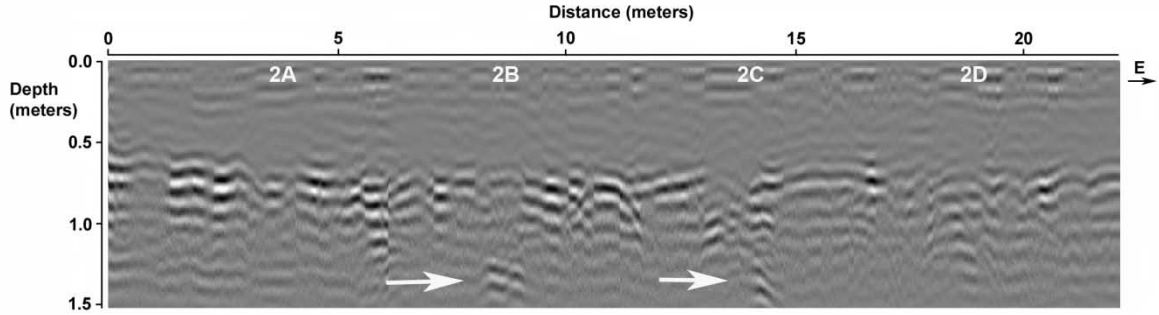

Figure 40: GPR reflection profile using the 500-MHz antenna of Row 2 at 14 months

MONTH 15

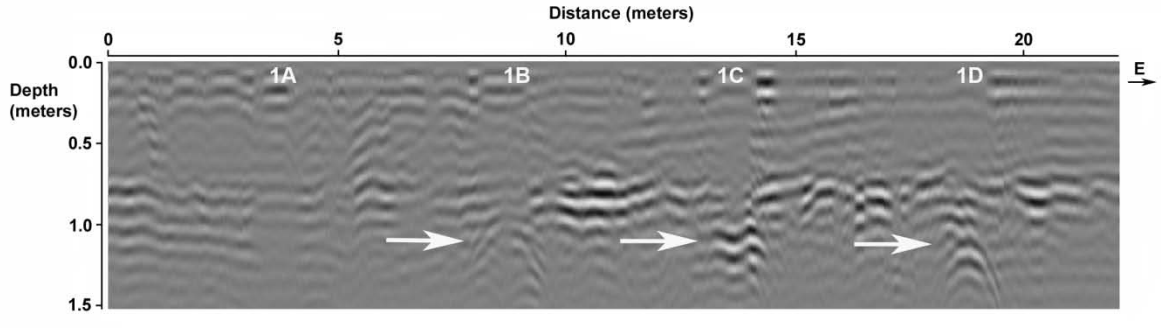

Figure 41: GPR reflection profile using the 500-MHz antenna of Row 1 at 15 months

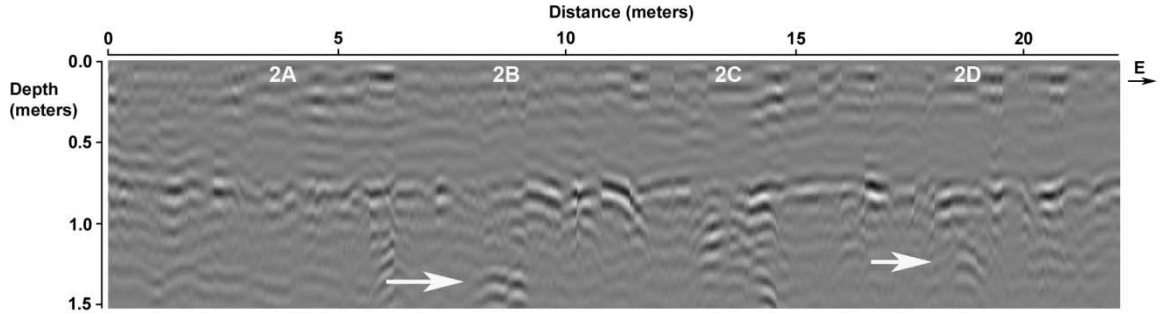

Figure 42: GPR reflection profile using the 500-MHz antenna of Row 2 at 15 months

MONTH 16

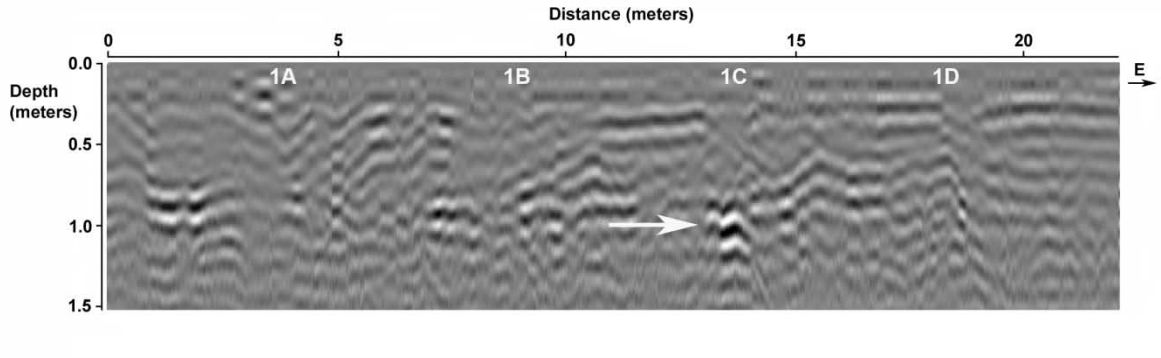

Figure 43: GPR reflection profile using the 500-MHz antenna of Row 1 at 16 months

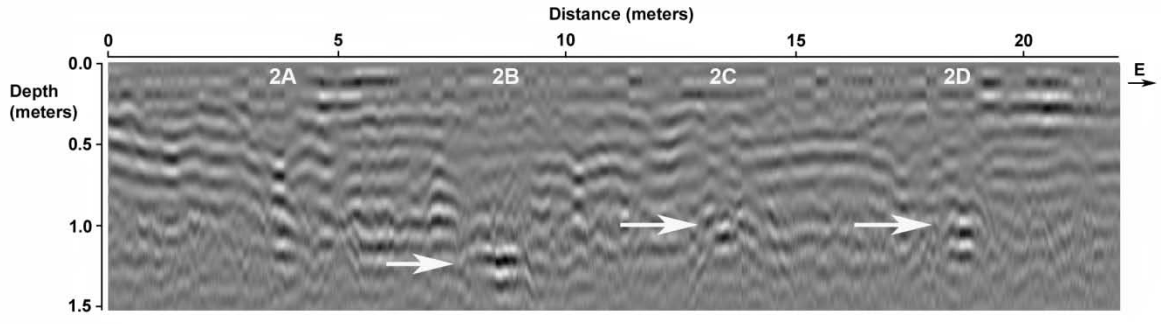

Figure 44: GPR reflection profile using the 500-MHz antenna of Row 2 at 16 months

MONTH 17

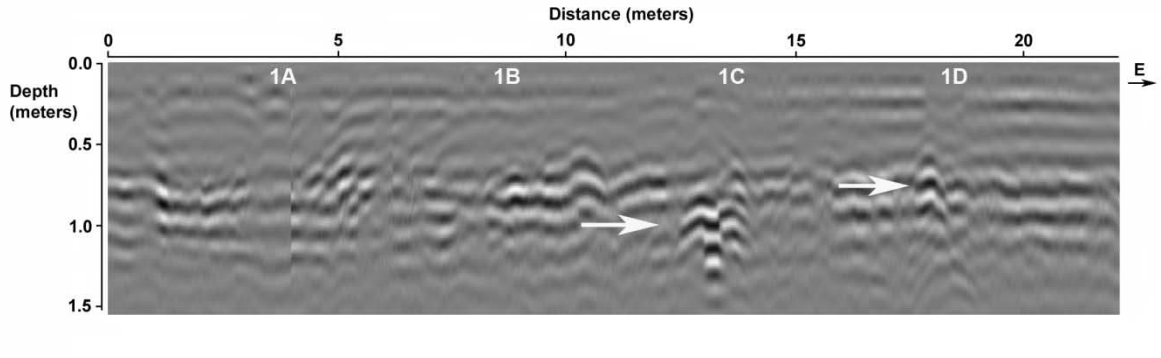

Figure 45: GPR reflection profile using the 500-MHz antenna of Row 1 at 17 months

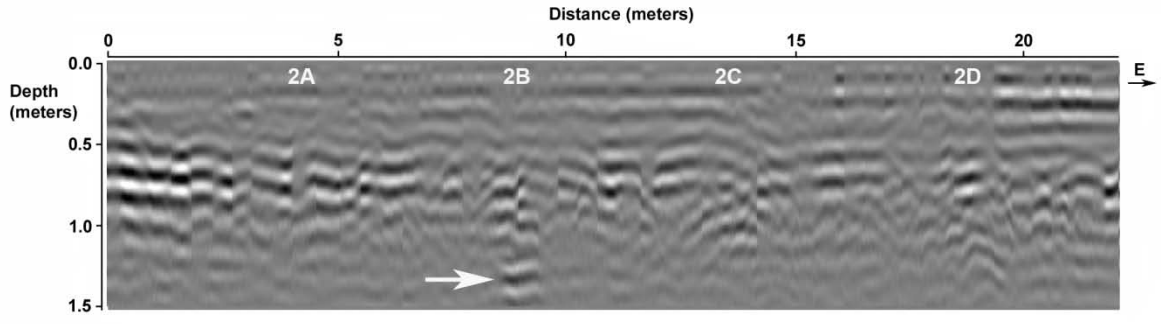

Figure 46: GPR reflection profile using the 500-MHz antenna of Row 2 at 17 months

MONTH 18

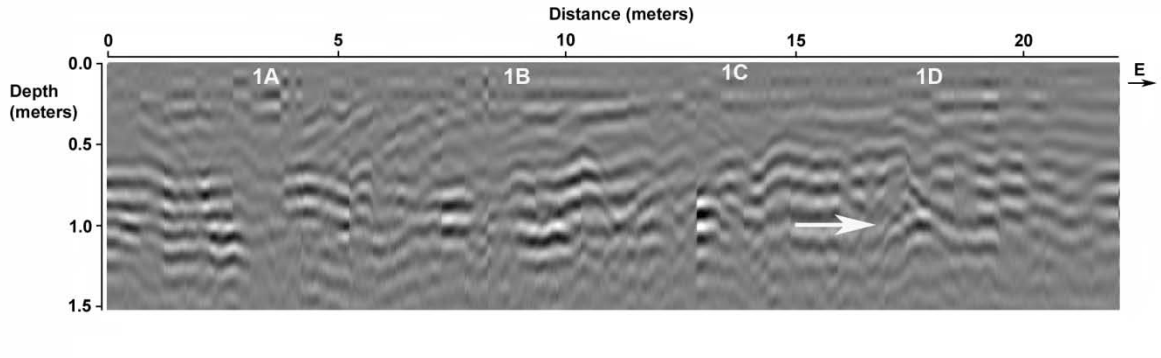

Figure 47: GPR reflection profile using the 500-MHz antenna of Row 1 at 18 months

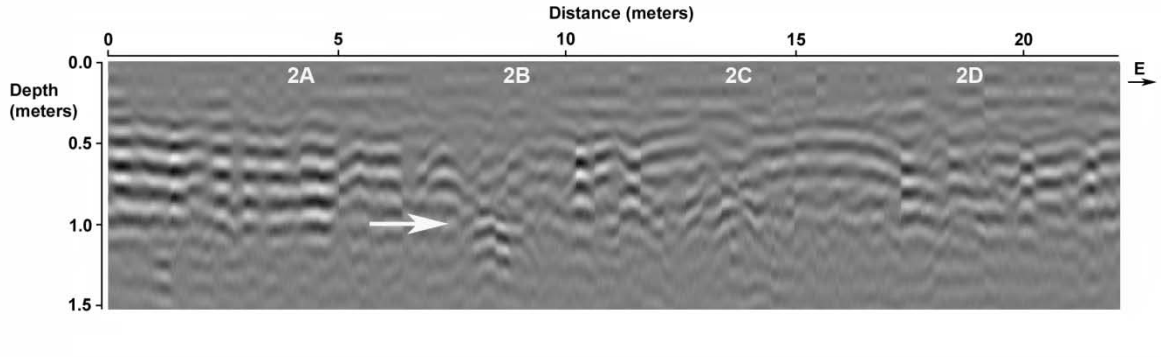

Figure 48: GPR reflection profile using the 500-MHz antenna of Row 2 at 18 months

MONTH 19

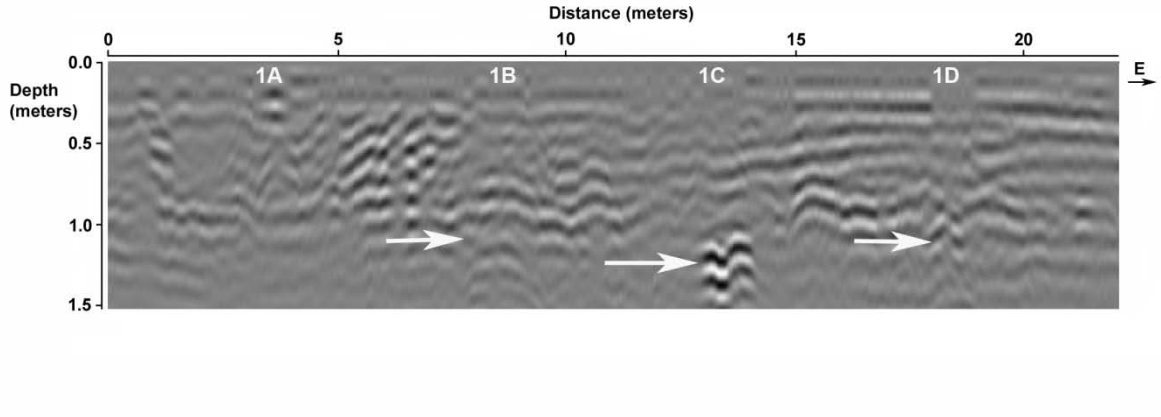

Figure 49: GPR reflection profile using the 500-MHz antenna of Row 1 at 19 months

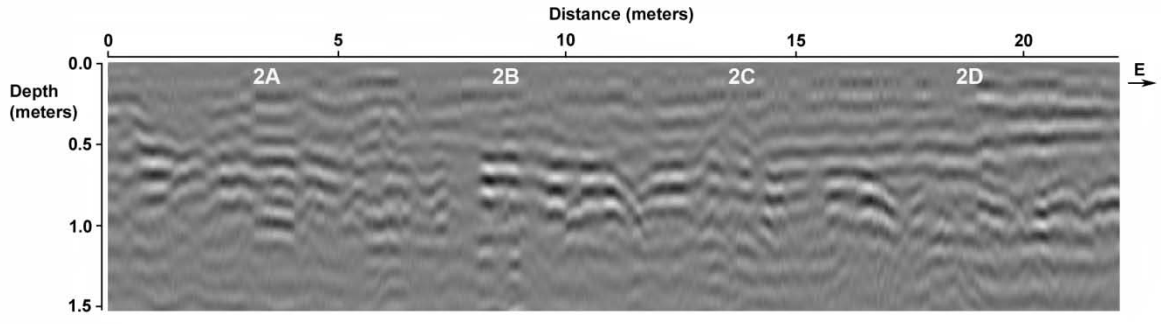

Figure 50: GPR reflection profile using the 500-MHz antenna of Row 2 at 19 months

MONTH 20

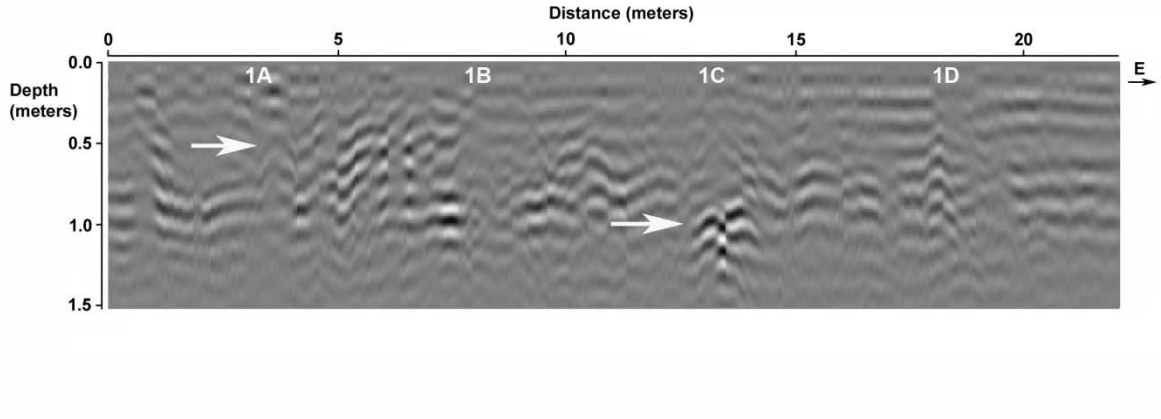

Figure 51: GPR reflection profile using the 500-MHz antenna of Row 1 at 20 months

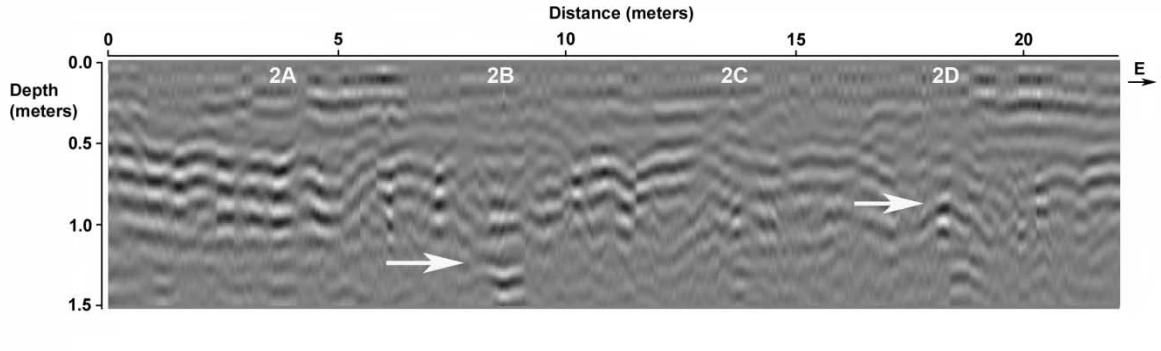

Figure 52: GPR reflection profile using the 500-MHz antenna of Row 2 at 20 months

MONTH 21

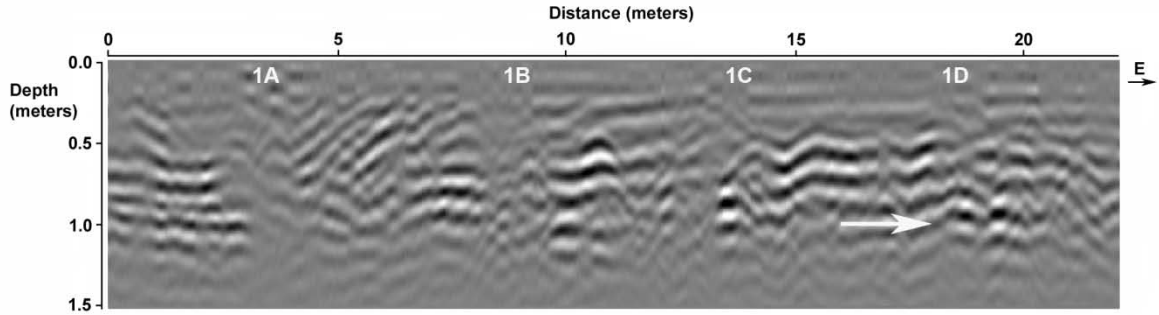

Figure 53: GPR reflection profile using the 500-MHz antenna of Row 1 at 21 months

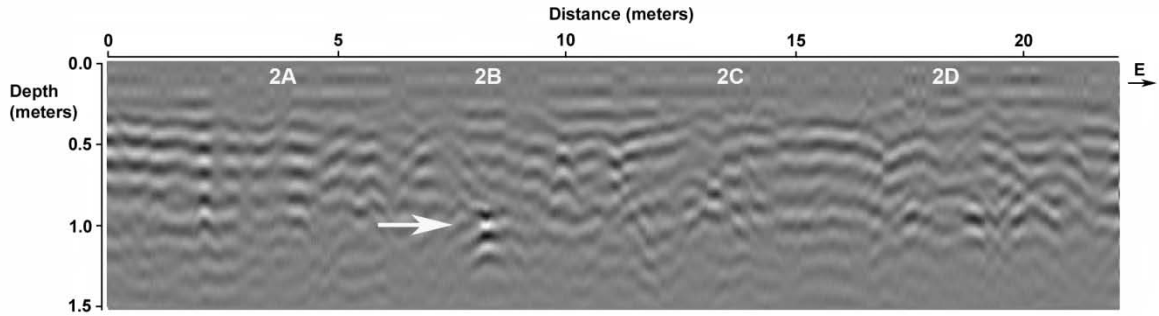

Figure 54: GPR reflection profile using the 500-MHz antenna of Row 2 at 21 months

MONTH 22

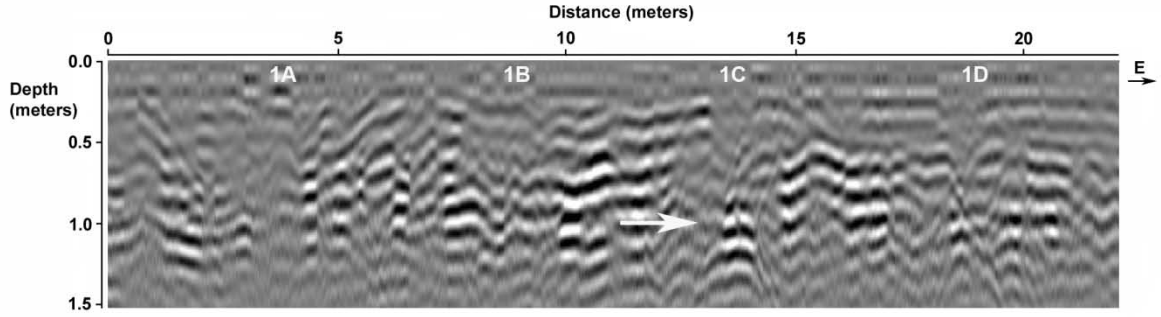

Figure 55: GPR reflection profile using the 500-MHz antenna of Row 1 at 22

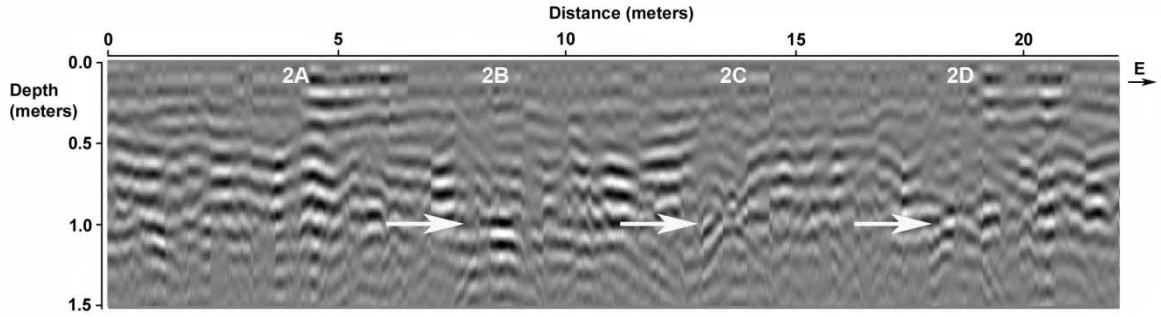

Figure 56: GPR reflection profile using the 500-MHz antenna of Row 2 at 22 months

MONTH 23

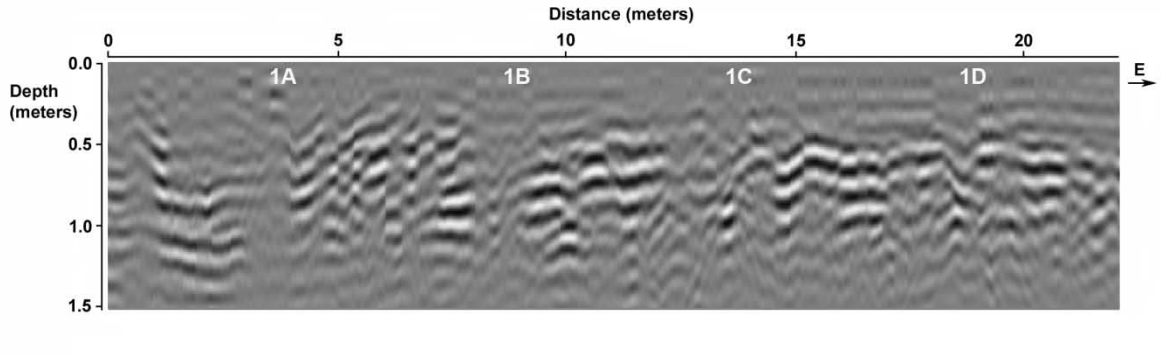

Figure 57: GPR reflection profile using the 500-MHz antenna of Row 1 at 23 months

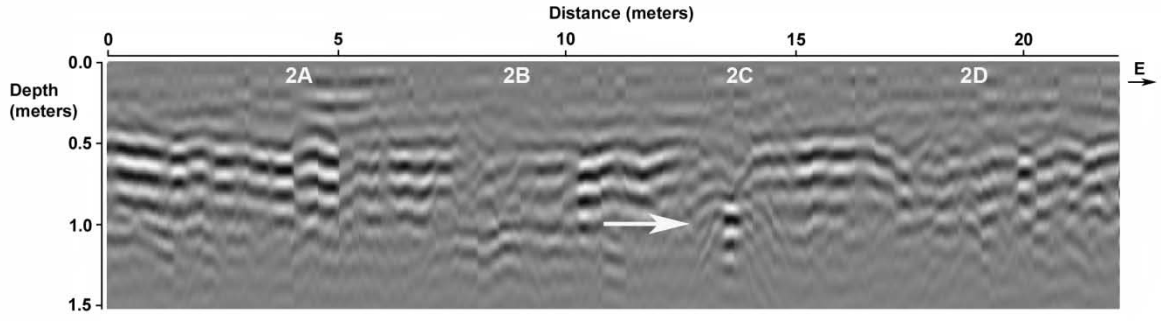

Figure 58: GPR reflection profile using the 500-MHz antenna of Row 2 at 23 months

MONTH 24

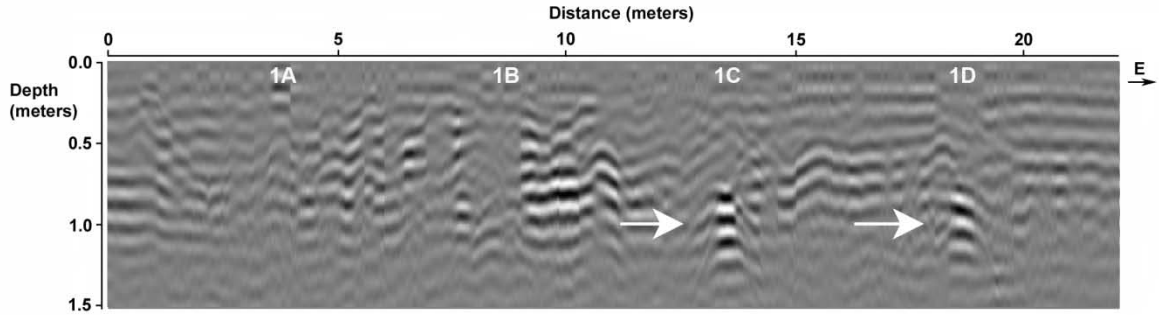

Figure 59: GPR reflection profile using the 500-MHz antenna of Row 1 at 24 months

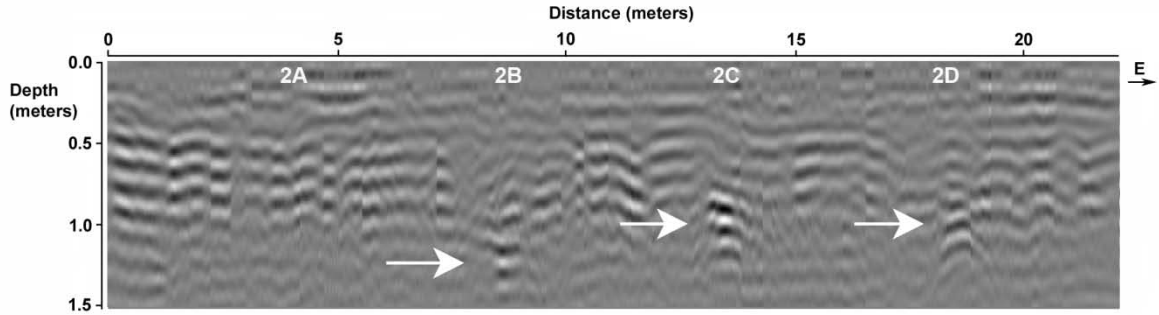

Figure 60: GPR reflection profile using the 500-MHz antenna of Row 2 at 24 months

APPENDIX C: GROUND-PENETRATING RADAR 500-MHZ HORIZONTAL SLICES

MONTH 13

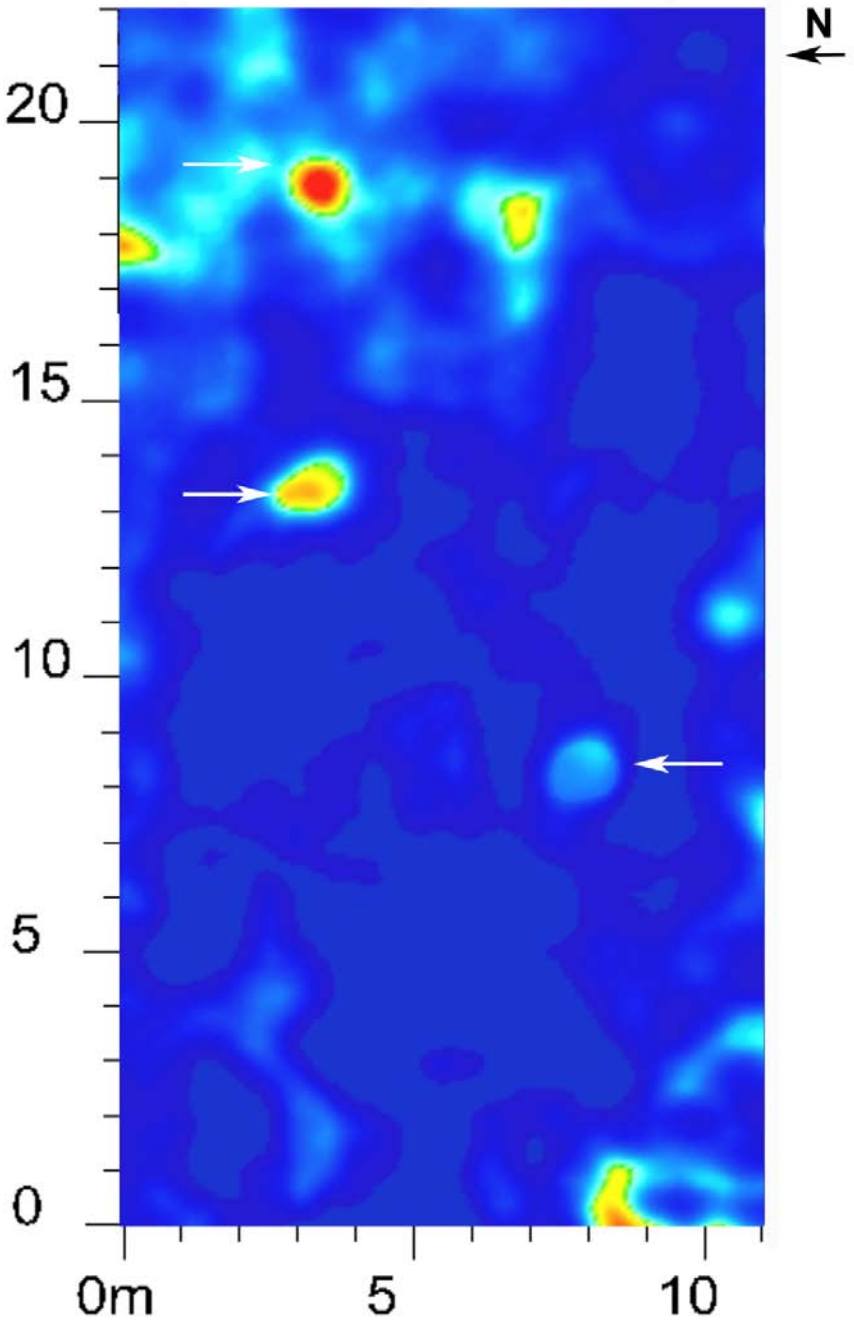

Figure 61: GPR horizontal slice using the 500-MHz antenna at 13 months. The horizontal slice is taken at 28.24 ns, approximately 1.14 m in depth.

MONTH 14
Shallow View

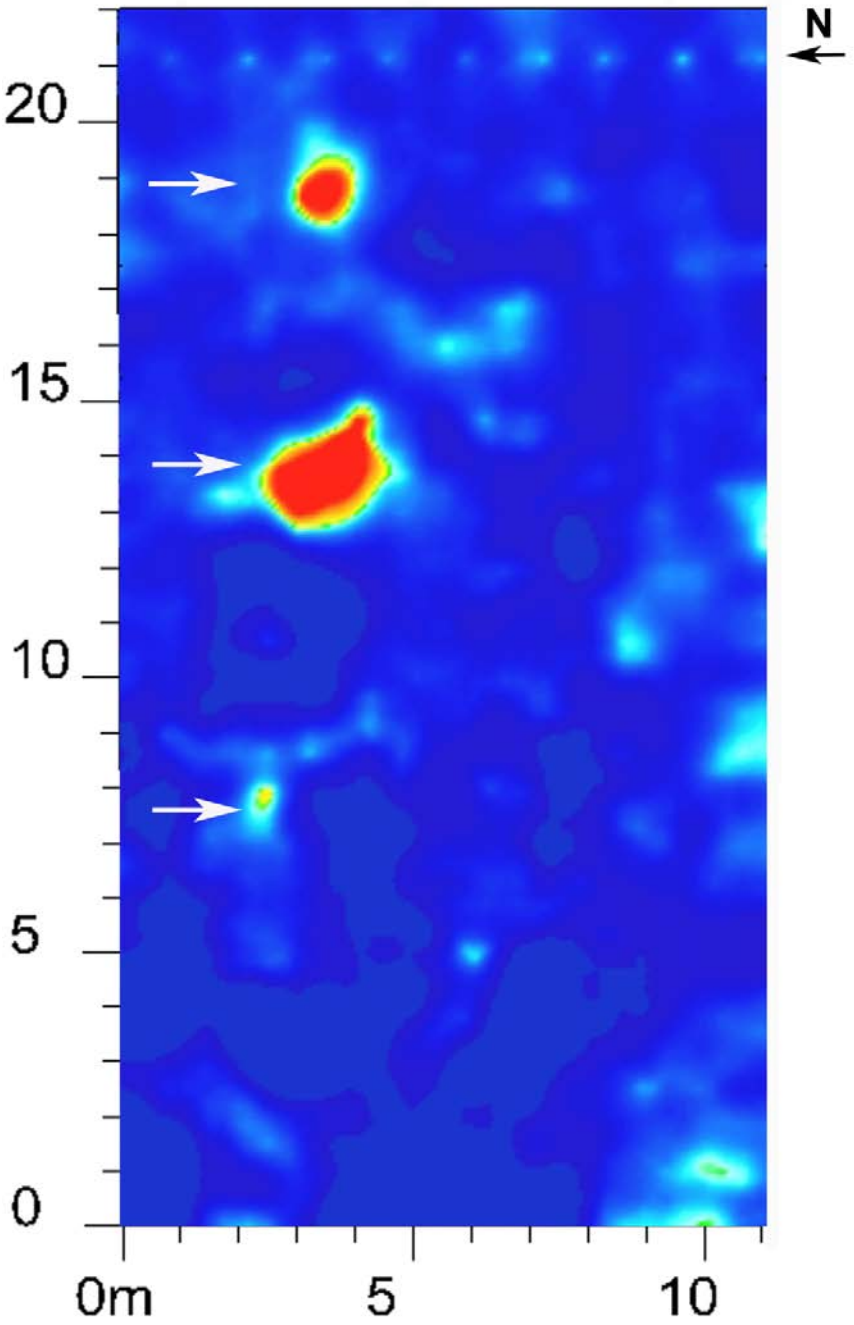

Figure 62: GPR horizontal slice using the 500-MHz antenna at 14 months, shallow view. The horizontal slice is taken at 29.88 ns, approximately 1.0 m.

MONTH 14
Deep View

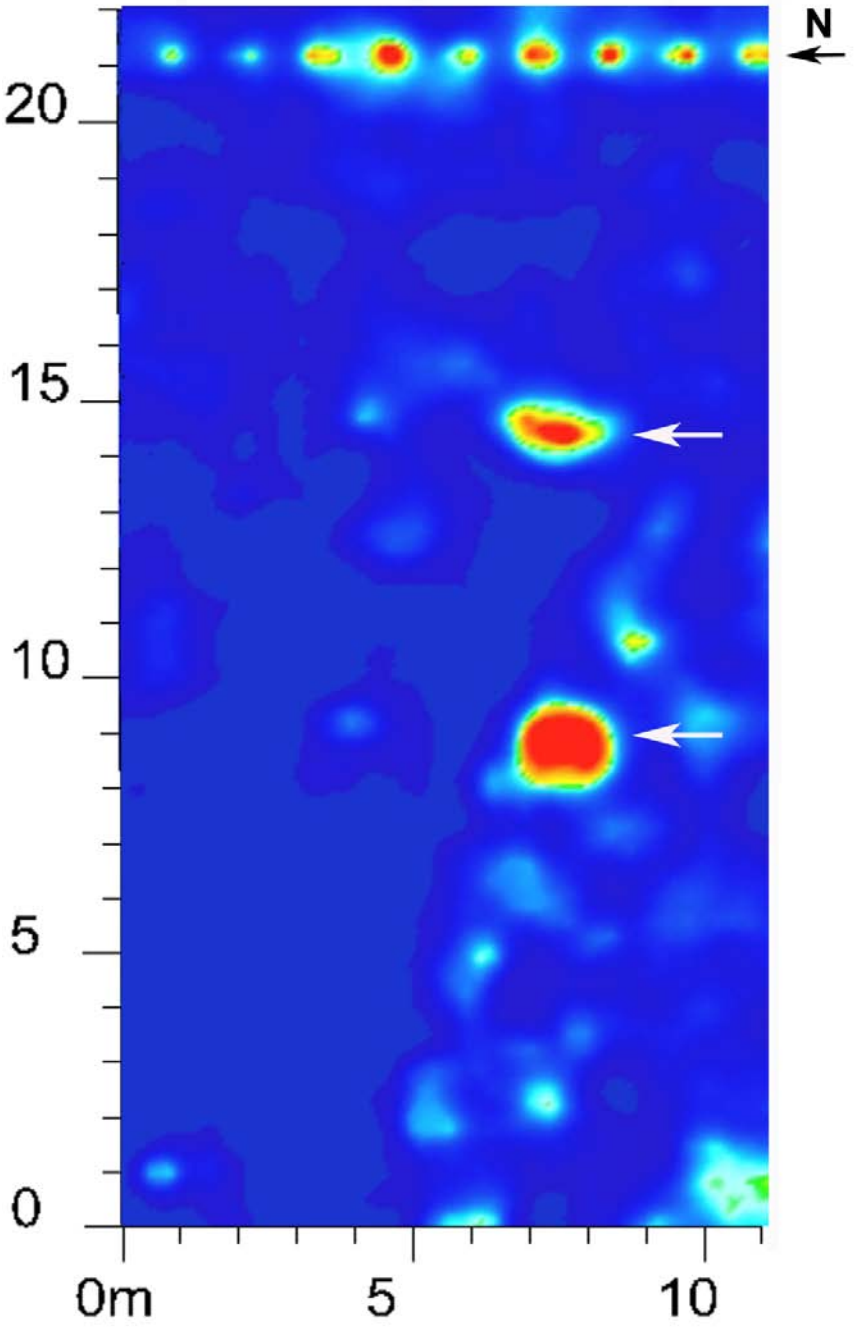

Figure 63: GPR horizontal slice using the 500-MHz antenna at 14 months, deep view. The horizontal slice is taken at 38.14 ns, approximately 1.50 m in depth.

MONTH 15
Shallow View

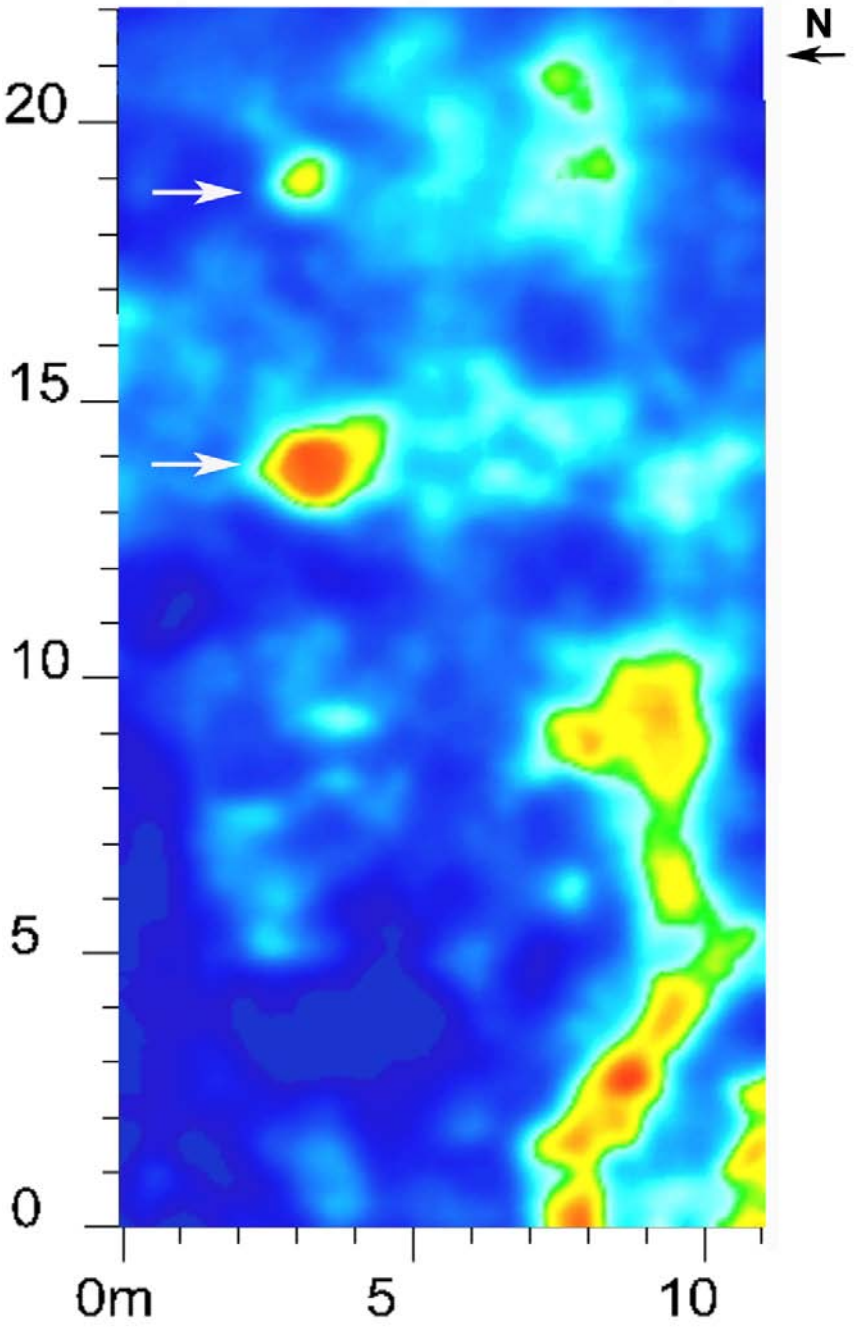

Figure 64: GPR horizontal slice using the 500-MHz antenna at 15 months, shallow view. The horizontal slice is taken at 29.24 ns, approximately 1.0 m in depth.

MONTH 15
Deep View

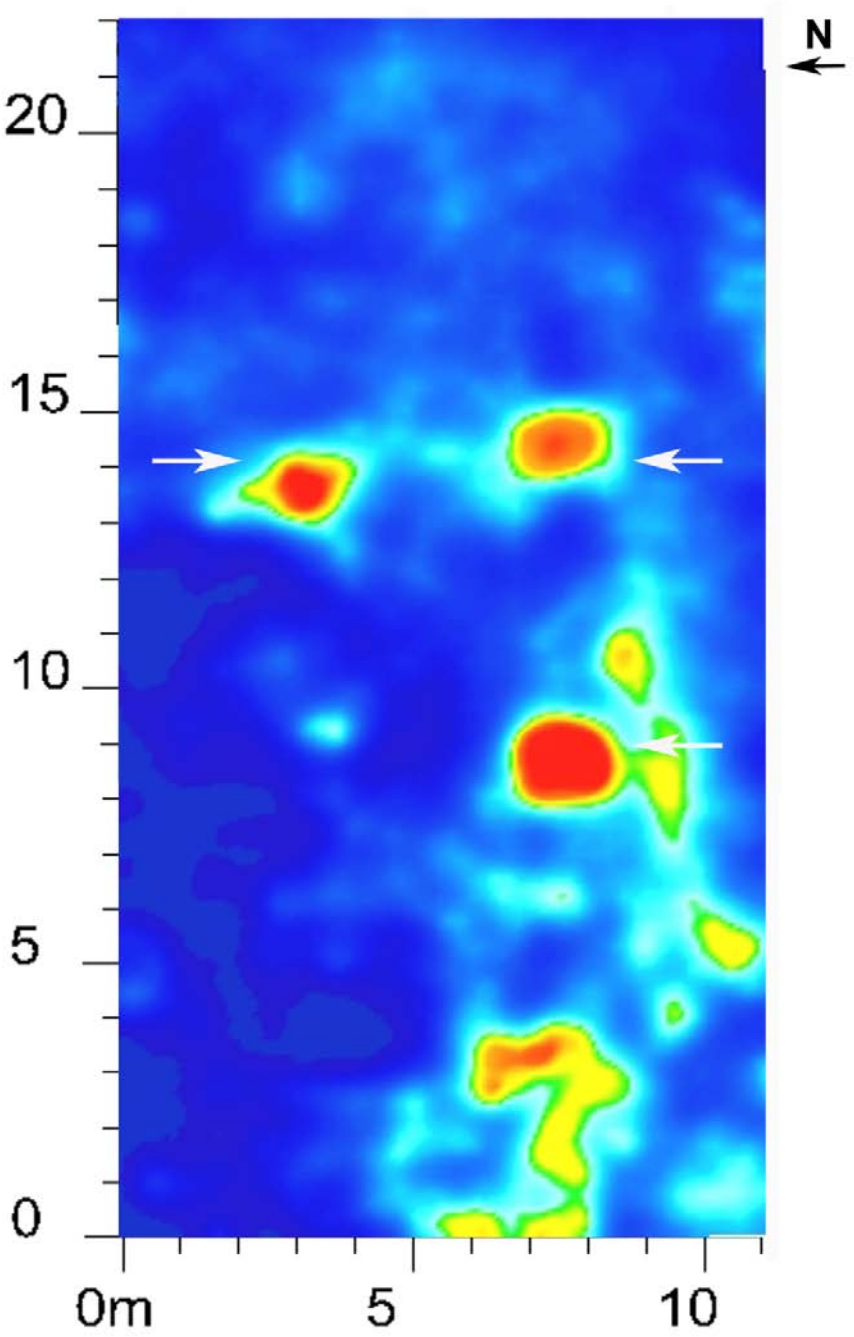

Figure 65: GPR horizontal slice using the 500-MHz antenna at 15 months, deep view. The horizontal slice is taken at 38.14 ns, approximately 1.5 m in depth.

MONTH 16

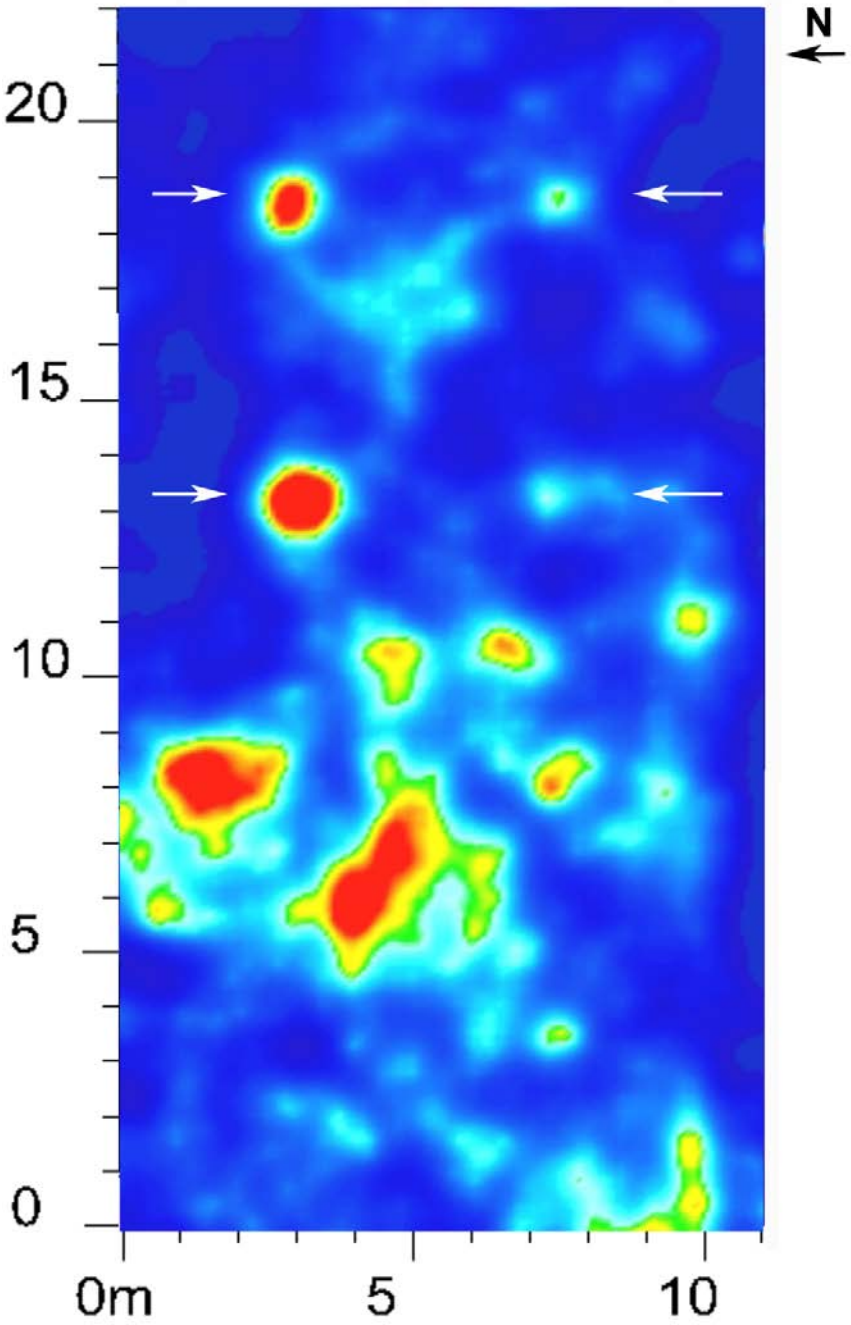

Figure 66: GPR horizontal slice using the 500-MHz antenna at 16 months. The horizontal slice is taken at 22.74 ns, approximately 1.14 m in depth.

MONTH 17
Shallow View

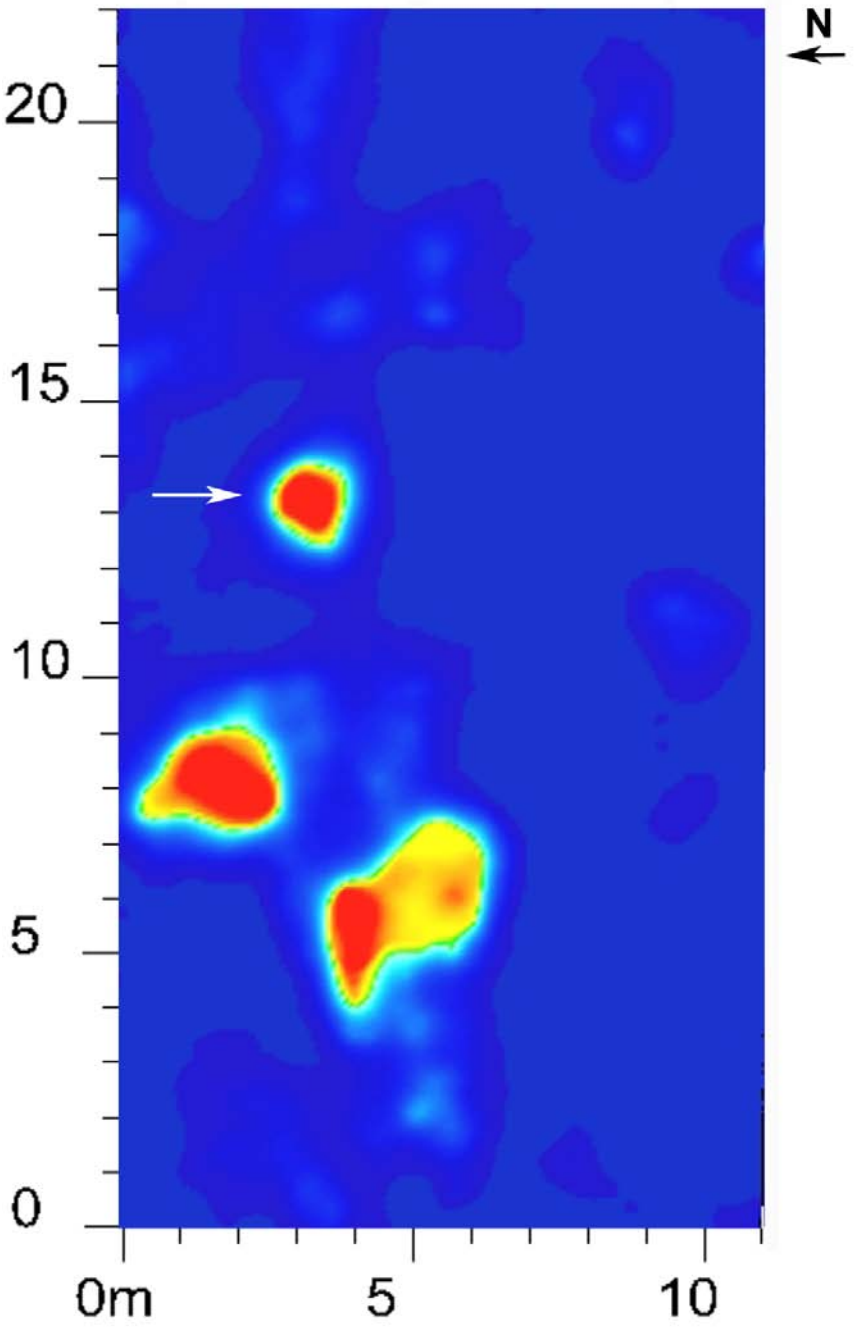

Figure 67: GPR horizontal slice using the 500-MHz antenna at 17 months, shallow view. The horizontal slice is 21.18 ns, approximately 1.10 m in depth.

MONTH 17
Deep View

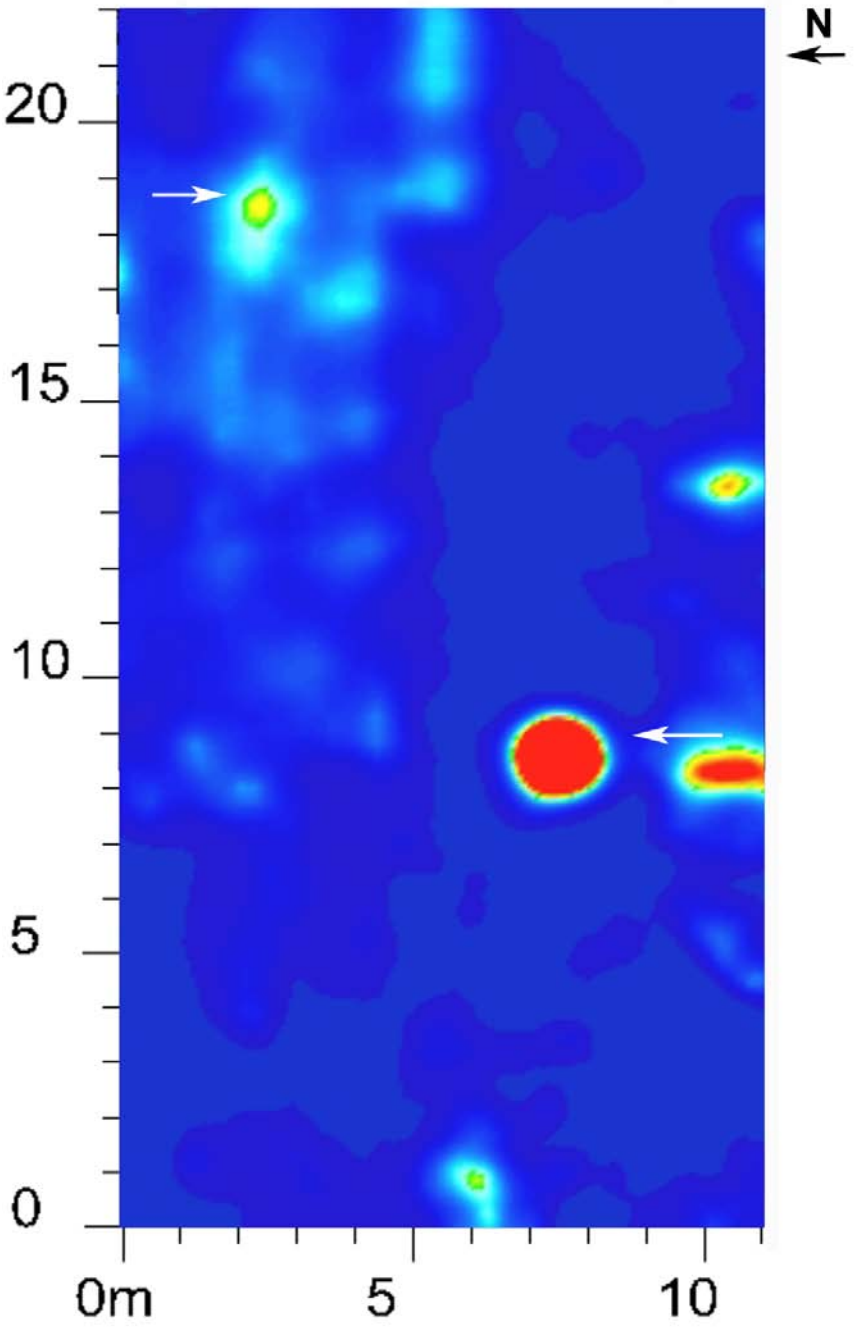

Figure 68: GPR horizontal slice using the 500-MHz antenna at 17 months, deep view. The horizontal slice is taken at 29.59 ns, approximately 1.0 m in depth.

MONTH 18

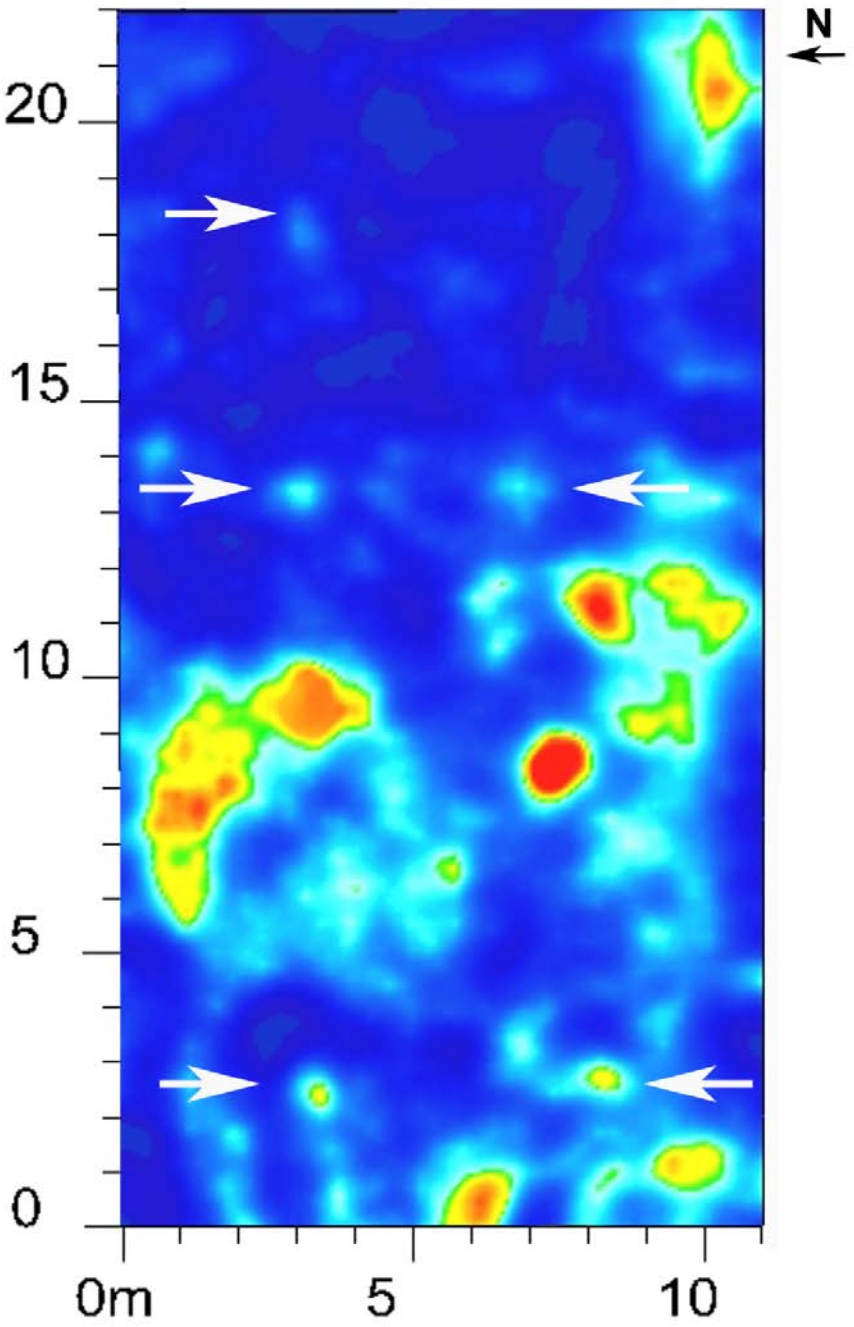

Figure 69: GPR horizontal slice using the 500-MHz antenna at 18 months. The horizontal slice is taken at 24.3 ns, approximately 1.15 m in depth.

MONTH 19

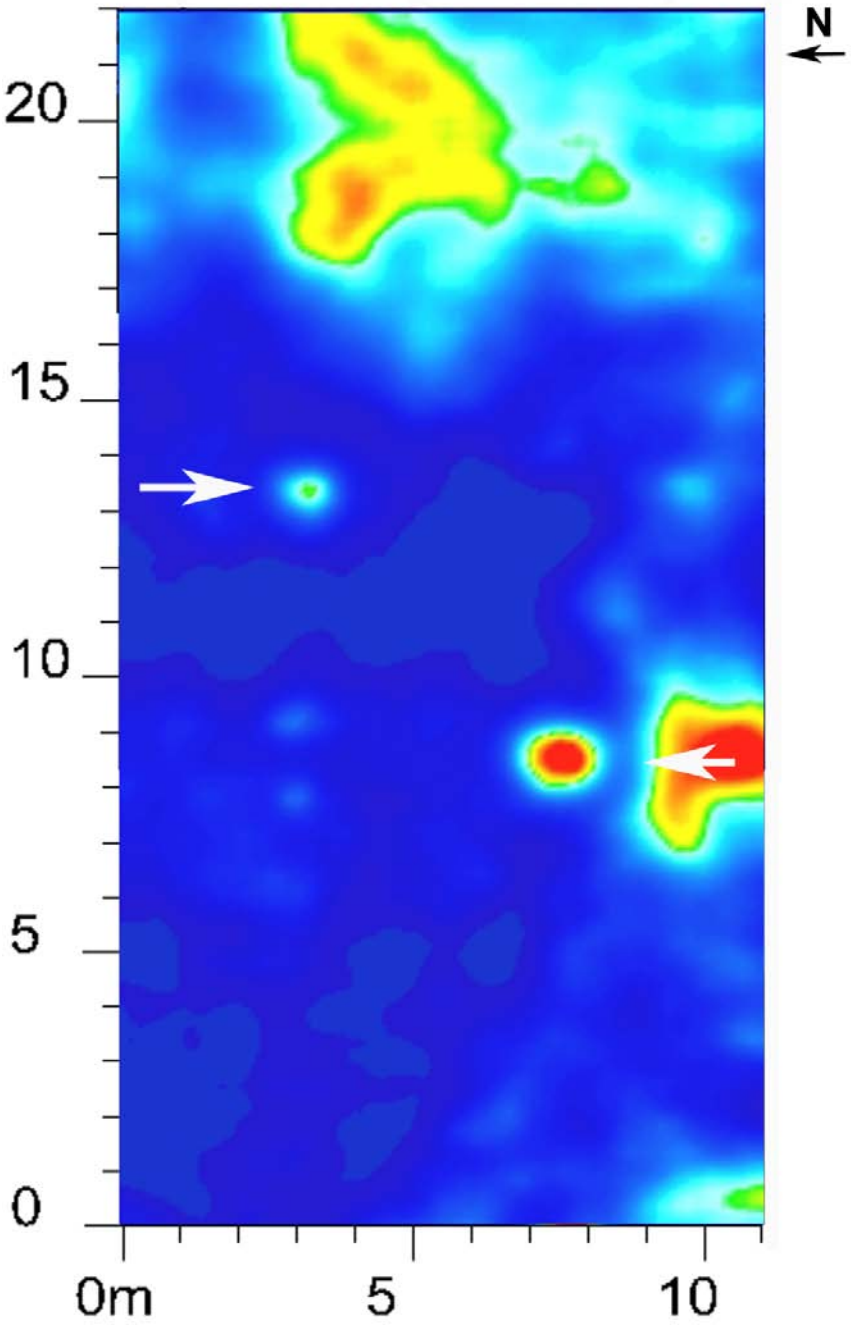

Figure 70: GPR horizontal slice using the 500-MHz antenna at 19 months. The horizontal slice is taken at 32.87 ns, approximately 1.50 m in depth.

MONTH 20
Shallow View

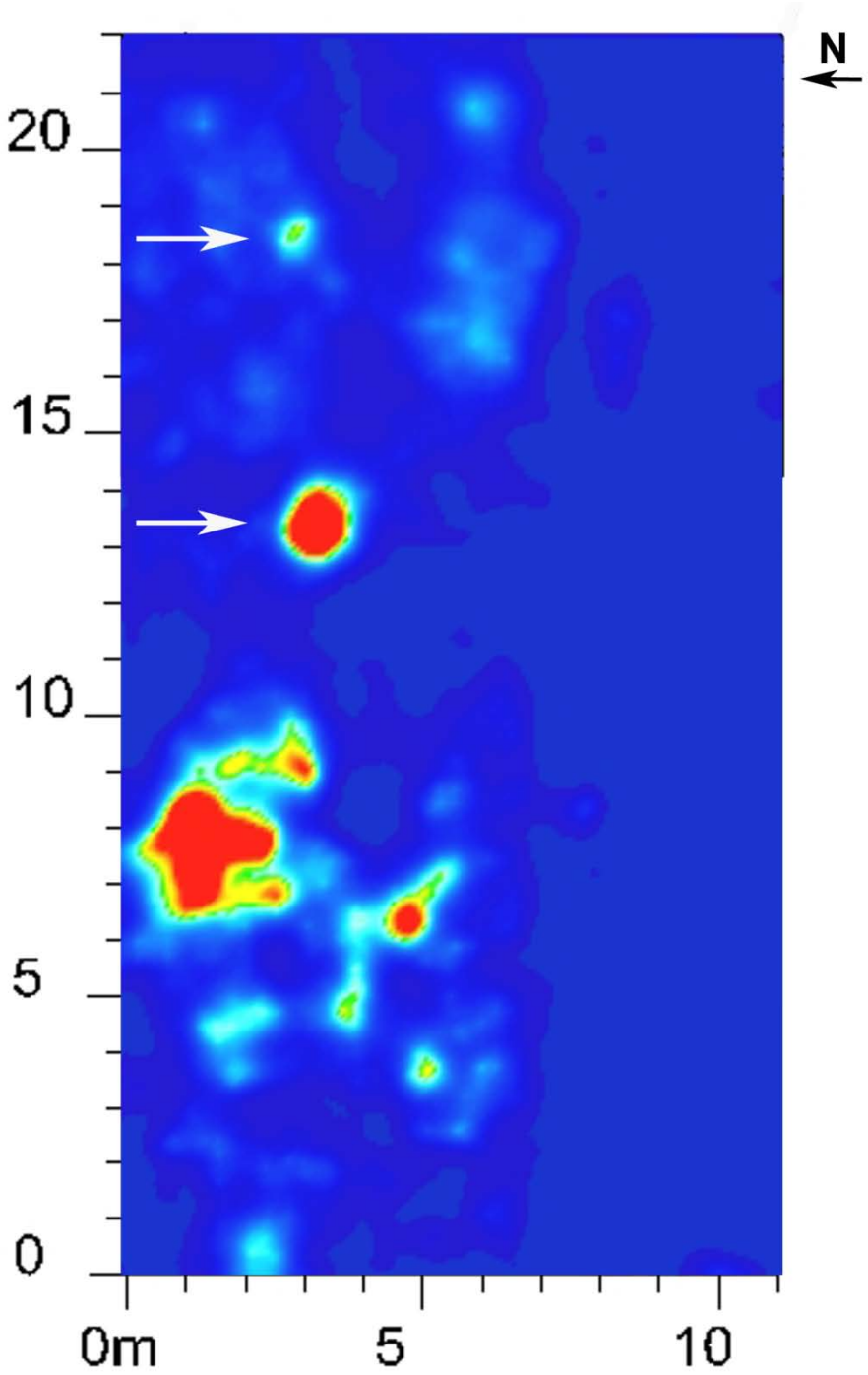

Figure 71: GPR horizontal slice using the 500-MHz antenna at 20 months, shallow view. The horizontal slice is taken at 24.49 ns, approximately 1.0 m in depth.

MONTH 20
Deep View

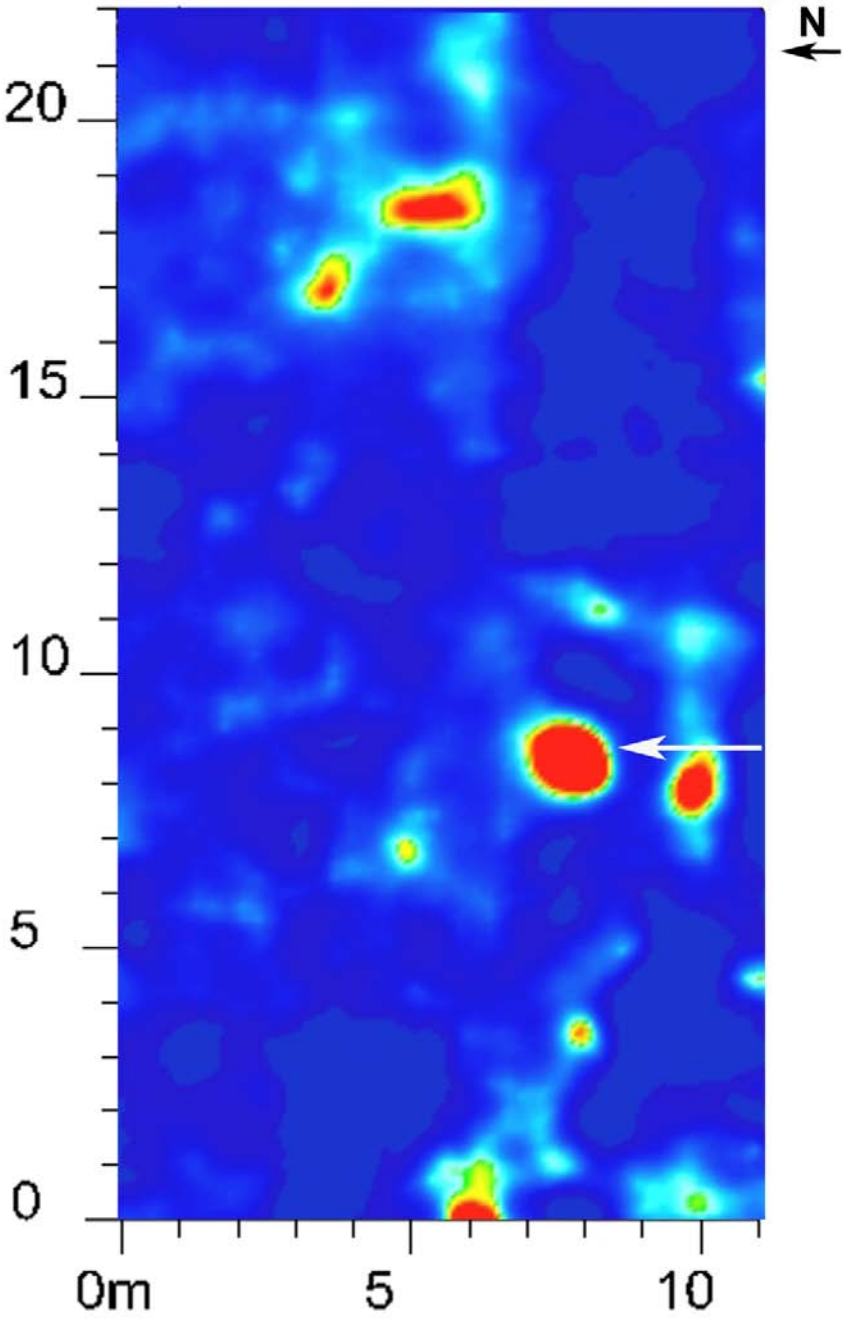

Figure 72: GPR horizontal slice using the 500-MHz antenna at 20 months, deep view. The horizontal slice is taken at 30.49 ns, approximately 1.5 m in depth.

MONTH 21

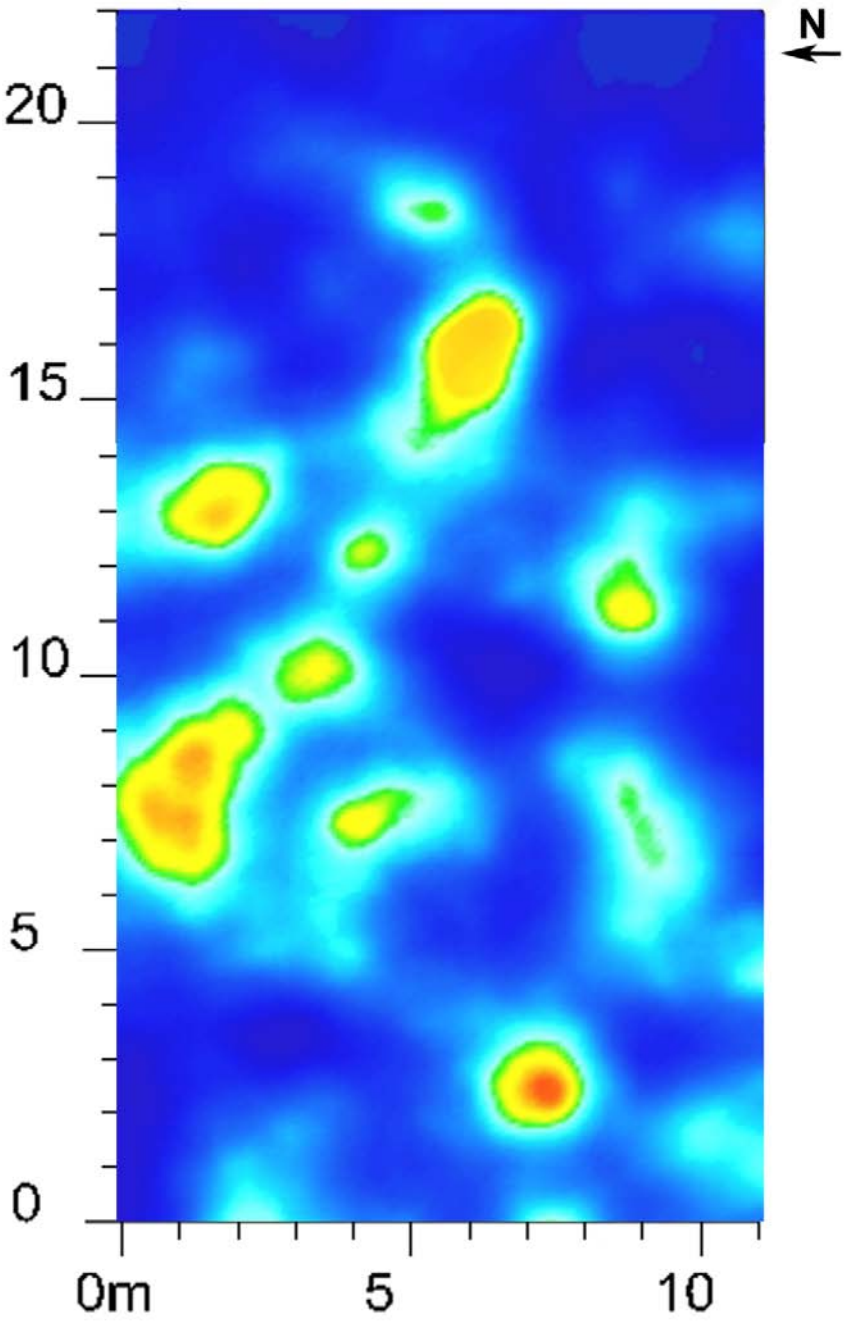

Figure 73: GPR horizontal slice using the 500-MHz antenna at 21 months. The horizontal slice is taken at 25.85 ns, approximately 1.25 m in depth.

MONTH 22

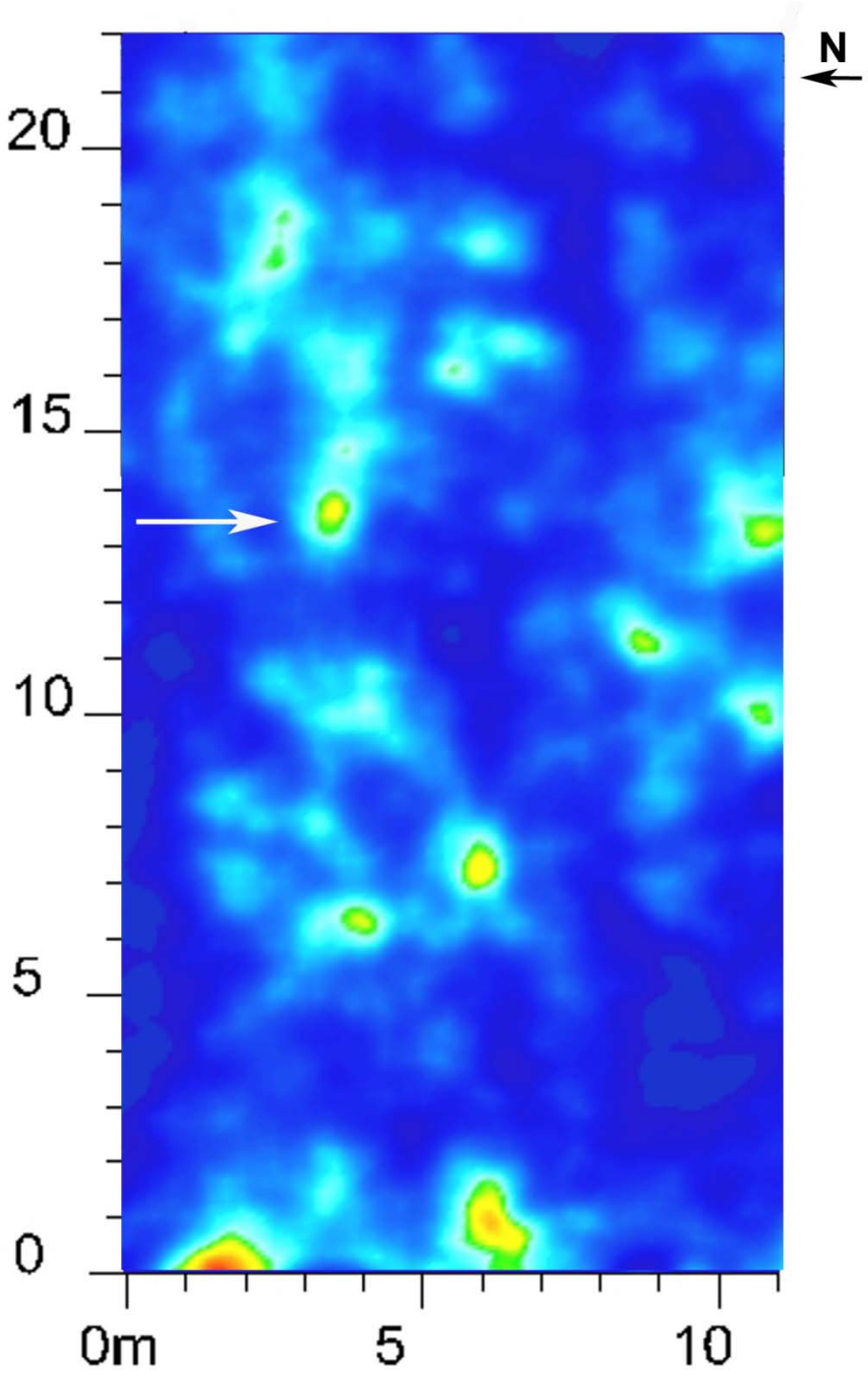

Figure 74: GPR horizontal slice using the 500-MHz antenna at 22 months. The horizontal slice is taken at 26.59 ns, approximately 1.25 m in depth.

MONTH 23

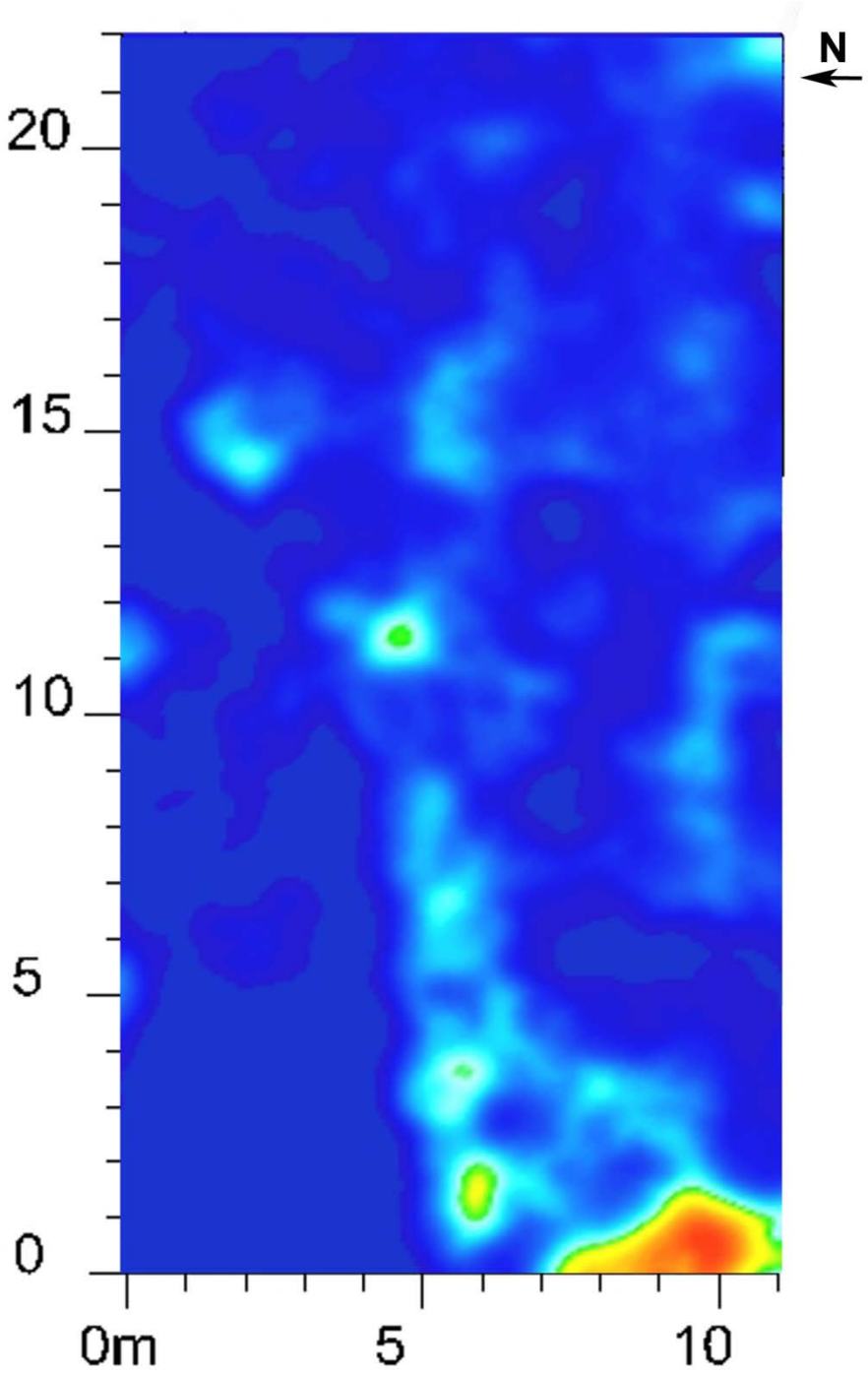

Figure 75: GPR horizontal slice using the 500-MHz antenna at 23 months. The horizontal slice is taken at 26.12 ns, approximately 1.25 m in depth.

MONTH 24

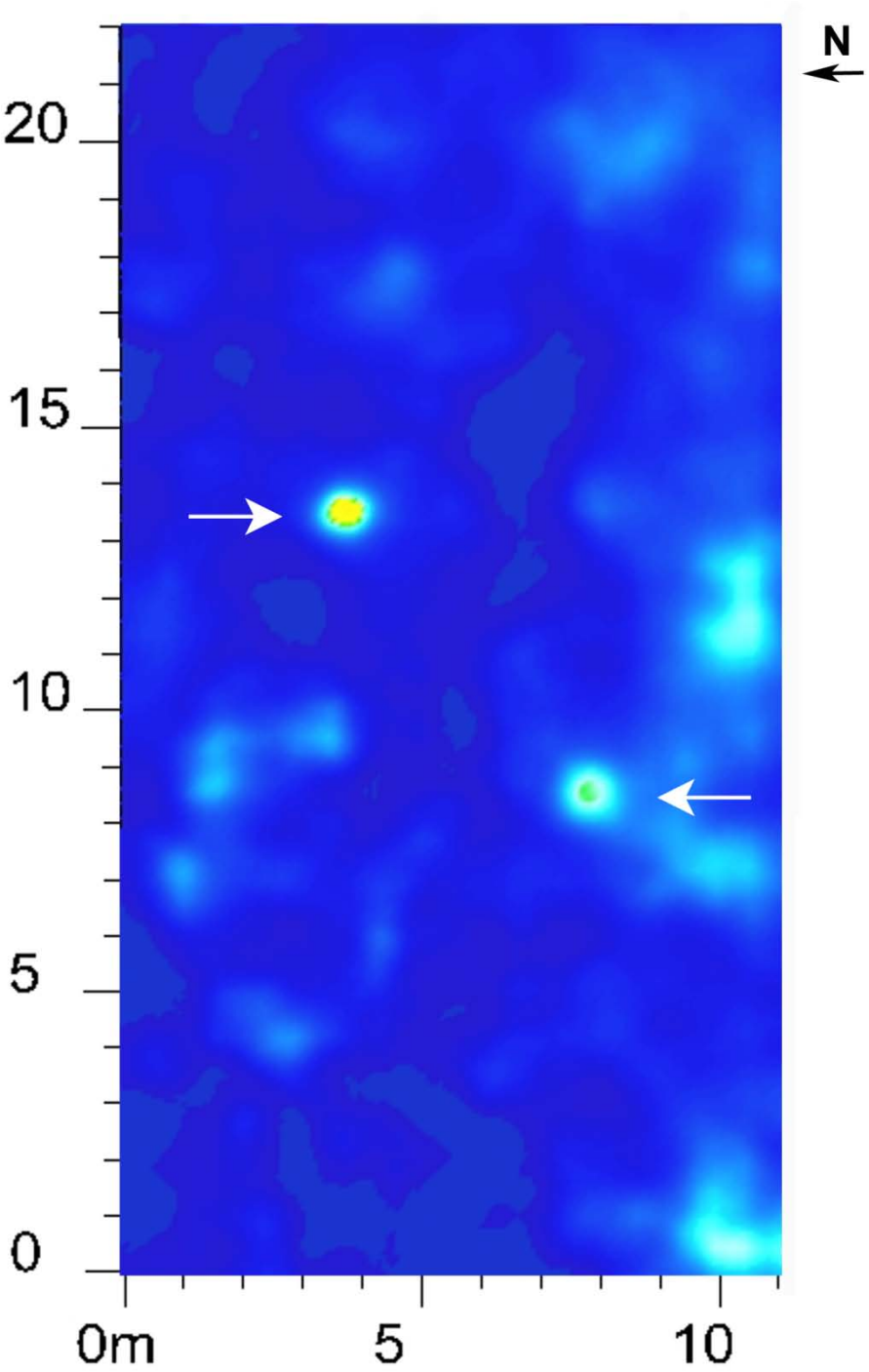

Figure 76: GPR horizontal slice using the 500-MHz antenna at 23 months. The horizontal slice is taken at 25.61 ns, approximately 1.30 m in depth.

APPENDIX D: GROUND-PENETRATING RADAR 250-MHZ REFLECTION PROFILES

MONTH 13

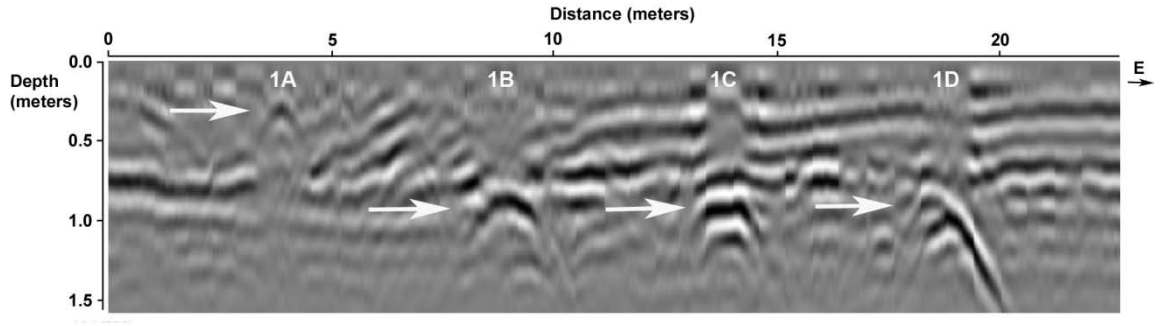

Figure 77: GPR reflection profile using the 250-MHz antenna of Row 1 at 13 months

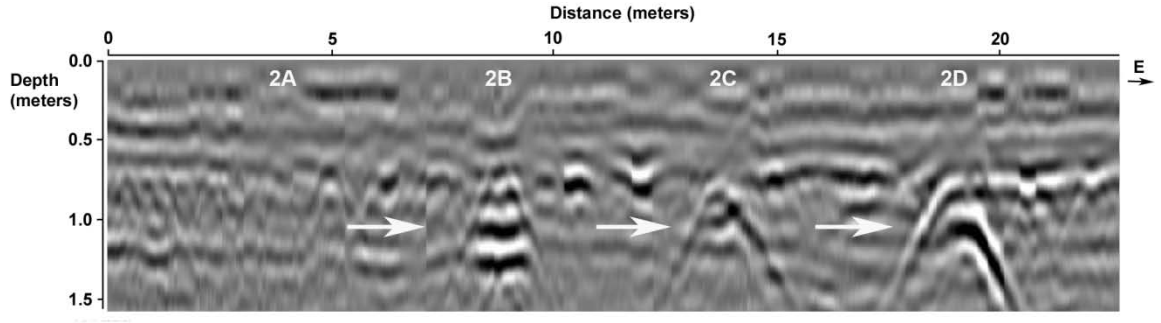

Figure 78: GPR reflection profile using the 250-MHz antenna of Row 2 at 13 months

MONTH 14

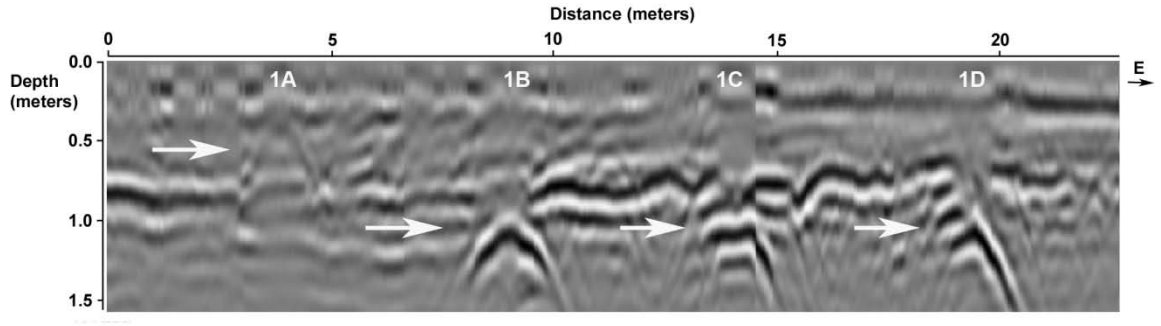

Figure 79: GPR reflection profile using the 250-MHz antenna of Row 1 at 14 months

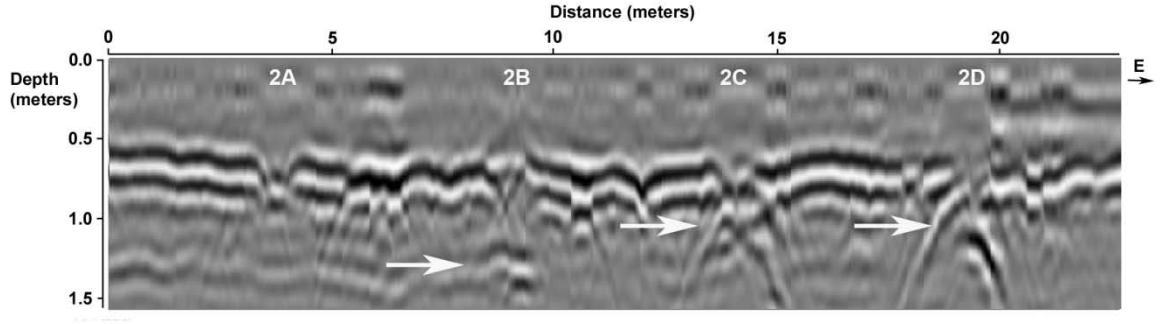

Figure 80: GPR reflection profile using the 250-MHz antenna of Row 2 at 14 months

MONTH 15

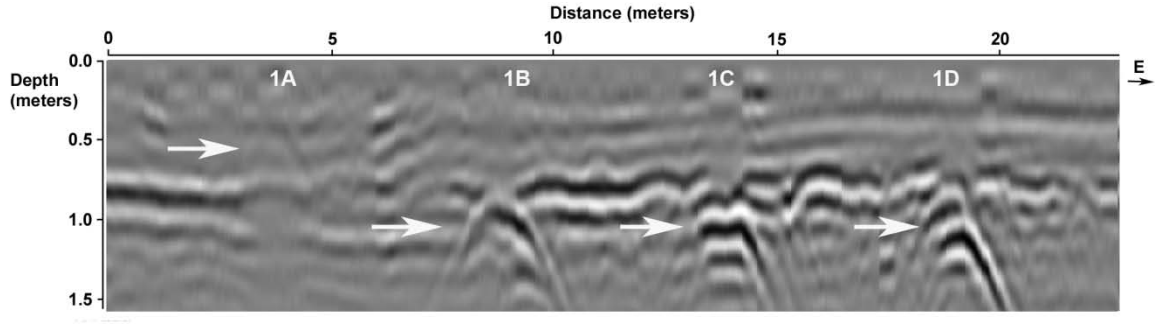

Figure 81: GPR reflection profile using the 250-MHz antenna of Row 1 at 15 months

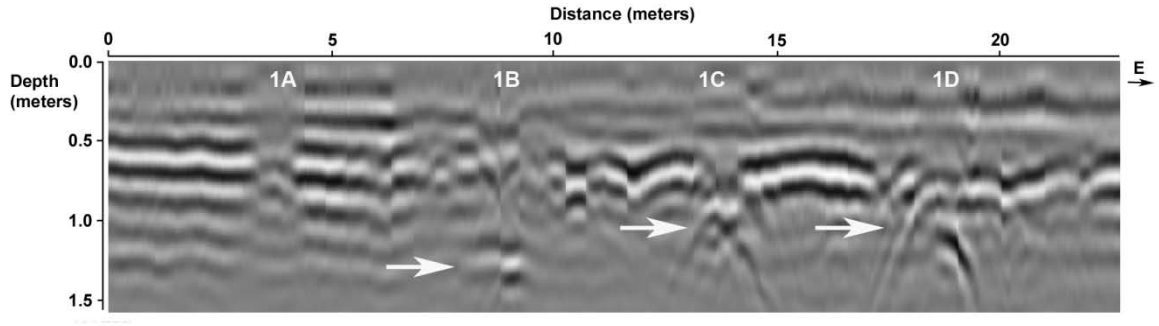

Figure 82: GPR reflection profile using the 250-MHz antenna of Row 2 at 15 months

MONTH 16

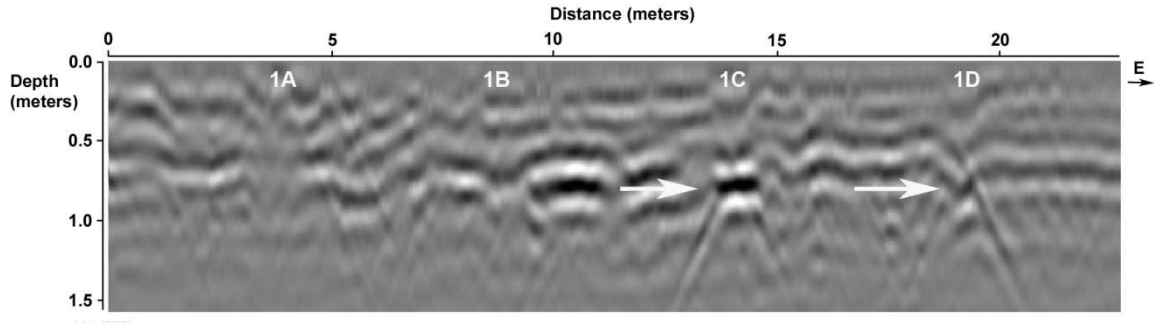

Figure 83: GPR reflection profile using the 250-MHz antenna of Row 1 at 16 months

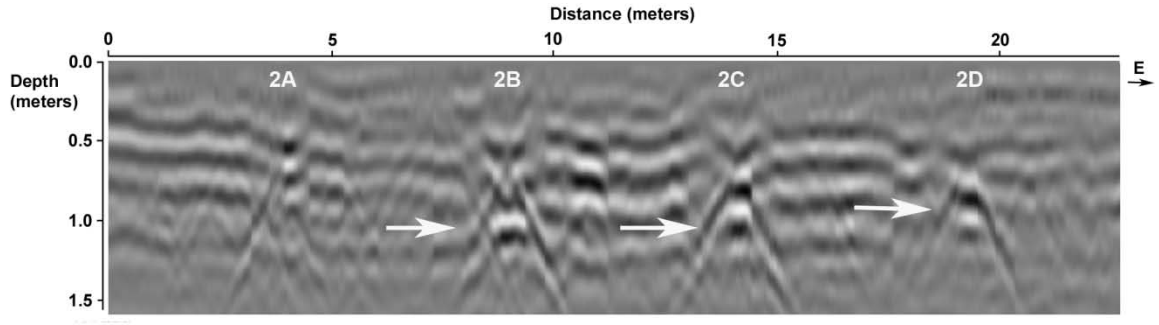

Figure 84: GPR reflection profile using the 250-MHz antenna of Row 2 at 16 months

MONTH 17

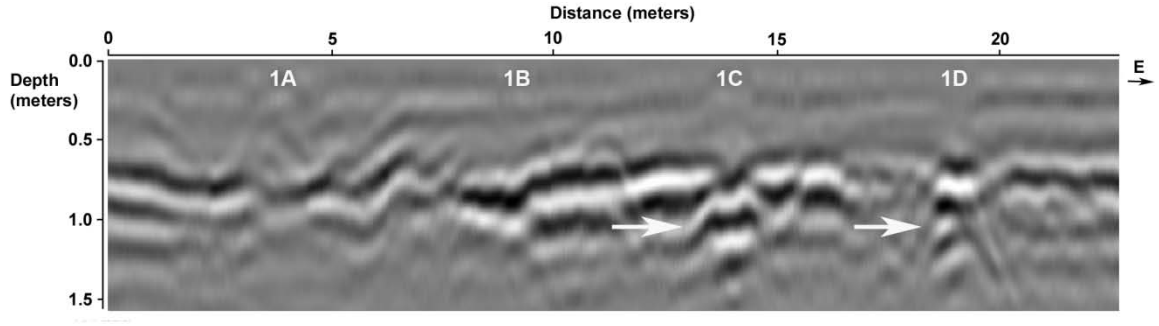

Figure 85: GPR reflection profile using the 250-MHz antenna of Row 1 at 17 months

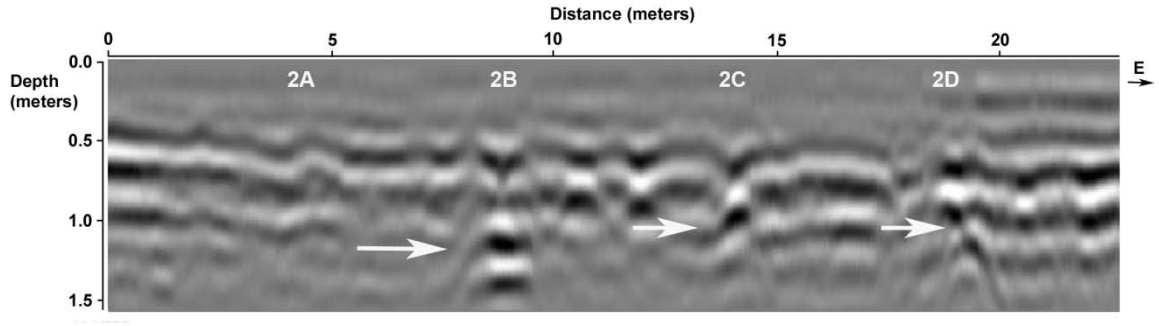

Figure 86: GPR reflection profile using the 250-MHz antenna of Row 2 at 17 months

MONTH 18

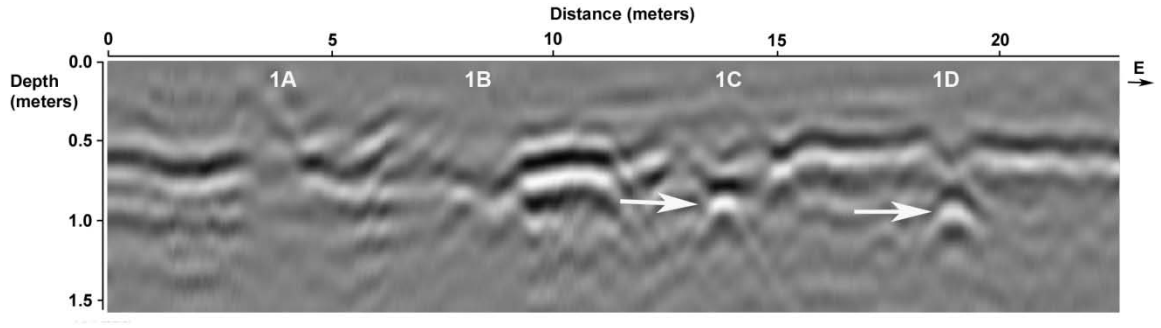

Figure 87: GPR reflection profile using the 250-MHz antenna of Row 1 at 18 months

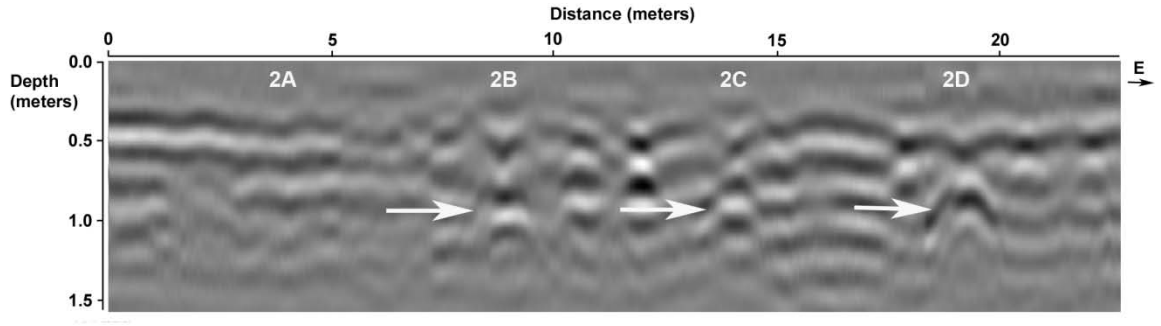

Figure 88: GPR reflection profile using the 250-MHz antenna of Row 2 at 18 months

MONTH 19

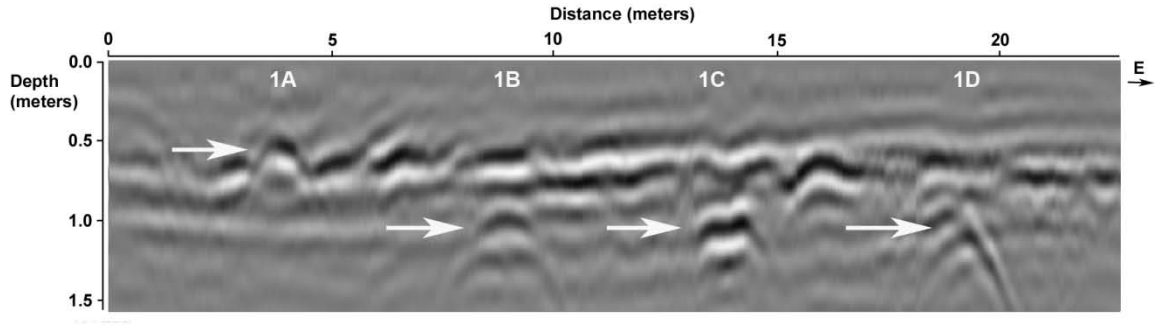

Figure 89: GPR reflection profile using the 250-MHz antenna of Row 1 at 19 months

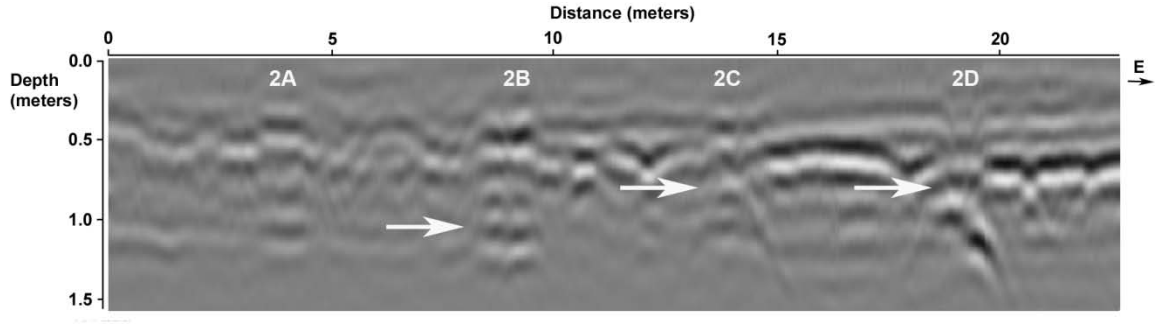

Figure 90: GPR reflection profile using the 250-MHz antenna of Row 2 at 19 months

MONTH 20

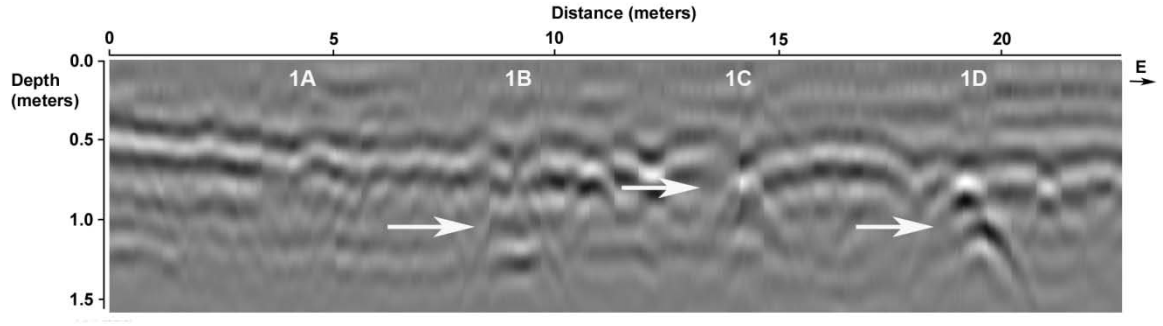

Figure 91: GPR reflection profile using the 250-MHz antenna of Row 1 at 20 months

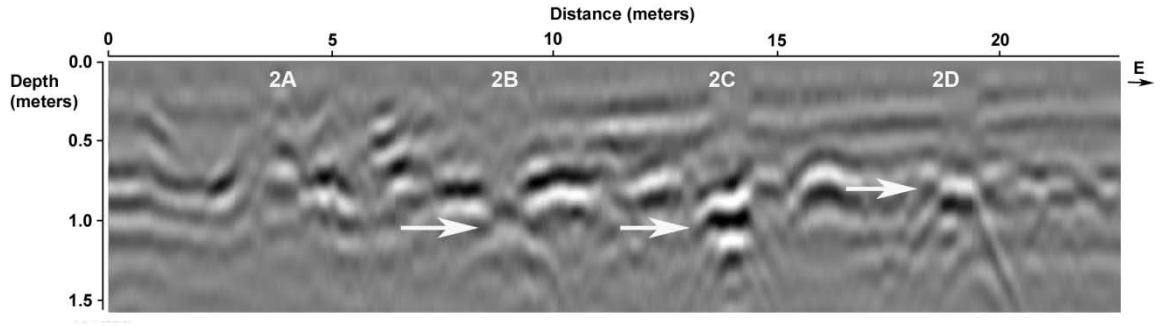

Figure 92: GPR reflection profile using the 250-MHz antenna of Row 2 at 20 months

MONTH 21

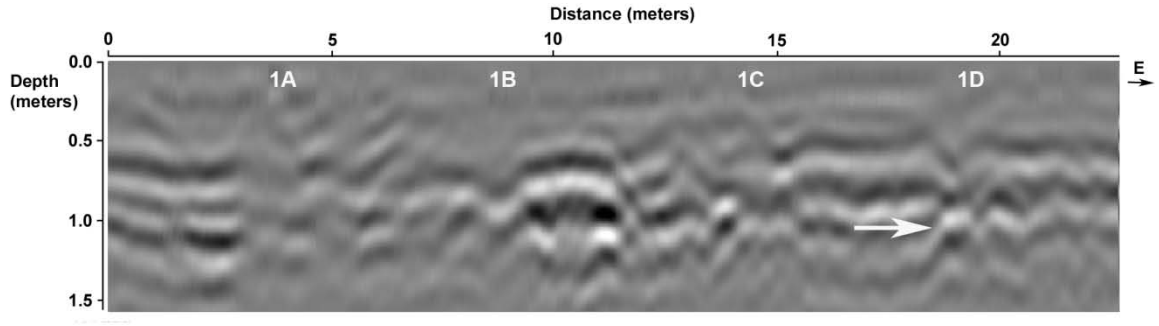

Figure 93: GPR reflection profile using the 250-MHz antenna of Row 1 at 21 months

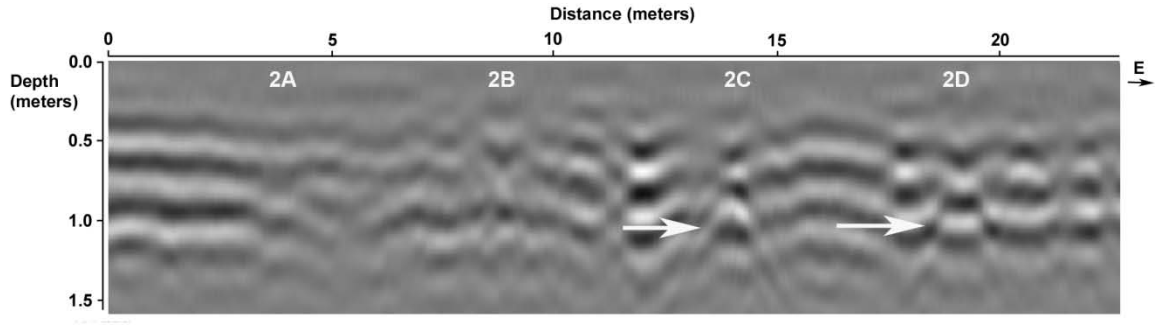

Figure 94: GPR reflection profile using the 250-MHz antenna of Row 2 at 21 months

MONTH 22

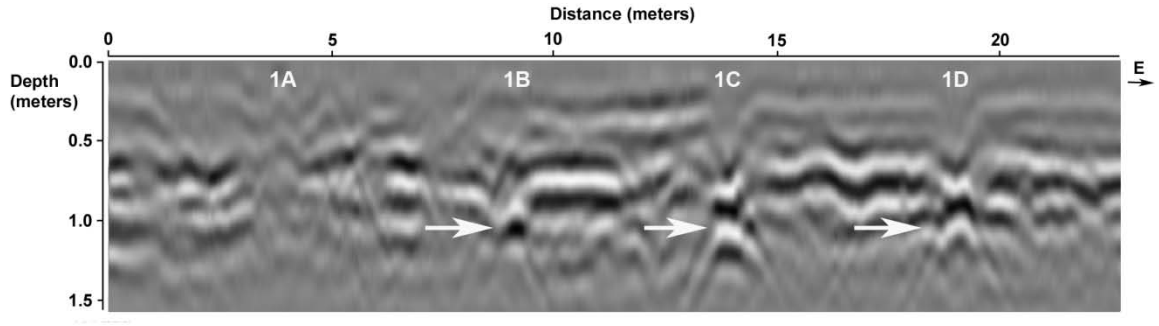

Figure 95: GPR reflection profile using the 250-MHz antenna of Row 1 at 22 months

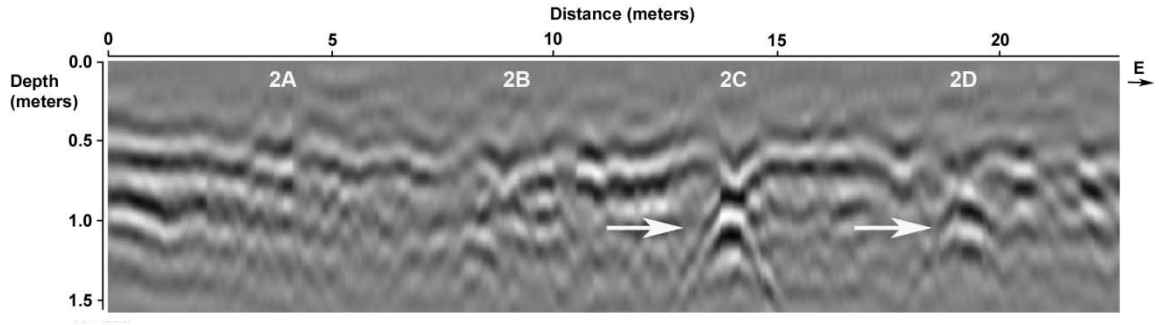

Figure 96: GPR reflection profile using the 250-MHz antenna of Row 2 at 22 months

MONTH 23

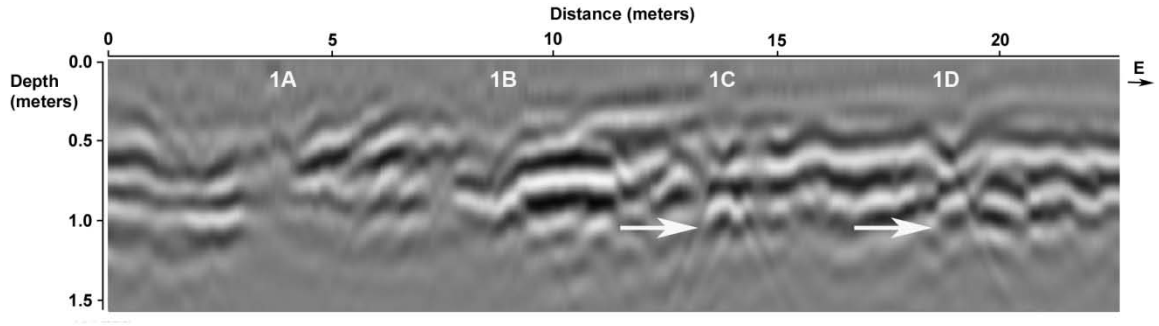

Figure 97: GPR reflection profile using the 250-MHz antenna of Row 1 at 23 months

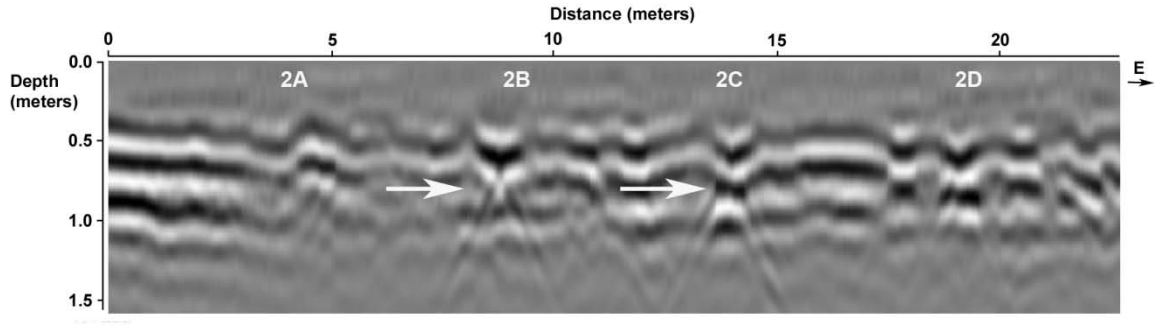

Figure 98: GPR reflection profile using the 250-MHz antenna of Row2 at 23 months

MONTH 24

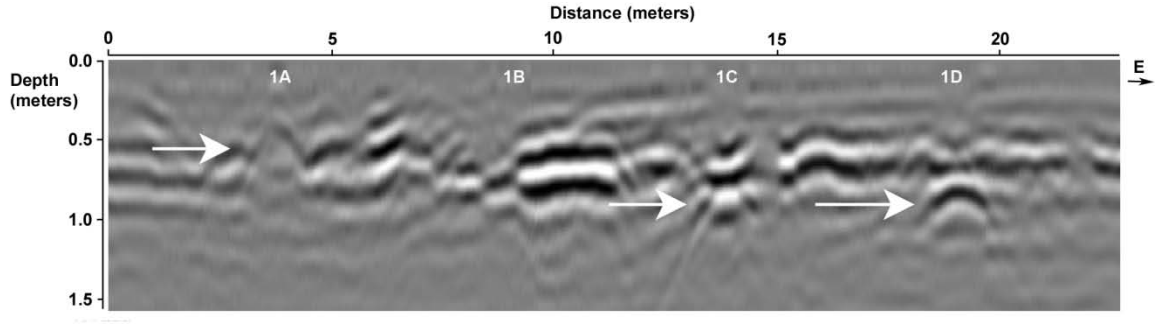

Figure 99: GPR reflection profile using the 250-MHz antenna of Row 1 at 24 months

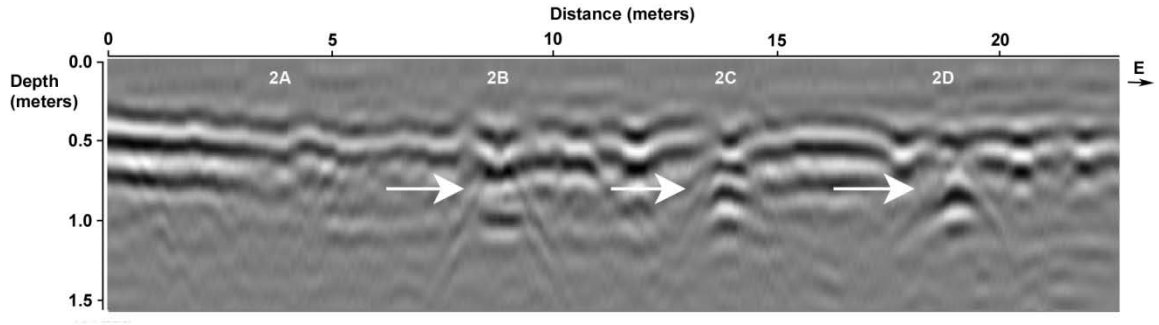

Figure 100: GPR reflection profile using the 250-MHz antenna of Row2 at 24 months

APPENDIX E: GROUND-PENETRATING RADAR 250-MHZ HORIZONTAL SLICES

MONTH 13

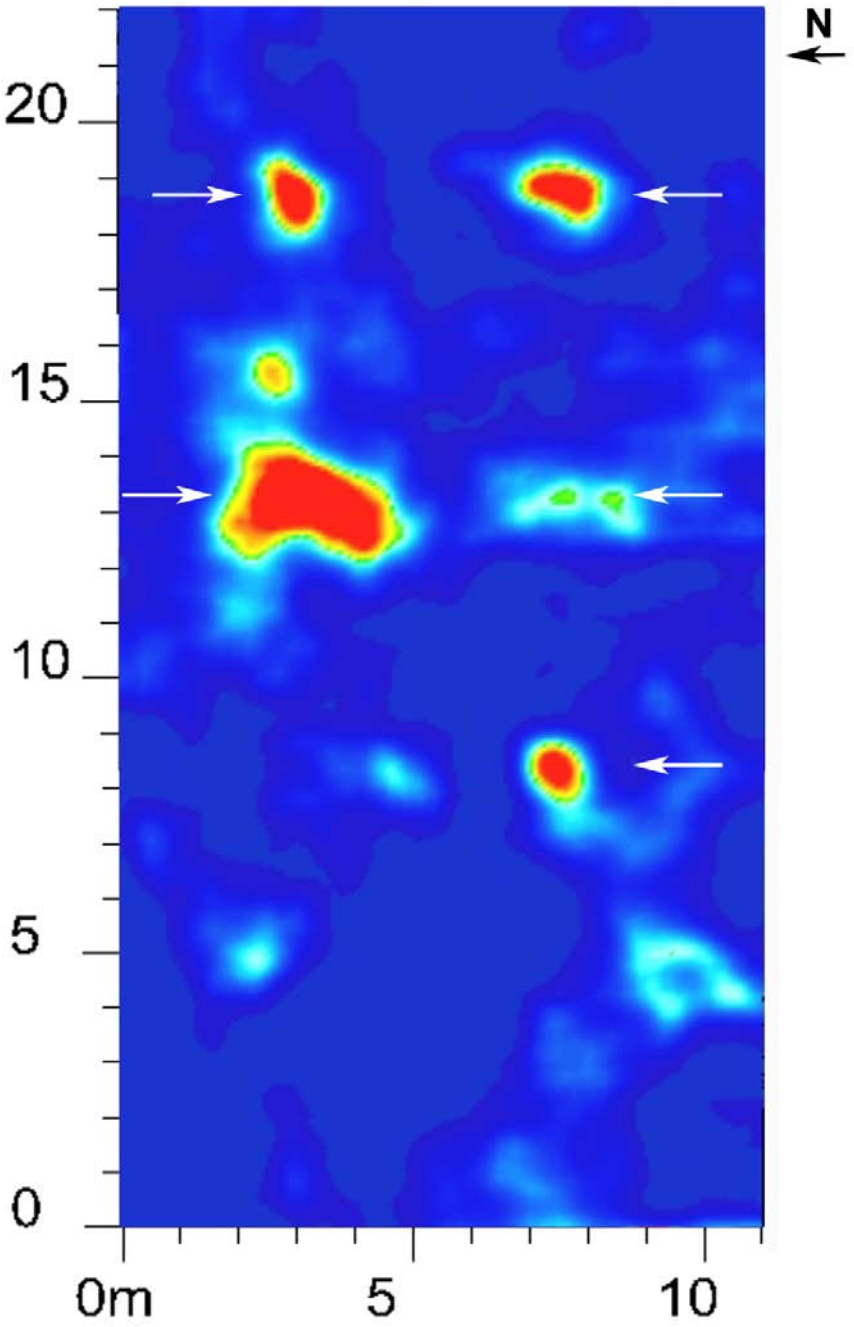

Figure E1: GPR horizontal slice using the 250-MHz antenna at 13 months. The horizontal slice is taken at 31.13 ns, approximately 1.06 m depth.

MONTH 14

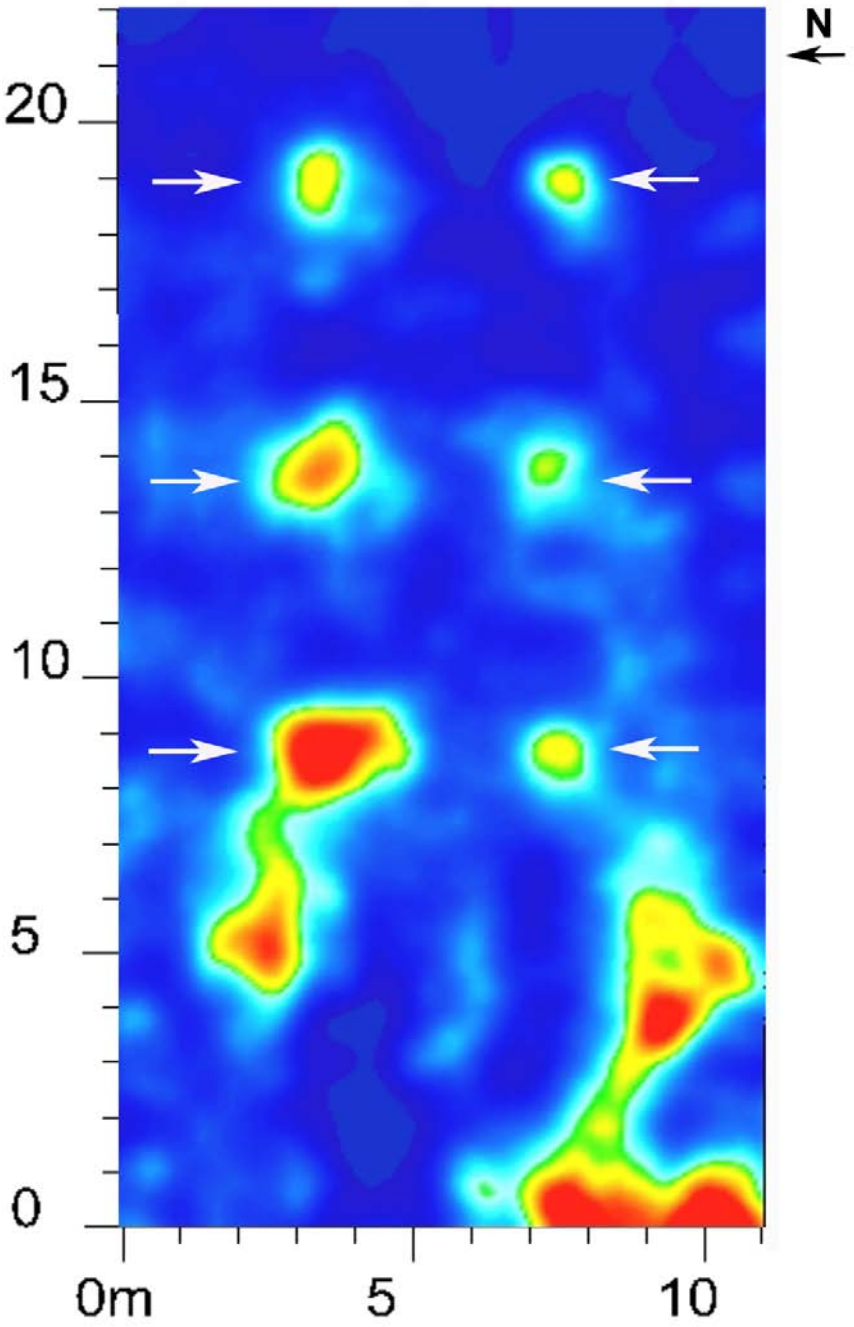

Figure 101: GPR horizontal slice using the 250-MHz antenna at 14 months. The horizontal slice is taken at 31.14 ns, approximately 1.14 m in depth.

MONTH 15

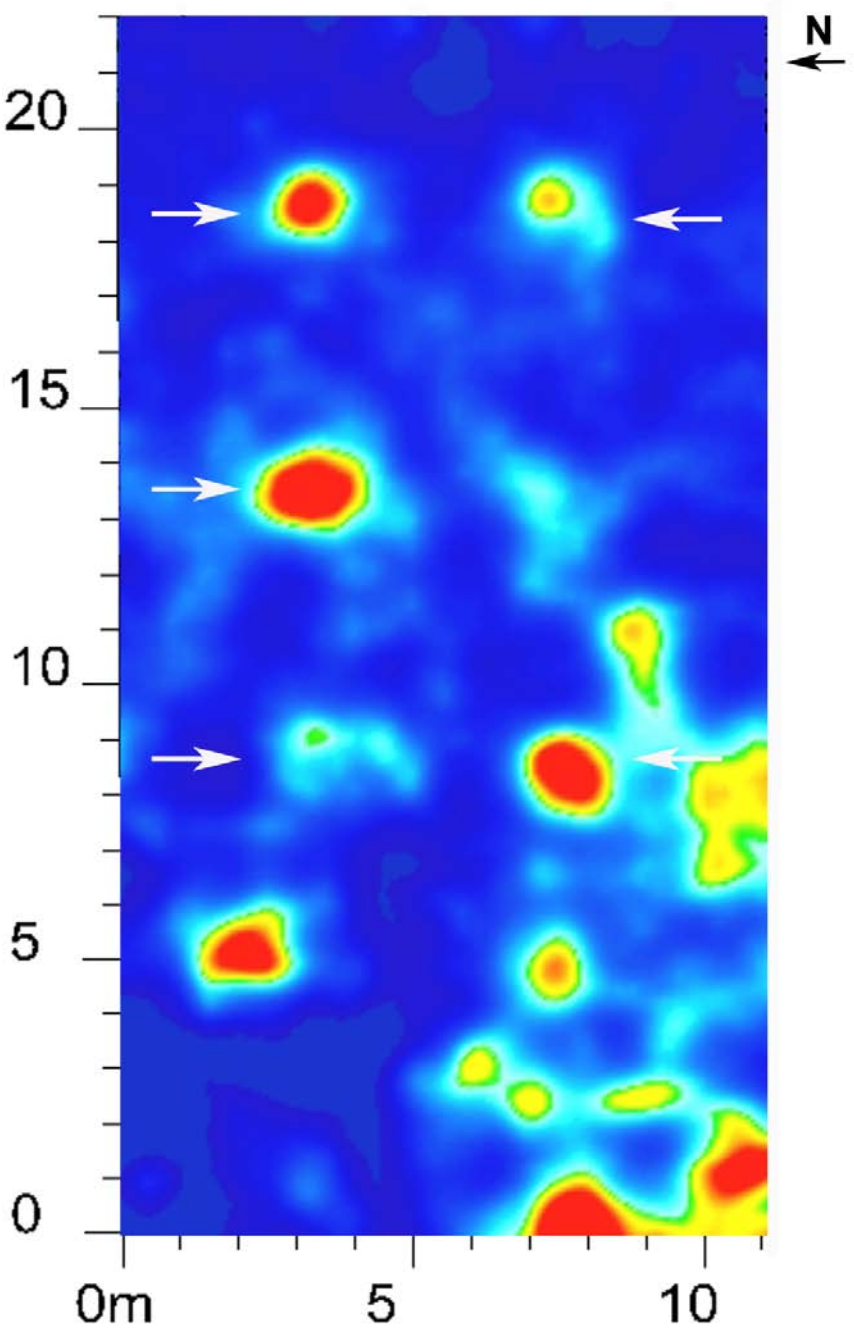

Figure 102: GPR horizontal slice using the 250-MHz antenna at 15 months. The horizontal slice is taken at 31.13 ns, approximately 1.14 m in depth.

MONTH 16

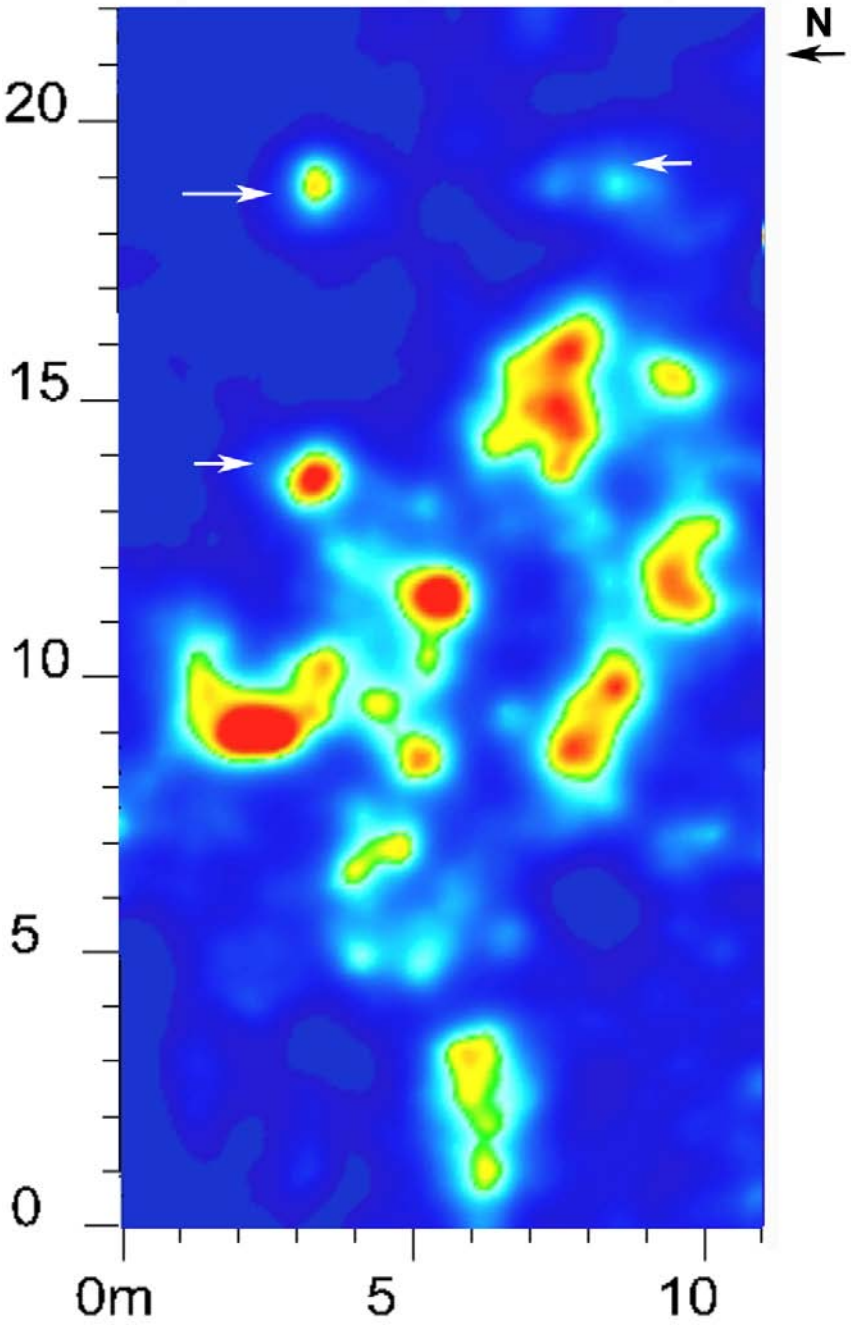

Figure 103: GPR horizontal slice using the 250-MHz antenna at 16 months. The horizontal slice is taken at 27.19 ns, approximately 1.11 m in depth.

MONTH 17

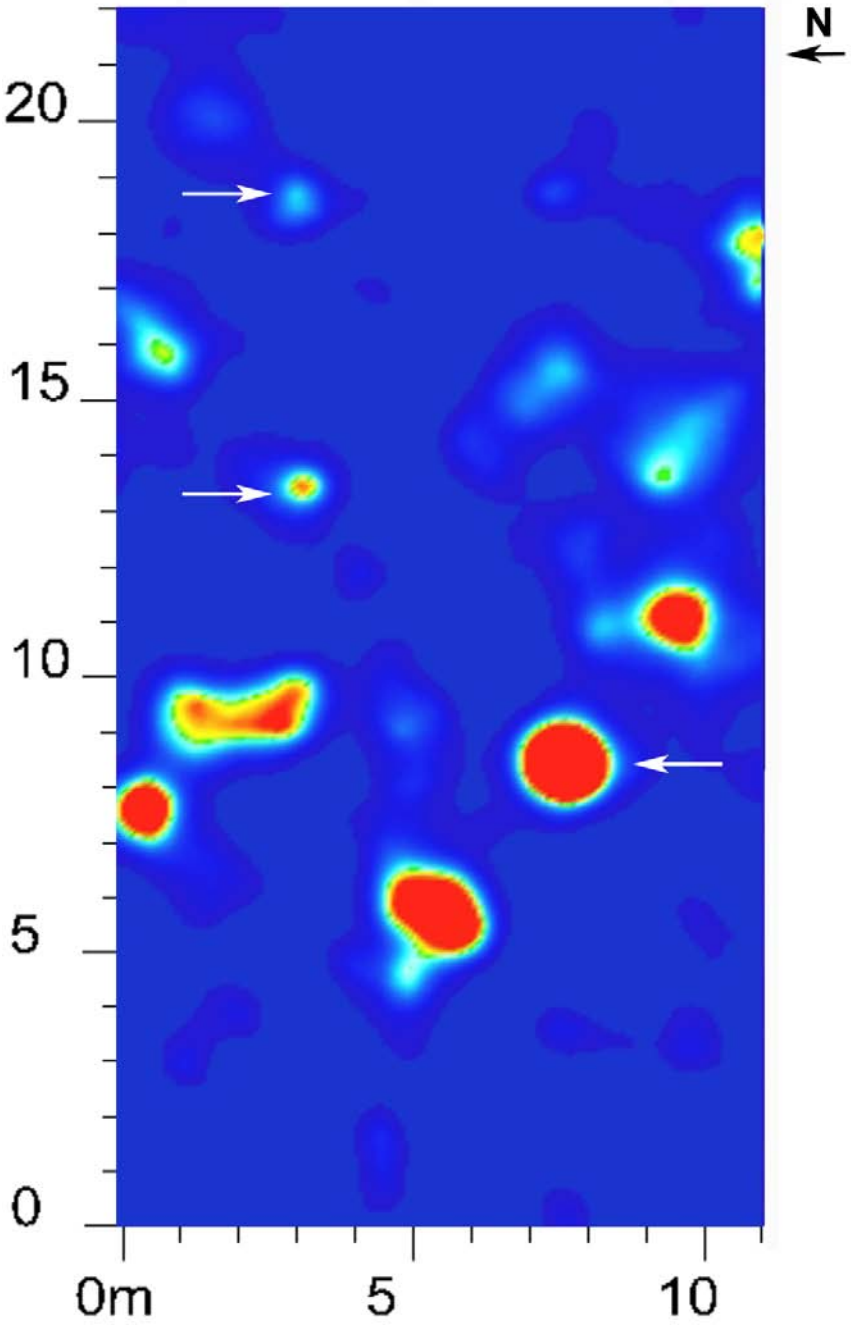

Figure 104: GPR horizontal slice using the 250-MHz antenna at 17 months. The horizontal slice is taken at 33.03 ns, approximately 1.30 m in depth.

MONTH 18

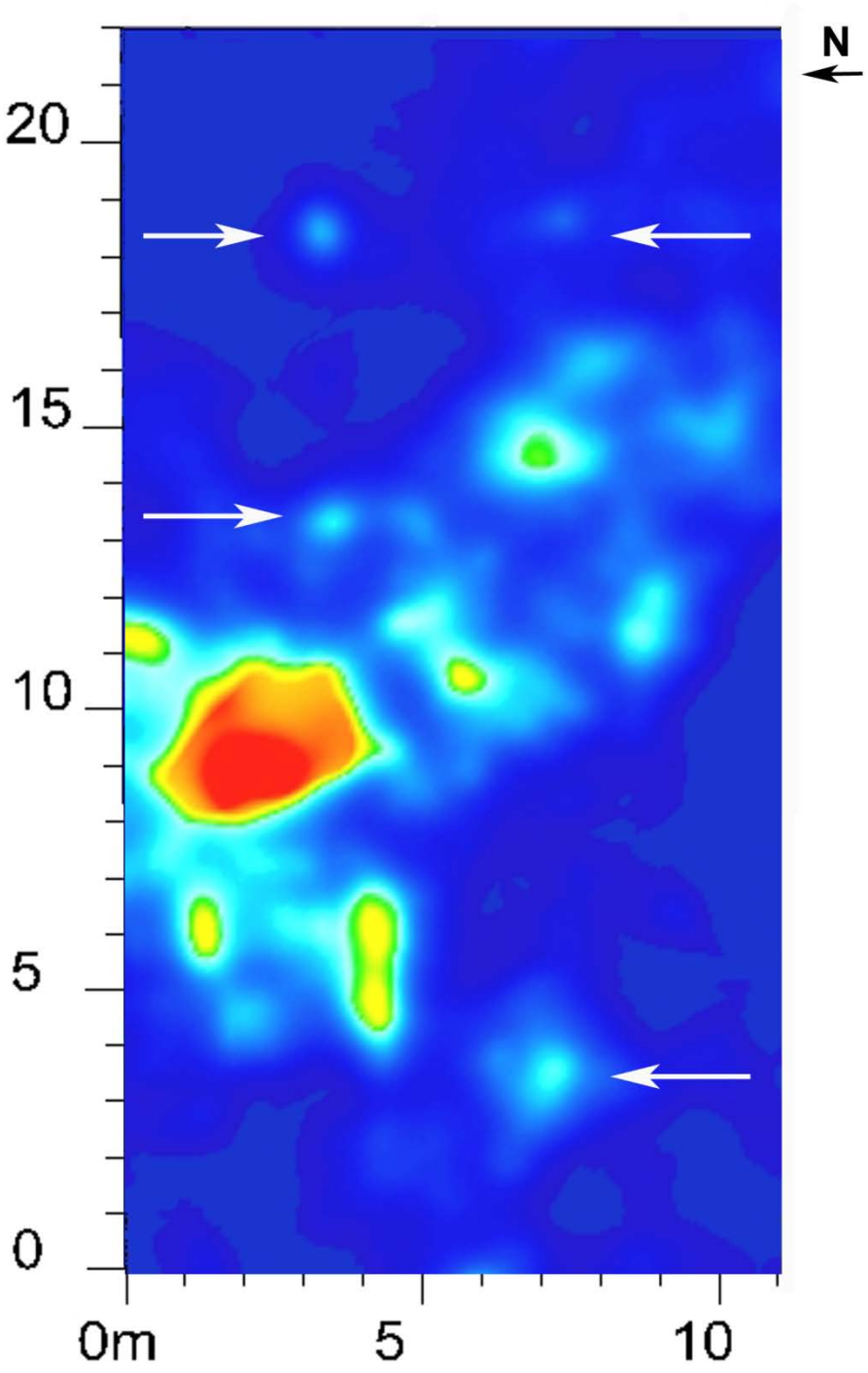

Figure 105: GPR horizontal slice using the 250-MHz antenna at 18 months. The horizontal slice is taken at 31.53 ns, approximately 1.21 m in depth.

MONTH 19

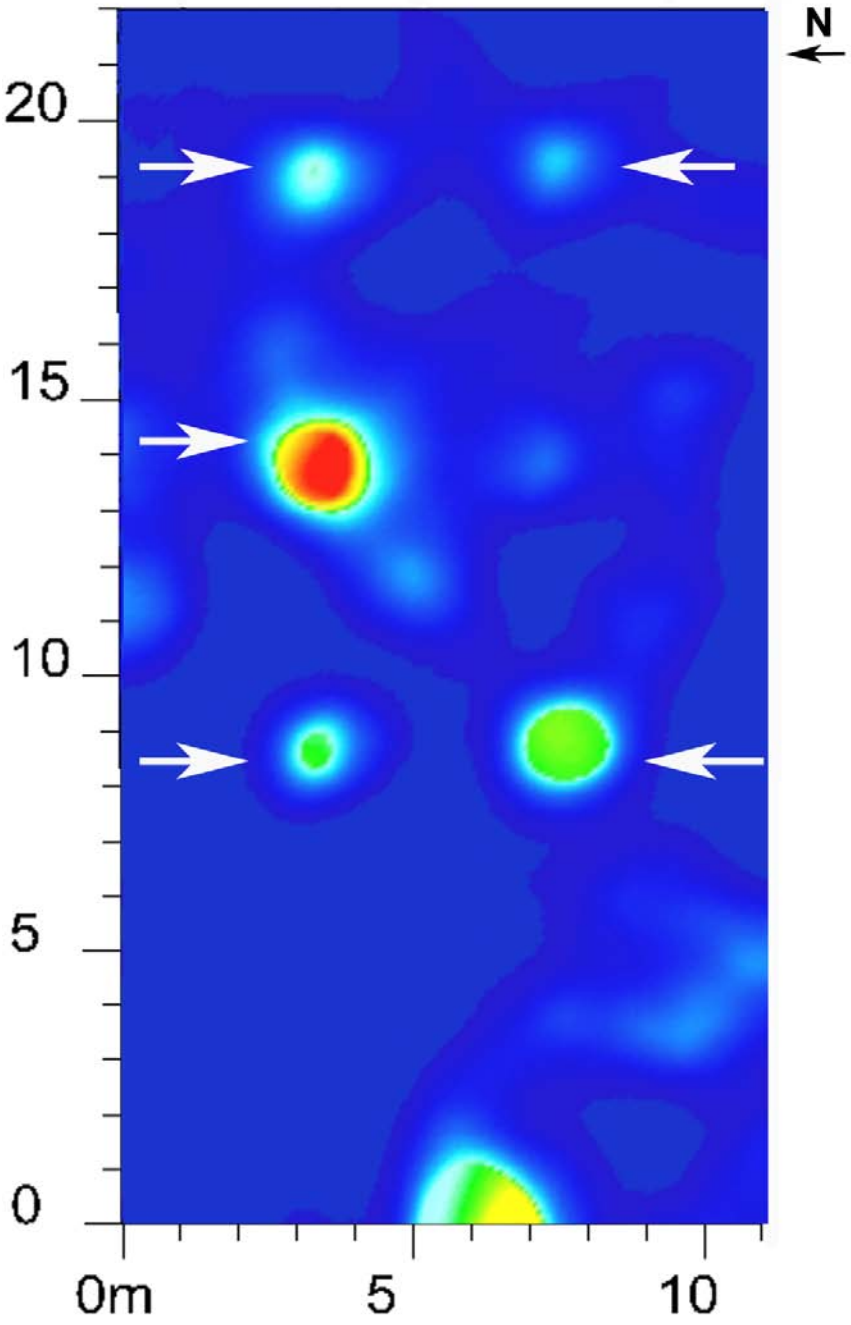

Figure 106: GPR horizontal slice using the 250-MHz antenna at 19 months. The horizontal slice is taken at 33.53 ns, approximately 1.33 in depth.

MONTH 20

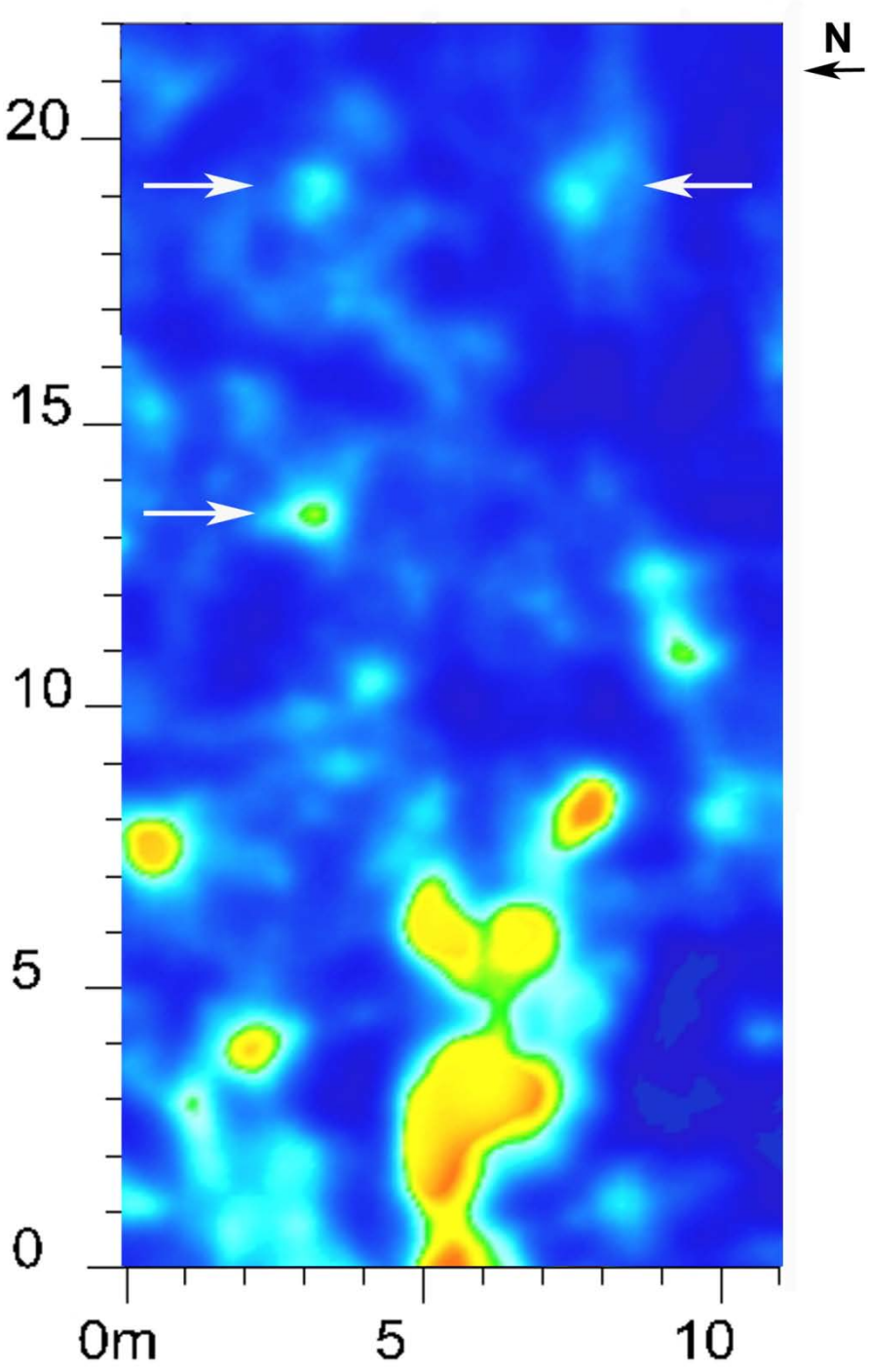

Figure 107: GPR horizontal slice using the 250-MHz antenna at 20 months. The horizontal slice is taken at 30.95 ns, approximately 1.28 m in depth.

MONTH 21

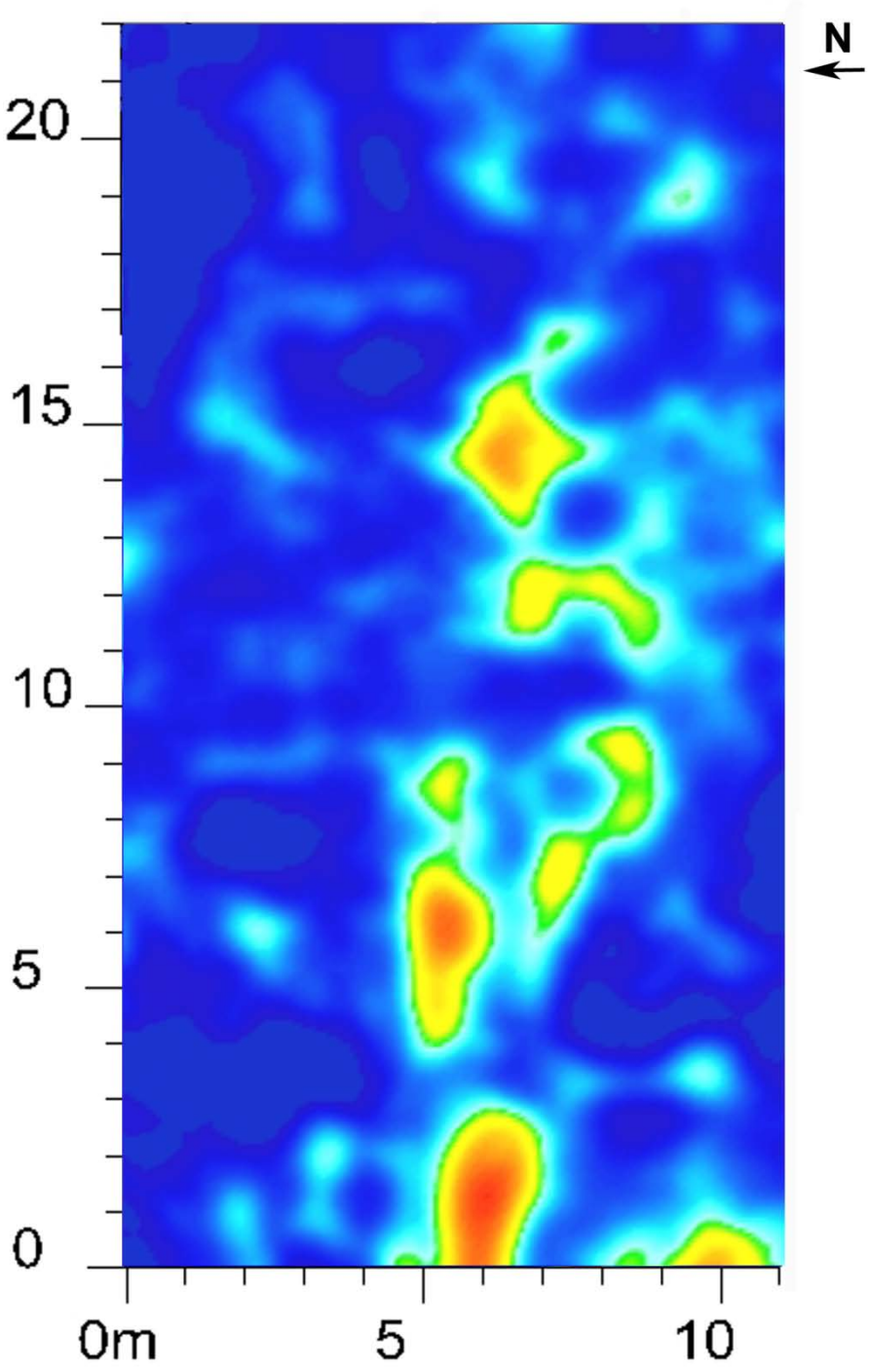

Figure 108: GPR horizontal slice using the 250-MHz antenna at 21 months. The horizontal slice is taken at 28.01 ns, approximately 1.25 m in depth.

MONTH 22

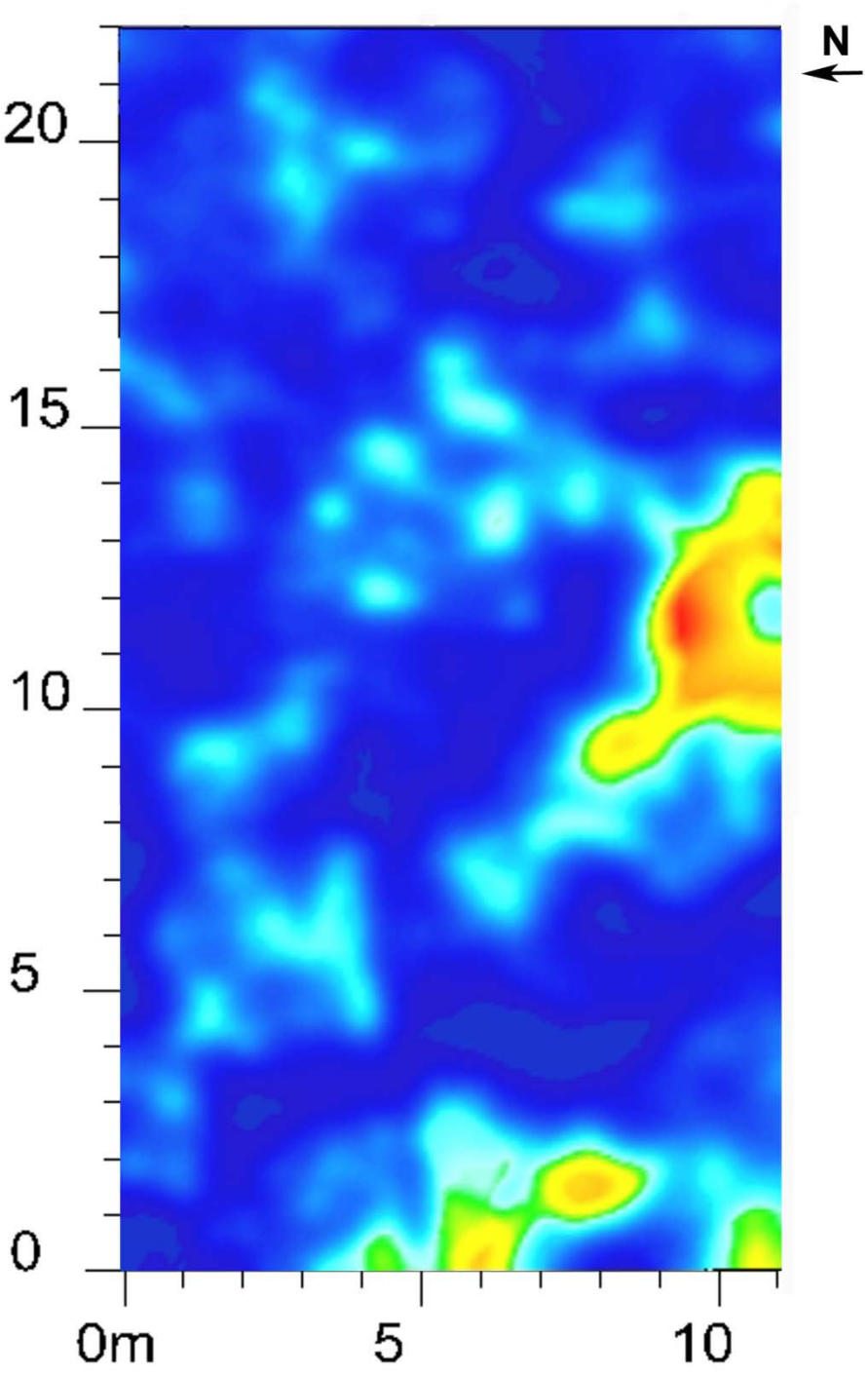

Figure 109: GPR horizontal slice using the 250-MHz antenna at 22 months. The horizontal slice is taken at 28.99 ns, approximately 1.25 m in depth.

MONTH 23

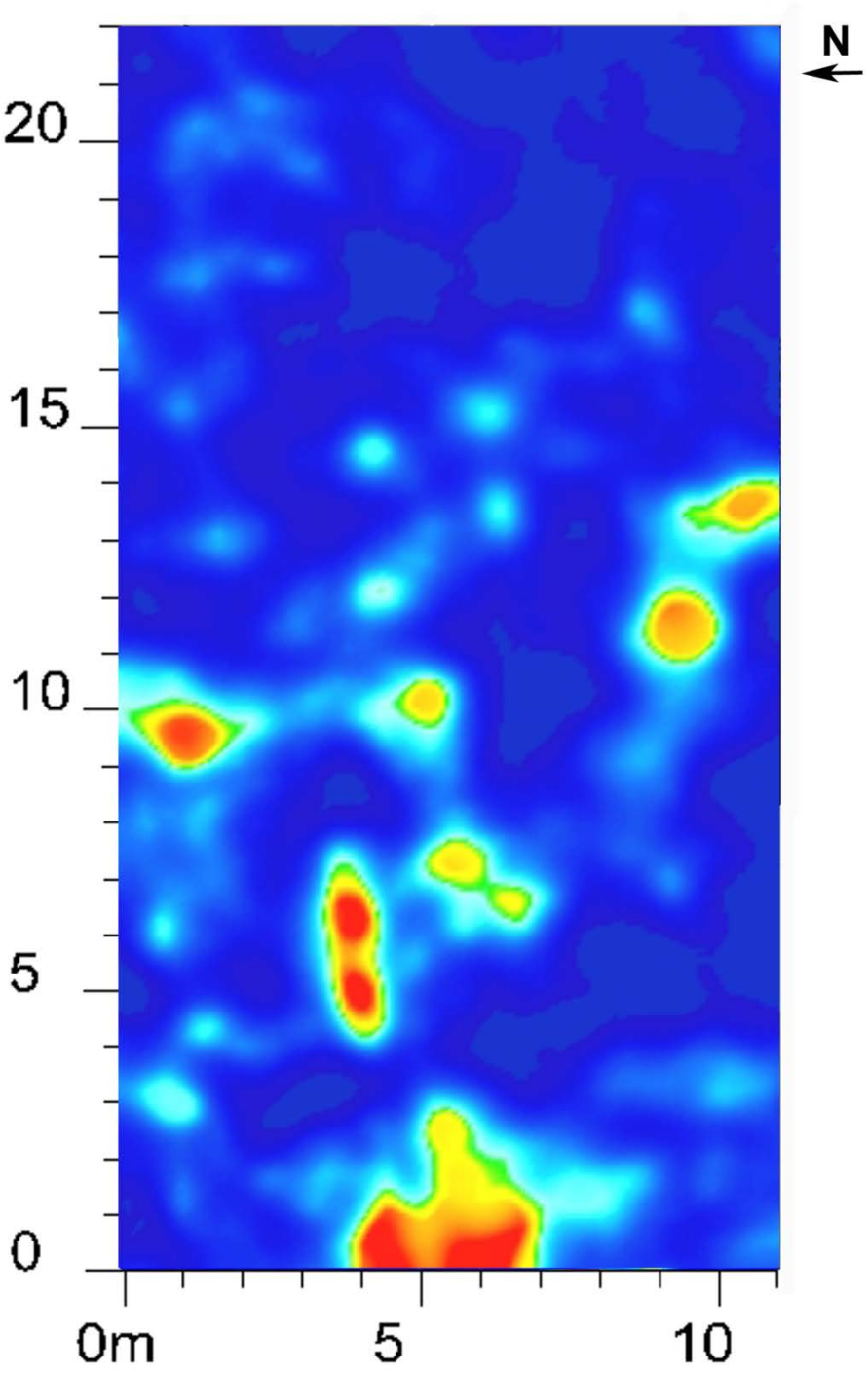

Figure 110: GPR horizontal slice using the 250-MHz antenna at 23 months. The horizontal slice is taken at 28.72 ns, approximately at 1.28 m in depth

MONTH 24

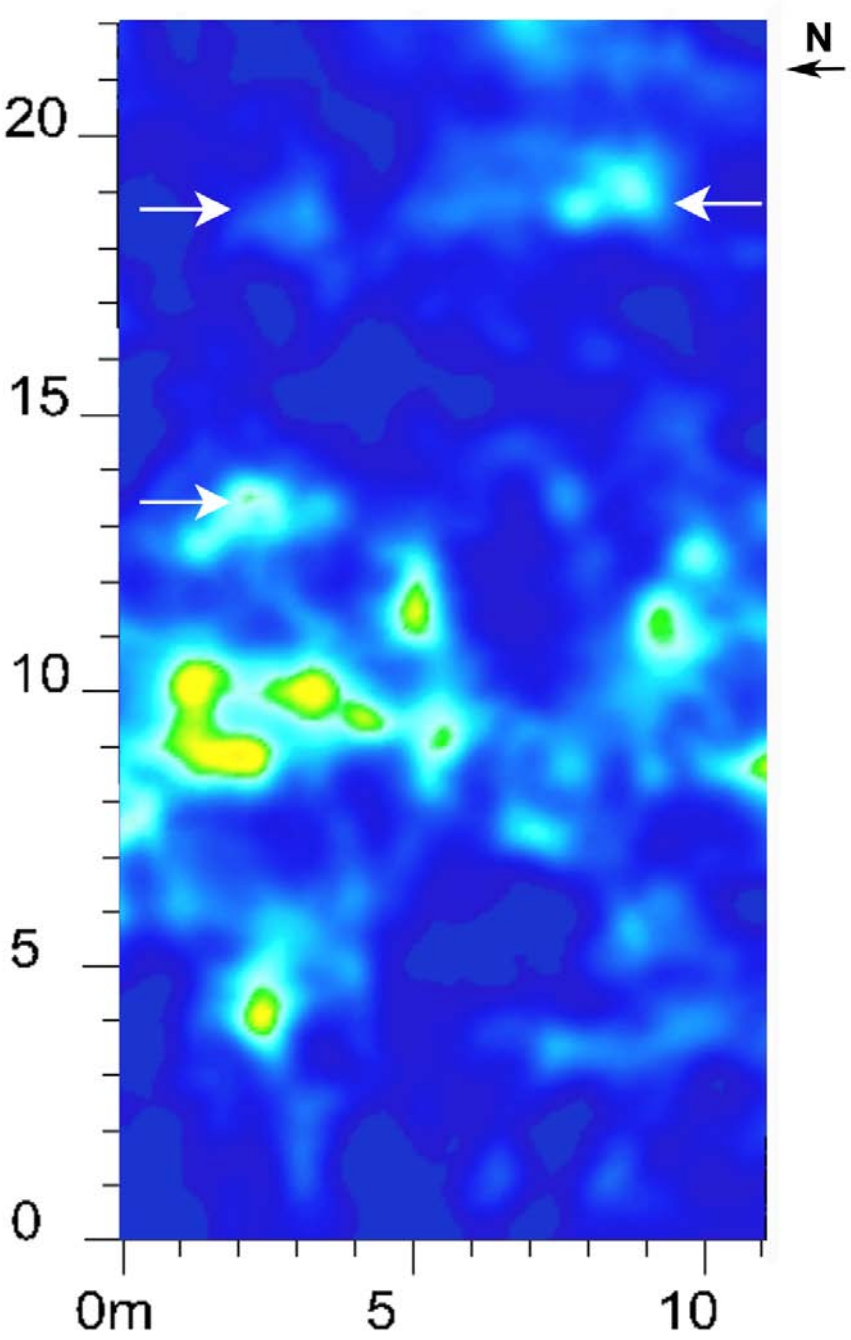

Figure 111: GPR horizontal slice using the 250-MHz antenna at 23 months. The horizontal slice is taken at 28.49 ns, approximately 1.15 m in depth.

APPENDIX F: MONTHLY MOISTURE DATA TABLES

Table 12: Moisture readings for 3/1/10- 13 month-500 MHz

Mark	1st Depth	2nd Depth	3rd Depth	Mark	1st Depth	2nd Depth	3rd Depth
N	0	-	-	1A	0	0	-
S	0	-	-	1B	0	0	0
E	0	-	-	1C	2	2	10
W	0	-	-	1D	2	2	2
NE	0	-	-	2A	0	0	-
NW	0	-	-	2B	0	2	3
SE	0	-	-	2C	2	3	6
SW	0	-	-	2D	2	2	2

Table 13: Moisture readings for 3/2/10- 13 month- 250 MHz

Mark	1st Depth	2nd Depth	3rd Depth	Mark	1st Depth	2nd Depth	3rd Depth
N	0	-	-	1A	10	10	-
S	0	-	-	1B	0	2	8
E	1	-	-	1C	2	8	10
W	0	-	-	1D	2	8	8
NE	1	-	-	2A	0	0	-
NW	0	-	-	2B	2	2	2
SE	0	-	-	2C	2	10	10
SW	0	-	-	2D	2	2	4

Table 14: Moisture readings for 3/31/10- 14 month-500 MHz

Mark	1st Depth	2nd Depth	3rd Depth	Mark	1st Depth	2nd Depth	3rd Depth
N	0	-	-	1A	6	8	-
S	0	-	-	1B	2	2	2
E	0	-	-	1C	2	4	6
W	0	-	-	1D	2	2	5
NE	0	-	-	2A	2	0	-
NW	0	-	-	2B	2	2	2
SE	0	-	-	2C	2	8	6
SW	0	-	-	2D	8	8	10

Table 15: Moisture readings for 4/1/10- 14 month-250 MHz

Mark	1st Depth	2nd Depth	3rd Depth	Mark	1st Depth	2nd Depth	3rd Depth
N	0	-	-	1A	0	2	-
S	0	-	-	1B	2	2	2
E	0	-	-	1C	2	8	8
W	0	-	-	1D	2	0	2
NE	1	-	-	2A	2	0	-
NW	0	-	-	2B	2	2	2
SE	0	-	-	2C	2	4	6
SW	0	-	-	2D	2	2	2

Table 16: Moisture readings for 4/27/10- 15 month- 500 MHz

Mark	1st Depth	2nd Depth	3rd Depth	Mark	1st Depth	2nd Depth	3rd Depth
N	0	-	-	1A	10	8	-
S	0	-	-	1B	0	2	2
E	0	-	-	1C	2	10	10
W	0	-	-	1D	2	2	2
NE	0	-	-	2A	0	0	-
NW	0	-	-	2B	2	2	0
SE	0	-	-	2C	2	10	8
SW	0	-	-	2D	2	2	2

Table 17: Moisture readings for 4/29/10- 15 month- 250 MHz

Mark	1st Depth	2nd Depth	3rd Depth	Mark	1st Depth	2nd Depth	3rd Depth
N	0	-	-	1A	10	10	-
S	0	-	-	1B	0	2	2
E	0	-	-	1C	2	4	10
W	0	-	-	1D	2	2	2
NE	0	-	-	2A	0	0	-
NW	0	-	-	2B	2	2	2
SE	0	-	-	2C	2	6	4
SW	0	-	-	2D	2	2	2

Table 18: Moisture readings for 5/31/10- 16 month-250 MHz

Mark	1st Depth	2nd Depth	3rd Depth	Mark	1st Depth	2nd Depth	3rd Depth
N	0	-	-	1A	0	0	-
S	0	-	-	1B	0	0	0
E	0	-	-	1C	0	2	8
W	0	-	-	1D	0	2	9
NE	0	-	-	2A	0	0	-
NW	0	-	-	2B	0	0	0
SE	0	-	-	2C	0	1	2
SW	0	-	-	2D	0	1	2

Table 19: Moisture readings for 6/2/10- 16 month- 500 MHz

Mark	1st Depth	2nd Depth	3rd Depth	Mark	1st Depth	2nd Depth	3rd Depth
N	0	-	-	1A	0	0	-
S	0	-	-	1B	0	0	0
E	0	-	-	1C	0	1	10
W	0	-	-	1D	0	4	1
NE	0	-	-	2A	0	1	-
NW	0	-	-	2B	0	0	0
SE	0	-	-	2C	0	0	4
SW	0	-	-	2D	0	0	2

Table 20: Moisture readings for 6/28/10- 17 month- 500 MHz

Mark	1st Depth	2nd Depth	3rd Depth	Mark	1st Depth	2nd Depth	3rd Depth
N	0	-	-	1A	2	4	-
S	0	-	-	1B	0	0	2
E	0	-	-	1C	0	0	0
W	0	-	-	1D	4	2	2
NE	0	-	-	2A	0	0	-
NW	0	-	-	2B	0	2	2
SE	0	-	-	2C	0	4	10
SW	0	-	-	2D	2	2	2

Table 21: Moisture readings for 6/30/10- 17 month- 250 MHz

Mark	1st Depth	2nd Depth	3rd Depth	Mark	1st Depth	2nd Depth	3rd Depth
N	0	-	-	1A	10	10	-
S	0	-	-	1B	0	0	0
E	0	-	-	1C	0	1	10
W	0	-	-	1D	0	2	1
NE	0	-	-	2A	0	0	-
NW	0	-	-	2B	0	0	1
SE	0	-	-	2C	0	2	8
SW	0	-	-	2D	0	2	2

Table 22: Moisture readings for 7/29/10- 18 month-250 MHz

Mark	1st Depth	2nd Depth	3rd Depth	Mark	1st Depth	2nd Depth	3rd Depth
N	0	-	-	1A	0	0	-
S	0	-	-	1B	0	0	0
E	0	-	-	1C	0	0	0
W	0	-	-	1D	0	0	0
NE	0	-	-	2A	0	0	-
NW	0	-	-	2B	0	0	0
SE	0	-	-	2C	0	0	0
SW	0	-	-	2D	0	0	0

Table 23: Moisture readings for 8/1/10-18 month-500 MHz

Mark	1st Depth	2nd Depth	3rd Depth	Mark	1st Depth	2nd Depth	3rd Depth
N	0	-	-	1A	0	0	-
S	0	-	-	1B	0	0	0
E	0	-	-	1C	0	0	0
W	0	-	-	1D	0	0	0
NE	0	-	-	2A	0	0	-
NW	0	-	-	2B	0	0	0
SE	0	-	-	2C	0	0	0
SW	0	-	-	2D	0	0	0

Table 24: Moisture readings for 8/30/10- 19 month- 250 MHz

Mark	1st Depth	2nd Depth	3rd Depth	Mark	1st Depth	2nd Depth	3rd Depth
N	0	-	-	1A	10	10	-
S	0	-	-	1B	0	0	1
E	0	-	-	1C	0	0	2
W	0	-	-	1D	1	1	1
NE	0	-	-	2A	0	2	-
NW	0	-	-	2B	0	1	1
SE	0	-	-	2C	0	1	10
SW	0	-	-	2D	2	1	2

Table 25: Moisture readings for 8/31/10- 19 month- 500 MHz

Mark	1st Depth	2nd Depth	3rd Depth	Mark	1st Depth	2nd Depth	3rd Depth
N	0	-	-	1A	1	10	-
S	0	-	-	1B	0	1	1
E	0	-	-	1C	0	0	4
W	0	-	-	1D	1	3	1
NE	0	-	-	2A	0	2	-
NW	0	-	-	2B	0	1	1
SE	0	-	-	2C	0	1	10
SW	0	-	-	2D	1	1	10

Table 26: Moisture readings for 9/30/10- 20 month- 250 MHz

Mark	1st Depth	2nd Depth	3rd Depth	Mark	1st Depth	2nd Depth	3rd Depth
N	0	-	-	1A	10	10	-
S	0	-	-	1B	4	4	4
E	0	-	-	1C	4	5	3
W	0	-	-	1D	3	4	4
NE	0	-	-	2A	4	5	-
NW	0	-	-	2B	4	5	5
SE	0	-	-	2C	3	3	3
SW	0	-	-	2D	3	3	3

Table 27: Moisture readings for 10/1/10- 20 month- 500 MHz

Mark	1st Depth	2nd Depth	3rd Depth	Mark	1st Depth	2nd Depth	3rd Depth
N	0	-	-	1A	10	10	-
S	0	-	-	1B	2	2	2
E	0	-	-	1C	2	2	2
W	0	-	-	1D	3	3	3
NE	0	-	-	2A	3	3	-
NW	0	-	-	2B	2	2	3
SE	0	-	-	2C	2	3	3
SW	0	-	-	2D	2	2	2

Table 28: Moisture readings for 10/28/10- 21 month- 500 MHz

Mark	1st Depth	2nd Depth	3rd Depth	Mark	1st Depth	2nd Depth	3rd Depth
N	0	-	-	1A	2	2	-
S	0	-	-	1B	0	1	1
E	0	-	-	1C	1	1	1
W	0	-	-	1D	1	1	2
NE	0	-	-	2A	2	2	-
NW	0	-	-	2B	3	2	2
SE	0	-	-	2C	1	1	1
SW	0	-	-	2D	1	1	1

Table 29: Moisture readings for 10/29/10- 21 month-250 MHz

Mark	1st Depth	2nd Depth	3rd Depth	Mark	1st Depth	2nd Depth	3rd Depth
N	0	-	-	1A	0	2	-
S	0	-	-	1B	0	0	0
E	0	-	-	1C	1	1	4
W	0	-	-	1D	1	1	1
NE	0	-	-	2A	0	0	-
NW	0	-	-	2B	0	0	1
SE	0	-	-	2C	1	2	3
SW	0	-	-	2D	1	1	1

Table 30: Moisture readings for 11/30/10- 22 month- 250 MHz

Mark	1st Depth	2nd Depth	3rd Depth	Mark	1st Depth	2nd Depth	3rd Depth
N	0	-	-	1A	10	10	-
S	0	-	-	1B	0	0	0
E	0	-	-	1C	0	0	4
W	0	-	-	1D	0	0	2
NE	0	-	-	2A	0	2	-
NW	0	-	-	2B	0	0	0
SE	0	-	-	2C	0	2	2
SW	0	-	-	2D	0	0	0

Table 31: Moisture readings for 12/1/10- 22 month- 500 MHz

Mark	1st Depth	2nd Depth	3rd Depth	Mark	1st Depth	2nd Depth	3rd Depth
N	0	-	-	1A	0	10	-
S	0	-	-	1B	0	0	0
E	0	-	-	1C	0	0	0
W	0	-	-	1D	0	0	0
NE	0	-	-	2A	0	2	-
NW	0	-	-	2B	0	0	0
SE	0	-	-	2C	0	0	0
SW	0	-	-	2D	0	0	1

Table 32: Moisture readings for 1/3/11- 23 month- 500 MHz

Mark	1st Depth	2nd Depth	3rd Depth	Mark	1st Depth	2nd Depth	3rd Depth
N	0	-	-	1A	4	10	-
S	0	-	-	1B	0	0	0
E	0	-	-	1C	0	0	0
W	0	-	-	1D	0	0	0
NE	0	-	-	2A	0	0	-
NW	0	-	-	2B	0	0	0
SE	0	-	-	2C	0	0	0
SW	0	-	-	2D	0	0	0

Table 33: Moisture readings for 1/4/11- 23 month-250 MHz

Mark	1st Depth	2nd Depth	3rd Depth	Mark	1st Depth	2nd Depth	3rd Depth
N	0	-	-	1A	10	10	-
S	0	-	-	1B	0	0	0
E	0	-	-	1C	0	2	0
W	0	-	-	1D	0	0	2
NE	0	-	-	2A	0	0	-
NW	0	-	-	2B	0	0	0
SE	0	-	-	2C	0	0	3
SW	0	-	-	2D	0	0	2

Table 34: Moisture readings for 2/1/11- 24 month-250 MHz

Mark	1st Depth	2nd Depth	3rd Depth	Mark	1st Depth	2nd Depth	3rd Depth
N	0	-	-	1A	0	1	-
S	0	-	-	1B	0	0	0
E	0	-	-	1C	0	0	0
W	0	-	-	1D	0	0	0
NE	0	-	-	2A	0	0	-
NW	0	-	-	2B	0	0	0
SE	0	-	-	2C	0	0	1
SW	0	-	-	2D	0	0	0

Table 35: Moisture readings for 2/2/11- 24 month-500 MHz

Mark	1st Depth	2nd Depth	3rd Depth	Mark	1st Depth	2nd Depth	3rd Depth
N	0	-	-	1A	0	1	-
S	0	-	-	1B	0	0	0
E	0	-	-	1C	0	0	0
W	0	-	-	1D	0	0	0
NE	0	-	-	2A	0	0	-
NW	0	-	-	2B	0	0	0
SE	0	-	-	2C	0	0	0
SW	0	-	-	2D	0	0	0

REFERENCES

Beauchaine AJ, Werdemann E. 2006. Using ground conductivity as a geophysical survey technique to locate potential archaeological sites in the Bad Axe river valley of western Wisconsin. UWL Journal of Undergraduate Research IX:1-6.

Bevan BW. 1991. The search for graves. Geophysics 56:1310-1319.

Clay RB. 2005. Conductivity survey: A survival manual. Cultural Resource Analysts, Inc.

Conyers LB, Cameron CM. 1998. Ground-penetrating radar techniques and three-dimensional computer mapping in the American Southwest. Journal of Field Archaeology 25:417-430.

Conyers LB. 2004. Ground-penetrating radar for archaeology. New York: Alta Mira Press.

Conyers LB. 2006. Ground penetrating radar, 2nd edition. Geoarchaeology 21(7):763-764.

Davenport GC. 2001. Remote sensing applications in forensic investigations. Historical Archaeology 35(1):87-100.

Davis JL, Heginbottom JA, Annan AP, Daniels RS, Berdal BP, Bergan T, Duncan KE, Lewin PK, Oxford JS, Roberts N, Skehel JJ, Smith CR. 2000. Ground penetrating radar surveys to locate 1918 Spanish flu victims in permafrost. Journal of Forensic Science 45(1): 68 76.

Dionne CA. 2009. Detecting buried metallic weapons in a controlled setting using a conductivity meter and a ground-penetrating radar. Master's Thesis. Department of Anthropology, University of Central Florida.

Dionne CA, Wardlaw DK, Schultz JJ. Delineation and resolution of cemetery graves using geophysical methods. Technical Briefs in Historical Archaeology 5:20-30.

Doolittle JA, and Bellantoni NF. 2009. The search for graves with ground-penetrating radar in Connecticut. Journal of Archaeological Science 37(5):941-949.

Doolittle JA, and Schellentrager G. 1989. Soil Survey, Orange County, Florida: US Dept. Agriculture, Soil Conservation Service.

Dupras TL, Schultz JJ, Wheeler SM, Williams LJ. 2006. Forensic recovery of human remains: archaeological approaches. Boca Raton: CRC Press, Taylor and Francis Group.

France DL, Griffin TJ, Swanburg JG, Lindemann JW, Davenport GC, Tranunell V,

Armbrust CT, Kondrateiff B, Nelson A, Castellano K, Hopkins D. 1992. A multidisciplinary approach to the detection of clandestine graves. Journal of Forensic Sciences 37(6):1445-1458.

Freeland RS, Miller ML, Yoder RE, Koppenjan SK. 2003. Forensic application of FM-CW and pulse radar. Journal of Environmental and Engineering Geophysics 8(2):97-104.

Geonics Limited. 2006. EM38 ground conductivity meter operating manual. Mississauga, Canada.

Hunter JR, Cox M. 2005. Forensic archaeology: advances in theory and practice. London: Routledge.

Imai T, Sakayama T, Kanemori T. 1987. Use of ground-probing radar and resistivity surveys for archaeological investigations. Geophysics 52(2):137-150.

Instanes A, Lønne I, Sandaker K. 2004. Location of avalanche victims with ground-penetrating radar. Cold Regions Science and Technology 38(1):55-61.

Killam EW. 2004. The detection of human remains. Springfield: Charles C. Thomas Publisher.

Kearey P, Brooks M, Hill I. 2002. An introduction to geophysical exploration. Oxford: Blackwell Science.

Leighty RG. 1989. Soil Survey, Orange County, Florida: US Dept. Agriculture, Soil Conservation Service.

Martin M. 2010. Detecting various burial scenarios in a controlled setting using ground-penetrating radar and conductivity. Master's Thesis. Department of Anthropology, University of Central Florida.

Manhein, MH. 1996. Decomposition rates of deliberate burials: a cases study of preservation. In: (William D. Haglund and Marcella H. Sorg, editors) Forensic Taphonomy: The Postmortem Fate of Human Remains, pgs. 469-481. CRC Press, Boca Raton.

McNeill JD. 1980. Electrical conductivity of soils and rocks. Technical Note TN-5. Geonics Limited. Mississauga, Ontario, Canada.

Mellett JS. 1992. Location of human remains with ground-penetrating radar. In: Hanninen P, Autio S, editors. Fourth International Conference on Ground Penetrating Radar, June 8-13. Rovaniemi, Finland: Geological Survey of Finland, Special Paper 16:359-365.

Modroo JJ, Olhoeft GR. 2004. Avalanche rescue using ground penetrating radar. Tenth International Conference on Ground Penetrating Radar: Delft, The Netherlands. p 785–788.

Morgan RM, Bull PA. 2007. Forensic geoscience and crime detection: identification, interpretation and presentation in forensic geoscience. Minerva Medicolegale 127(2): 73-89.

Nobes DC. 2000. The search for "Yvonne": a case example of the delineation of a grave using near-surface geophysical methods. Journal of Forensic Sciences 45(3):715-721.

Pomfret J. 2006. Ground-penetrating radar profile spacing and orientation for subsurface resolution of linear features. Archaeological Prospection 13:151-153.

Pye K, Croft DJ. 2004. Forensic geosciences: introduction and overview. In: Pye K, Croft DJ, editors. Forensic geoscience: principles, techniques and applications. London: Geological Society. pp 1-5.

Reynolds JM. 1997. An introduction to applied and environmental geophysics. John Wiley & Sons, West Sussex.

Rodgriuez, WC. Decompostion of buried and submerged bodies. In: (William D. Haglund and Marcella H. Sorg, editors) Forensic Taphonomy: The Postmortem Fate of Human Remains, pgs. 459-467. CRC Press, Boca Raton.

Ruffell A. 2005. Searching for the IRA "disappeared": ground-penetrating radar investigation of a churchyard burial site, Northern Ireland. Journal of Forensic Sciences 50:1-6.

Ruffell A, McKinley J. 2005. Forensic geosciences: applications of geology, geomorphology and geophysics to criminal investigations. Earth-Science Reviews 69:235-247.

Schultz JJ, Collins ME, Falsetti AB. 2006. Sequential monitoring of burials containing large pig cadavers using ground-penetrating radar. Journal of Forensic Sciences 51(3):607-616.

Schultz JJ. 2007. Using ground-penetrating radar to locate clandestine graves of homicide victims: forming forensic archaeology partnerships with law enforcement. Homicide Studies 11(11):15-29.

Schultz JJ. 2008. Sequential monitoring of burials containing small pig cadavers using ground penetrating radar. Journal of Forensic Sciences 53(2):279-287.

Schultz JJ, Martin M. 2011. Controlled GPR grave research: comparison of reflection profile between 500 MHz and 250 MHz antennae. In press- Forensic Science International.

Scott J, Hunter JR. 2004. Environmental influences on resistivity mapping for the location of clandestine graves. In: Pye K, Croft DJ, editors. Forensic geoscience: principles, techniques and applications. London: Geological Society. pp 33-38.

Strongman KB. 1992. Forensic applications of ground-penetrating radar. In: Pilon J, editor. Ground-penetrating radar. Ottawa: Geological Survey of Canada. pp 203-211.

Watters M, Hunter JR. 2004. Geophysics and burials: field experience and software development. In: Pye K, Croft DJ, editors. Forensic geoscience: principles, techniques and applications. London: Geological Society. pp 21-31.